# Improved Technique and Function of Agricultural Soil Mapping Using Visible and Near Infrared Real-time Soil Sensor

2015.3

Agricultural and Environmental Engineering
United Graduate School of Agricultural Science
Tokyo University of Agriculture and Technology

SITI NOOR ALIAH BINTI BAHAROM

学 位 論 文 要 旨

# Improved Technique and Function of Agricultural Soil Mapping Using Visible and Near Infrared Real-time Soil Sensor
# 可視・近赤外光リアルタイム土壌センサーを用いた農地土壌のマッピング手法改善

農業環境工学専攻　農業環境工学大講座
SITI NOOR ALIAH BINTI BAHAROM

The visible and near infrared (Vis-NIR) based real-time soil sensor (RTSS) is found to be a great tool for determining distribution of various soil properties and visualized it on digital soil maps. However there are still many aspects that need to be improved as to optimize the used of Vis-NIR soil sensor for better agriculture management either for precision agriculture or precision carbon farming purposes. This study describes on improved technique and function of agriculture soil mapping using Vis-NIR real-time soil sensor as to optimize the used of this state-of-the-art technology. Three aspects have been investigated. The first aspect is to investigate the potential of a Vis-NIR real-time soil sensor for mapping of paddy soil properties at multiple soil depths. The second aspect is to demonstrate the potential of Vis-NIR real-time soil sensor for high-resolution mapping of up to 24 paddy soil properties and the third aspect is to introduce integrated calibration model approach and compare its performance with local model for mapping of soil properties. Results from this study showed that the accuracy of the calibration models of the RTSS improved when the datasets from three soil depths used to develop the model. The three depths maps generated from the prediction value which were predicted using the three depth models exhibited that the soil properties were not only varied horizontally but also at different depths. Furthermore, the incorporation of multiple soil depths maps provided comprehensive information on soil variability for making precisions agronomic decisions. Hence, the Vis-NIR real-time soil sensor has great potential for determining the soil properties at

multiple soil depth. The used of the Vis-NIR real-time soil sensor for mapping of 24 soil properties is another pace that has been introduced in this study for optimizing the use of this sensor for precision agriculture practice. The investigated 24 soil properties were moisture content (MC), soil organic matter (SOM), pH, electrical conductivity (EC), cation exchange capacity (CEC), total carbon (C-t), total nitrogen (N-t), ammonium nitrogen (N-a), hot water extractable nitrogen (N-h), nitrate nitrogen (N-n), available phosphorus (P-a), exchangeable calcium (Ca), exchangeable potassium (K), exchangeable magnesium (Mg), hot water soluble soil boron (B), soluble copper (Cu), easily reducible manganese (Mn), soluble zinc (Zn), phosphate absorption coefficient (PAC), calcium saturation percentage (CSP), base saturation percentage (BSP), bulk density (BD), ratio of magnesium to potassium (Mg/K) and ratio of calcium to magnesium (Ca/Mg). The results indicated that 22 out of 24 soil properties can be predicted by just a single scan of Vis-NIR using a single action of soil sensing in real-time with different levels of model accuracy. The coefficient of determination ($R^2_{val}$) ranged from 0.43 to 0.90. Of these 24 soil properties, 8 soil properties' models were categorized as excellent, 14 as good and 2 as unreliable based on their residual prediction deviation (RPD) values. Reasonable spatial similarity exhibited between the measured and predicted maps is sufficient to declare that the Vis-NIR real-time soil sensor measurement system has potential to be used for the real-time measurement of numerous soil properties. Another approach to improve the use of RTSS for soil mapping is by introducing an integrated calibration model that was developed using the dataset from three different fields at three different regions of Japan with different soil nutrient management. The integrated calibration model has improved the prediction accuracy of the local calibration model. The comparison between measured and maps generated through prediction on the independent validation set using the integrated model showed spatial similarity for moisture content (MC), soil organic matter (SOM), total carbon (C-t) and total nitrogen (N-t). This showed that the integrated calibration model approach has good potential for minimizing the repetitiveness of developing calibration model for RTSS every time for every different field. This result could be used as a step towards establishment a robust calibration model for agriculture soil in Japan. The technique developed in this research would capable in reducing the cost and time in analysis of soil spatial variability for the precision agriculture and precision carbon farming practices. Furthermore, the approaches and recommendations on the techniques of soil properties measurement and mapping in this study could improve and optimize the utilization of Vis-NIR real-time soil sensor towards better agriculture production such as optimize production efficiency; optimize quality; minimize environmental impact; minimize risk at the site-specific level management practice in precision agriculture and carbon sequestration practices.

# Acknowledgement

*In the name of Allah, who is Beneficent and Merciful*

First of all, I would like to express my deepest gratitude to my supervisor, Prof. Dr. Sakae Shibusawa for offering me this precious research opportunity, guiding me to every progress, teaching me all research skills, helping me on both scientific and personal life aspects. Without his patience and unconditionally support, I would be impossible to carry out and finish this study.

I equally thank my other two co-supervisors, Prof. Tadashi Chosa from Tokyo University of Agriculture and Technology and Prof. Masakazu Komatsuzaki from Ibraki University for their contribution and encouragement during my study. I also gratefully acknowledge technical support by Mr. Masakazu Kodaira for his comments, ideas, opinions and suggestions in field work, laboratory analysis and journal writing.

I am also indebted to the Malaysian Agricultural Research and Development Institute (MARDI) for providing me adequate scholarship for my PhD. program and also Japan Science and Technology Agency for the research funding.

I would like to thank my colleagues: Kana Inoue, Ryuhei Kanda, Ida Ayu Bintang Madrini, Qichen Li, Shun Hosaka and Hui Li for their collaboration during the study.

This appreciation also for my supportive husband, Dr. Mohd Rosdzimin Abdul Rahman, my sons, Ahmad Aqil Iman and Ahmad Afif Iman who always have been encouraging and inspiring me through hard times, who always stayed beside me in times of difficulties, I would like also acknowledge my parents and my family members in Malaysia for their pray and sacrifices. I am really grateful their love and support.

Again, I would like to thank everybody, including those who may not have been mentioned above for the limited space, for everything they did to help this thesis make its way out to the world.

Thank you very much!

Jazak Allah Khayr

# TABLE OF CONTENT

# List of Figures

# List of Tables

# Abbreviations

| | |
|---|---|
| ANN | artificial neural networks |
| APCRL | Agricultural Product Chemical Research Laboratory |
| B | hot water soluble boron |
| BD | bulk density |
| BSP | base saturation percentage |
| C | carbon |
| C-t | total carbon |
| Ca | exchangeable calcium |
| Ca/Mg | ratio of calcium to magnesium |
| CCD | charge-coupled device |
| CEC | cation exchange capacity |
| CH | carbon-hydrogen |
| CM1 | calibration model that combined the dataset for depths of 10 and 15cm |
| CM2 | calibration model that combined the dataset for depths of 15 and 20cm |
| CM3 | calibration model that combined the dataset for depths of 10, 15 and 20cm |
| CSP | calcium saturation percentage |
| Cu | soluble copper |
| CV | coefficient of variation |
| DGPS | digital Global Positioning System |
| EC | electrical conductivity |
| GPS | global positioning system |
| IDW | inverse distance weighting |
| IM | integrated calibration model |
| InGaAs | indium gallium arsenide |
| INS | inelastic neutron scattering |
| K | exchangeable potassium |
| LIBS | laser induced breakdown spectroscopy |
| M | local calibration model for Matsuyama field |
| MARS | multivariate adaptive regression splines |
| MC | moisture content |
| Mg | exchangeable magnesium |
| Mg/K | ratio of magnesium to potassium |
| MIR | mid infrared |
| Mn | easily reducible manganese |
| Mo | molybdenum |

| | |
|---|---|
| MRA | multiple regression analysis |
| MSC | multiplicative scatter correction |
| MY | calibration model for combination of Matsuyama and Yamatsuri field |
| N | nitrogen |
| N-a | ammonium nitrogen |
| N-h | hot water extractable nitrogen |
| N-n | nitrate nitrogen |
| N-t | total nitrogen |
| NH | nitrogen-hydrogen |
| NIR | near infrared |
| Ob | local calibration model for Obihiro field |
| OH | oxygen-hydrogen |
| PAC | phosphate absorption coefficient |
| PC | principal components |
| Vis | visible |
| Vis-NIR | visible and near infrared |
| RTSS | real time soil sensor |
| P | phosphorous |
| P-a | available phosphorus |
| PCR | principle component regression |
| PLSR | partial least square regression |
| $R^2_{cal}$ | coefficient of determination of calibration |
| $R^2_{val}$ | coefficient of determination of full cross-validation |
| RPD | ratio prediction to deviation |
| RBFN | radial basis function networks |
| $RMSE_{cal}$ | root mean square error of calibration |
| $RMSE_{val}$ | root mean square error of full cross-validation |
| SD | standard deviation |
| SD(ym) | standard deviation of measured values |
| SMLR | stepwise multiple linear regression |
| SNV-D | standard normal variate and detrending |
| SOC | soil organic carbon |
| SOM | soil organic matter |
| SVM | support vector machines |
| TUAT | Tokyo University of Agriculture and Technology |
| Y | local calibration model for Yamatsuri field |
| Zn | soluble zinc |

# Chapter 1

# Introduction

## 1.1 Background

Information on spatial and temporal soil variability is essential in order to assist farmers in making agronomic decision for farm management and for environmental concern. This information is to ensure high crop yield and low cost production with minimal unintended environmental effects. Practical assessment of soil properties variability and soil nutrient availability, however, remains a challenging task because it requires the integrated consideration of multiple soil properties involved in soil functioning and their variation in space and time. Moreover, reports have shown that there is large variability in soil, crop, diseases, weed and/or yield, not only in large-size but also in small-size fields (Mouazen et al. 2003). In conventional method of soil properties quantification, the soil cores are collected at limited number of samples and analyze them intensively in laboratory. This practice is not only laborious but also high cost and time consuming. It is also impractical when the quantification of the soil properties involves mapping of large field areas for precision agriculture purposes. The

laboratory analysis of soil properties in the conventional method are usually measured using standardized analytical procedures, which are costly, time consuming and need a skilled operator. Therefore, these procedures are based on a limited number of mixed soil samples representative of a large area up to 2 ha of land (Vanden Auweele et al., 2000). This type of limited sampling strategy makes it impossible to generate high-resolution map for establishment of management zones. Therefore, alternative measurement methods are needed to replace the conventional method for providing intensive information about soils at low cost, acceptable level of reliability and in a timely manner.

To overcome the limitations in the conventional method of soil assessment, the spectroscopic technique was exploited in the region of visible (Vis), near-infrared (NIR), and mid-infrared (MIR) to determine the soil constituents (Sudduth et al. 1991; Morra et al. 1991; Shonk et al. 1991; Viscarra Rossel et al. 1998; Ehsani et al. 1999; Chang et al. 2001; Hummel 2001; Slaughter et al. 2001; Martin et al. 2002; Cozzolino and Moron 2006). The soil properties investigated in previous studies resulted in different levels of accuracy, using various types of spectroscopic instrument. The visible and infrared technique has gained huge interest among researchers because it is more straightforward than conventional soil analysis and most attractively, multiple soil properties can be derived from a single scan (Viscarra Rossel et al. 2006b). Once a soil is scanned, the same spectra can be used for estimation of various soil properties such as moisture and organic matter (Hummel et al. 2001), phosphorous (Maleki et al. 2006), pH, lime requirement, organic carbon, clay, silt, sand, cation exchange capacity, exchangeable calcium, exchangeable aluminum, nitrate–nitrogen, available phosphorus, exchangeable potassium and electrical conductivity (Viscarra Rossel et al. 2006a), total organic carbon, total nitrogen, clay content and cation exchange capacity (Genot et al. 2011).

Those previous studies have proven that Vis-NIR is a promising technique to provide information on soil constitutions.

The measurements of soil properties in those studies mentioned above were however not in real-time or on-the-go where the spectra scanning process for developing the calibration model and prediction was performed in the laboratory environment. The soil samples need to be crushed, sieved, dried and smoothed prior to the spectra scanning. Although this method may provide better accuracy due to the controlled condition in the laboratory, it is laborious when it involved such huge number of samples for generating high-resolution maps and it also cannot provide information of the field condition in real-time. For this reason, a Vis-NIR based real-time soil sensor (RTSS) was developed by Shibusawa (1999) and this RTSS has been used by Imade Anom et al. (2001) for the mapping of moisture content (MC), soil organic matter (SOM), $NO_3$-N, pH and electric conductivity (EC). The successor model of this RTSS (SAS1000) was employed by Kodaira and Shibusawa (2013) to provide high-resolution maps of 12 soil properties for upland agriculture fields. Mouazen et al. (2005) has also developed a Vis-NIR based on-line sensor which then was evaluated for mapping MC, total carbon (C-t), pH and available phosphorous (P-a). Tekin et al. (2013) used this online sensor to develop a soil pH map for variable-rate lime recommendations. Another real-time sensor was introduced by Christy (2008) for the measurement of soil organic matter and was later adopted for the estimation of not only organic carbon, but also clay, Mg, and K (Bricklemyer et al. 2010; Debaene et al. 2010).

Measurement of soil properties in real-time has raised several challenges and limitations in previous studies, particularly in the accuracy of the real-time measurement. The variation on the spectra sampling depth as the real-time sensor running across the field might also need to be taken into account for the reliability of the

real-time measurement. Moreover, the issues on the robustness of calibration model remain unresolved as the sensor system still need to be calibrated separately for every field. In addition, the Vis-NIR spectroscopy is not yet fully explored as to fully make use the advantage features of spectroscopy. These challenges need to be resolved as to improve and optimize the use of real-time soil sensor for measurement of soil properties towards sustainable agricultural practices.

## 1.2 Literature Review

### 1.2.1 Soil Properties

Soils have many different properties, including MC, SOM, pH, EC, cation exchange capacity (CEC) and carbon (C). The sufficiency of these soil properties determines the efficiency of nutrient supply from soil for the plant growth as most plants grow by absorbing nutrients from the soil. In other words the amount of these soil properties determines the extent to which nutrients are available to plants.

Soil nutrients are divided into two groups; macronutrient and micronutrients. Macronutrients can be broken into two more groups: primary and secondary nutrients. The primary nutrients are nitrogen (N), phosphorus (P), and potassium (K). These major nutrients usually are lacking from the soil first because plants use large amounts for their growth and survival.

The secondary nutrients are calcium (Ca), magnesium (Mg), and sulfur (S). There are usually enough of these nutrients in the soil so fertilization is not always needed (Troeh and Thompson, 2005). Also, large amounts of calcium and magnesium are added when lime is applied to acidic soils. Sulfur is usually found in sufficient amounts from the slow decomposition of soil organic matter.

Micronutrients are those elements essential for plant growth which are needed in only very small (micro) quantities. These elements are sometimes called minor elements or trace elements. The micronutrients are boron (B), copper (Cu), iron (Fe), chloride (Cl), manganese (Mn), molybdenum (Mo) and zinc (Zn). Recycling organic matter such as grass clippings and tree leaves is an excellent way of providing micronutrients (as well as macronutrients) to growing plants (Troeh and Thompson, 2005).

Since the soil provides most essential nutrients to the crops, it is important to know numerous soil properties and nutrient availability that associated to plant growth. In addition to the soil nutrients mentioned above, other main soil properties that crucial to be considered for sustainable agricultural production are phosphorous absorption coefficient (PAC), calcium saturation percentage (CSP), base saturation percentage (BSP), bulk density (BD) etc.

### 1.2.2 Soil Variability

Site-specific management has received considerable attention due to the three main potential benefits of increasing input efficiency, improving the economic margins of crop production, and reducing environmental risks (Fathi et al., 2014). Uniform management of crops grown under spatially variable conditions can result in less than optimum yields due to nutrient deficiencies as well as excessive fertilizer application that may potentially reduce environmental quality (Redulla et al., 1996). Site-specific management of nutrients gives the farmer the potential to apply the exact requirement of nutrients at each given location in a field. Spatial variability in soils occurs naturally from pedogenic factors. Natural variability of soil results from complex interactions between

geology, topography, climate as well as soil use (Quine and Zahng, 2002). In addition, variability can occur as a result of land use and management strategies. As a consequence, soils can exhibit marked spatial variability at the macro– and micro –scale (Vieira and Paz Gonzalez, 2003; Brejda et al., 2000). Demands for more accurate information on spatial distribution of soils have increased with the inclusion of the spatial dependence and scale in ecological models and environmental management systems. This is because the variation at some scales may be much greater than at others (Yemefack et al., 2005). Spatial dependence has been observed for a wide range of soil physical, chemical, and biological properties and processes (Lyons et al.,1998; Raun and et al,. 1998). Incorporation of functions that relate distance and variance among points into spatial analysis of soils data results in more accurate estimates of soil properties and processes than those that consider only spatial independence between points (Warrick and Nielsen, 1980).

Soil nutrient variability mapping has been reported as an important component for establishing management zones (Castrignano et al., 2000), although there are reports on recommendations affected by time of sampling (Hoskinson et al., 1999) and by variability in laboratory result (Brenk et al., 1999). Cahn et al. (1994) showed the importance of spatial variation of soil fertility for site specific crop management. Haneklause et al. (1998) also suggested that correctly mapping soil fertility parameters is important for variable rate application. Therefore, spatial information of nutrient status should be characterized when making fertilizer recommendations.

### 1.2.3 Emerging Technologies in Agricultural Soil Sensing

#### *1.2.3.1 Precision Agriculture*

Precision agriculture has become a very important sector in agriculture during the last two decades, particularly in countries, whose lands are dominated by large-size fields. Reports have showed that there is a large variability in soil, crop, diseases, weed and/or yield, not only in large-size fields (McBratney and Pringle, 1997; Corwin et al., 2003; Godwin and Miller, 2003; Vrindts et al., 2005) but in small-size fields too (Mouazen et al., 2003). The concept of management zones' was evolved in response to this large variability, aiming at better land management and reduction of the amount of inputs applied into the environment (Franzluebbers and Hons, 1996; Malhi et al., 2001). Applying appropriate doses would result in reducing costs, reducing groundwater contamination by herbicides, pesticides and fertilizers and occasionally increasing yield. But, a proper establishment of management zones relies heavily on several factors regarding availability of information about soil, crop, diseases, weed and yield.

In order to effectively implement the precision agriculture practice, detailed spatial information on soil properties is required to manage the crop production with increased farm profits and reduced environmental impacts. Detailed soil properties maps provide essential information for site-specific decision making in choosing appropriate management practices. For example, nitrogen concentrations in the soil surface or several centimeters below the soil surface are needed to determine site-specific application rates of some crop production inputs, including fertilizers and herbicides (Blackmer and White 1998)

The importance of describing the variability of soil properties at either small- or large-scale field size and present it on map has resulted in the exploitation of several new sensor technologies for soil properties measurement in the field. Sensor technologies is an important element in precision agriculture as to facilitate the generation of soil map of the spatial variation in several entities, namely crop yield, crop growth, soil characteristics, and others (Tekin et al., 2013). The output of these technologies is useful information for variable rate nutrient and pesticide application, irrigation control, tillage, etc. Therefore, precision agriculture makes extensive use of sensors in order to identify proper targets and needs of crops for applying locally varying doses of chemicals (Lee at al., 2010). Various types of soil sensor technologies are used, but in many cases these are insufficient for the in situ monitoring of plant beds conditions, such as the nutrient concentration, soil compaction, and pH, because particle sizes and plant roots in the solution are non-uniform distributed spatially and with depth (Futagawa et al., 2012)

The development of sensors is expected to increase the effectiveness of precision agriculture. In particular, sensors developed for on-the-go measurement of soil properties have the potential to provide benefits from the increased density of measurements at a relatively low cost (Sonka et al., 1997). Several emerging technologies that have been exploited for measurement of soil properties are near-infrared spectroscopy (Sudduth and Hummel 1993; Shibusawa, 1999; Christy et al. 2003; Mouazen, 2005), electromagnetic induction (Sudduth et al., 2003) ion-selective electrodes (Adamchuk et al., 2003; Viscarra Rossel and Walter, 2004), and Landsat Enhanced Thematic mapper (ETM) (Huang et al., 2007)

#### *1.2.3.2 Precision Carbon Farming*

More recently, global climate change studies have shown that increasing carbon storage by soils is a practical method to mitigate greenhouse gas emissions (Robertson et al., 2000; Lal, 2004). Conservation management practices that enhance soil carbon storage, e.g. no-till and cover cropping can stimulate carbon sequestration (Young, 2003; Lal et al., 2004). Growers may be able to benefit when switching their management practices to those that store more soil carbon by getting paid for stored carbon by private markets or government programs (Young, 2003). This agriculture approach is known as carbon farming. However, quick, reliable and cost-effective techniques are needed for ensuring soil carbon changes in response to changes in land management on an agricultural field.

Conventional laboratory analysis involves a substantial amount of resources to make relatively few measurements of soil carbon. Development of methods for soil carbon analysis that address and minimize the uncertainties associated with conventional methodologies are important for improving estimates of terrestrial carbon inventories and fluxes (Gehl and Rice, 2007). Online methods for determination of soil carbon are important due to the comparatively rapid and potentially cost-effective benefits of these methods, and the reduction in sampling and laboratory errors (Gehl and Rice, 2007). The greatest benefit of field analysis of soil carbon may lie in the potential to minimize soil disturbance while increasing the ability to analyze large areas of soil (Gehl and Rice, 2007). Advanced field methods of carbon analysis should be capable of providing repetitive, sequential measurements for evaluation of spatial and temporal variation at a scale that was previously unfeasible.

The increased interest in assessing carbon inventories and dynamics has resulted in the advent of several new technologies for soil carbon measurement in the field. Visible and near infrared reflectance spectroscopy have each been assessed as a means to determine soil organic carbon (SOC) content (Dalal and Henry 1986; Ben-Dor and Banin 1995; Janik et al. 1998; Chang and Laird 2001; Reeves et al. 2001; McCarty et al. 2002). More research attempts to measure soil carbon in situ have included Laser Induced near-infrared spectroscopy (Sudduth and Hummel 1996; Christy et al. 2003), Breakdown Spectroscopy (LIBS, Ebinger et al. 2003; Bricklemeyer, et al., 2011), Inelastic Neutron Scattering (INS, Wielopolski et al. 2003) airborne imaging spectroscopy (Stevens, et al., 2006) and remote sensing imagery (Chen et al. 2000).

### 1.2.4 Visible and Near Infrared (Vis-NIR) Spectroscopy

Vis-NIR is a molecular technique where spectral signatures of materials are characterized by their reflectance, or absorbance, as a function of wavelength. It is highly sensitive to both organic and inorganic phases of the soil, making their use in the agricultural and environmental sciences particularly relevant (Viscarra Rossel et al., 2006b). Intense fundamental molecular frequencies related to soil components occur in the mid infrared (MIR) between wavelengths 2500 and 25 000 nm with overtones and combinations found in the near-infrared region (400 – 2500 nm) (Clark, 1999; Shepherd & Walsh, 2002). The visible and infrared portions of the electromagnetic spectrum are highlighted in Figure 1.1. Weak overtones and combinations of these fundamental vibrations due to the stretching and bending of NH, OH and CH groups dominate the NIR (700–2500nm) and electronic transitions the Vis (400–700 nm).

Several studies have shown Vis-NIR spectroscopy to be useful for rapidly characterizing soil (Baumgardner et al., 1985; Dalal & Henry, 1986; Ben-Dor & Banin, 1995; Reeves & McCarty, 2001; Adamchuk et al., 2004; Barthes et al., 2006; Brown et al., 2005; Viscarra Rossel et al., 2006b). Vis-NIR provides an established method for the quantitative and semi-quantitative determination of soil clay mineralogy, iron oxyhydroxides, clay-size particles, soil organic C, carbonates (soil inorganic C), and CEC in a laboratory setting (Shepherd & Walsh, 2002; Islam et al., 2003; Barthes et al., 2006; Brown et al., 2006; Van Vuuren et al., 2006; Viscarra Rossel et al., 2006a; b; Wetterlind et al., 2008) for intact soil cores (Waiser et al., 2007; Kusumo et al., 2008; Morgan et al., 2009), and "real-time" (Shonk et al., 1991; Shibusawa et al., 1999; Mouazen et al., 2005; Christy, 2008; Bricklemyer & Brown, 2010).

Visible and infrared reflectance spectroscopy has advantages over some of the conventional techniques of soil analysis such as they are rapid, timely and less expensive, hence are more efficient when a large number of analyses and samples are required. This technique does not require expensive and time-consuming sample pre-processing or the use of (environmentally harmful) chemical extractants. Furthermore, and in particular with infrared spectroscopy, a single spectrum allows for simultaneous characterization of various soil constituents because one spectrum holds information about various soil constituents. Hence, several soil properties can be measured from a single scan (Viscarra Rossel et al., 2006b). Visible and infrared spectroscopy may, on instances, be more straightforward than conventional soil analysis and on occasions also more accurate. For example, McCauley et al. (1993) suggested that Vis spectroscopy may be more accurate than dichromate digestions for analysis of soil organic carbon. One other advantage is the potential adaptability of

the techniques for real-time field use (Viscarra Rossel and McBratney, 1998). These are particularly important advantages now that there is an increasing global need for larger amounts of good quality inexpensive spatial soil data to be used in precision agriculture and environmental monitoring and modelling.

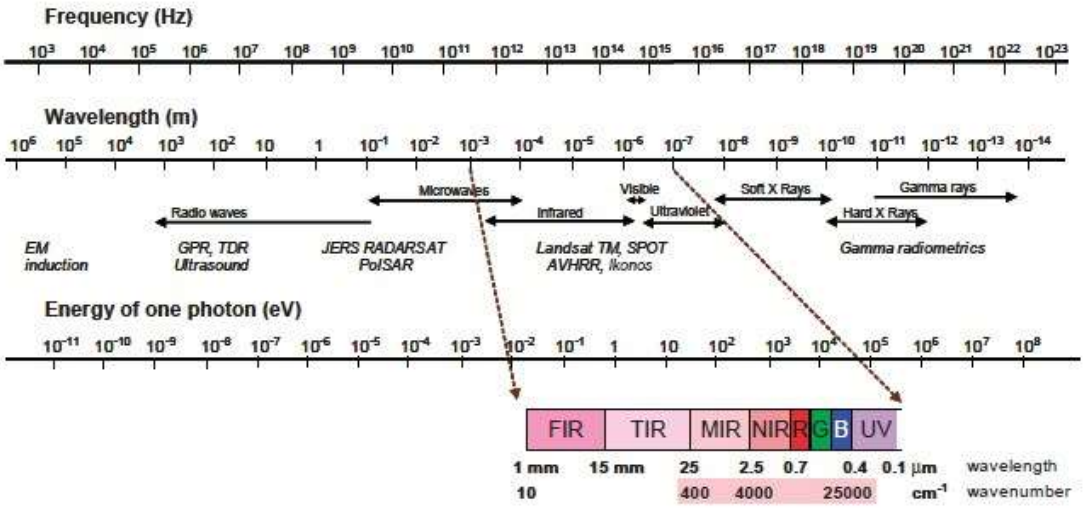


Fig. 1.1 The electromagnetic (EM) spectrum highlighting the visible and infrared portions (McBratney et al., 2003, Viscarra Rossel et. al, 2006b).

### 1.2.5 Use of the Vis-NIR Techniques for real-time Measurement of Soil Properties and its Limitations

Very few studies are available on using the Vis–NIR spectroscopy to perform real-time measurement of soil properties. This is attributed to the difficulties in building a real-time measurement system. Inserting the illumination and detection units within the soil leads to delicate and fragile instrumentation, particularly when measurement is to be done in fields with gravels and stones (Mouazen at al., 2007). Shonk et al. (1991) reported that MC and surface preparation significantly affected the online sensor output. Sudduth and Hummel (1993b) found a 40% standard error

of prediction under laboratory measurement conditions that increased under on-line measurement in the field due to the movement of soil past the sensor during data acquisition. The online soil sensing units developed by Sudduth and Hummel (1993b) and Shibusawa et al. (2003) suffered from inaccuracies in spectroscopic measurements due to problems associated with the variation of soil-to-sensor distance. In another study on the online measurement of soil MC using Vis–NIR spectroscopy based sensor, Mouazen et al. (2005) claimed that they minimized the soil-to-sensor optical unit distance variation. They proved their claim by introducing reasonably similar maps of MC developed by on-line sensor and oven drying method.

Real-time Vis-NIR measurements also have unique concerns related to continuously collecting data while moving across the field. Soil passing the sensor during scanning could cause different wavelengths to be captured at different physical locations (Christy, 2008; Sudduth and Hummel, 1993b). This problem could be overcome by employing an array spectrometer that capture the entire spectrum simultaneously by using a grating to separate the reflected light according to wavelength, and then projected the light onto an InGaAs detector. Scanning type spectrometers, such as the lab-based instrument used in many laboratory basis of spectra scanning measure one wavelength at a time (Bricklemeyer and Brown, 2010). A scanning type spectrometer used on-the-go could degrade accuracy by measuring soil reflectance across different soil scenes as it collects data through the spectrum (Bricklemeyer and Brown, 2010). The scanning nature of the lab-based instrument was a non-issue because soil samples were stationary when interrogated in the laboratory (Bricklemeyer and Brown, 2010).

Real-time Vis-NIR measurement has also introduced additional unique challenges for accurate determination of soil properties compared to the controlled conditions in the laboratory. Natural soil heterogeneity, macro-aggregation, and field moisture content have also been identified as variables that can reduce the predictive accuracy of Vis-NIR methods (Sudduth & Hummel, 1993b; Waiser et al., 2007; Christy, 2008; Morgan et al., 2009). Sensors moving through the soil can also cause inconsistent soil presentation, smearing, and spectral data that are averaged over some distance traveled, dependent on acquisition time and velocity, all of which can degrade accurate Vis-NIR predictions (Morgan et al., 2009; Sudduth and Hummel, 1993b; Waiser et al., 2007).

The rational for the use of real-time soil sensing in agriculture is that although measurements maybe less accurate than those produced by lab-based instrument and measurement, real-time soil sensing facilitates the collection of larger amounts of spatial data using cheaper, simpler and less laborious techniques (Viscarra Rossel at al., 2009). Thus, real-time soil sensing improves the efficiency of soil data collection and provides more information on the patterns of soil variation than lab-based measurement where only few very accurate measurements are used (Viscarra Rossel and Walter, 2004). The large amount of information could be used to generate high-resolution soil properties map which the distribution of soil constituents can be visualized by farm manager for making more precise agronomic decisions. For instance, when a fine resolution of pH requirement is crucial for implementing variable rate liming, the off-line (laboratory basis of spectra scanning) is impractical to generate a high-resolution map for precise of variable rate lime application. This is where a real-time sensing technology plays an important role where the real-time measurement of soil pH could be performed at fine resolution

sampling rate (Tekin et al. 2010). The sampling density could be increased with less time-consuming. Furthermore, real-time measurements are made in situ, providing the information at field conditions and in a timely manner.

Although some limitations particularly in accuracy of the real-time measurement were addressed in earlier studies, several more recent studies have revealed the accuracy improvement in the real-time measurement. Adamchuk et al., (2007) concluded that with certain field conditions, online soil mapping can significantly increase the accuracy of soil pH maps and therefore increase the potential profitability of variable rate liming. Another study by Viscarra Rossel et al. (2009) also reported that the prediction of clay content using the spectra collected in situ was slightly more accurate than those using the laboratory-collected spectra. The more recent studies have proven that the accuracy of real-time measurement of soil constituents cannot be underestimated and there is always a room for improvement. The reliability and robustness of the real-time measurement of soil properties could be further improved by taking into account several factors such as increases in number of samples for developing the model so that it covers as much of the soil variation as possible at wider geographical area and incorporate samples and spectra from several depth of the fields.

### 1.2.6 Chemometrics for Data Analysis

Soil Vis–NIR spectra are largely non-specific, quite weak and broad due to overlapping absorptions of soil constituents and their often small concentrations in soil. Therefore, the information need to be mathematically extracted from the spectra so that they may be correlated with soil properties. Hence, the analysis of soil reflectance or absorbance spectra requires the use of chemometric techniques and

multivariate calibration (Martens and Naes, 1989). In these cases, to be useful quantitatively, spectra must be related to a set of known reference samples through a calibration model.

The spectra need to be pretreated prior to the multivariate calibration analysis because the spectral data contain a great deal of physical and chemical information which cannot be extracted straightforwardly for two reasons, one intrinsic and the other practical (Ozaki et al., 2007). The intrinsic reason is because Vis-NIR spectra consist of number of band arising from overtones and combination modes overlapping with each other causing multicollinearity (Ozaki et al., 2007). The practical reason is appears because Vis-NIR spectroscopy often involves "real-world" samples which may produce relatively poor signal-to-noise ratios, baseline fluctuations and severe overlapping band due to the various components present (Ozaki et al., 2007). To overcome those two difficulties, spectral pretreatment or preprocessing is needed.

#### *1.2.6.1 Spectra Pretreatment*

The spectral data should be pretreated before any statistical analysis is carried out. This is due to by the fact that pretreated spectral data may improve the Vis-NIR prediction accuracy (Barnes et al., 1989). Many available software packages for instance Unscrambler, MATLAB and SpectraPro can be used for spectral preprocessing and data reduction. Some of the common processes of spectral pretreated are waveband filtering, spectra smoothing, data reduction and derivative transformation

Noisy regions may occur at the edges of a spectrum even though the sensor is placed close to the object. Mouazen et al. (2005) removed edges of noisy regions so spectra data collected at 306.5-1710.9 nm were reduced to 401.4-1699 nm. Kodaira and Shibusawa (2013) also removed the left and right ends of the spectra from the original spectra of 350-1700 nm and reduced to 500-1600 nm.

The original Vis-NIR spectra are rich in information but highly repetitive or heavily over-sampled with a highly degree of correlation between many neighboring bands. This data redundancy can be reduced by data reduction. One of the simplest methods of data reduction is by averaging several adjacent spectral points. Chang and Laird (2002) collected spectral samples from 1100-1498 nm with 2-nm interval and reduced spectral data into 140 new data by averaging 5 adjacent spectral points, so one data point represents a 10-nm interval. Kodaira and Shibusawa (2013) used the interpolation method to convert the absorbance spectra to 5-nm-interval and formed 220 new spectral data.

After the noise removal at the edges of the spectra and the subsequent data reduction, the spectra need to be transformed in order to eliminate specific interferences. The interferences are such as light scattering caused by particle size distribution, and path length differences, large baseline variations, and overlapping peaks (Kusumo, 2009). Some of spectra transformation techniques are first or second derivative (Savitzky and Golay, 1964), maximum normalization, standard normal variate and detrending (SNV-D: Barnes et al., 1989) and multiplicative scatter correction (MSC: Martens and Naes, 1989). The derivative with Savitzky-Golay method is the most common used of spectra transformation technique as this technique allows useful and rapid calculation of smoothed derivatives (Brereton, 2003). Previous studied have successfully used this

technique to transform the spectral for prediction of numerous soil properties (Scheinost et al., 1998; Malengreau et al., 1996; Reeves III and McCarty, 2001; Brown et al., 2005; Kodaira and Shibusawa, 2013). Thus, the second derivative with Savitzky-Golay method was chosen as spectral pretreatment technique in this study.

### *1.2.6.2 Multivariate Statistical Analysis for Calibration and Validation*

The Vis-NIR pretreated spectra must be related to a set of known reference samples through a calibration model. The set of reference samples used in the models need to be representative of the range of soils in which the models are to be used. Several statistical methods have been used to establish the relationship between the pretreated spectra with a set of known reference samples such as principle component regression (PCR) (Chang et al., 2001; Christy, 2008), partial least square regression (PLSR) (Mouazen et al., 2005; Bricklemeyer and Brown, 2010; Kodaira and Shibusawa, 2013; Tekin et al., 2013), stepwise multiple linear regression (Dalal and Henry, 1986), artificial neural networks (ANN) (Daniel et al., 2003), multivariate adaptive regression splines (MARS) (Shepherd and Walsh, 2002), boosted regression trees (Brown et al., 2006), PLSR with bootstrap aggregation (bagging-PLSR) (Viscarra Rossel, 2007), support vector machines SVM and penalised spline signal regression (Stevens et al., 2008), multiple regression analysis (MRA) (Ben-Dor and Banin, 1995), stepwise multiple linear regression (SMLR) (Shibusawa et al., 2001) radial basis function networks (RBFN) (Fidêncio et al., 2002).

Amongst of these statistical methods, partial least squares regression (PLSR) are the most common algorithm used to calibrate Vis-NIR spectra to soil properties (Wold et al., 1983; Cheng and Wu, 2006). It is used to construct predictive models when there are many predictor variables that are highly collinear. Both PLSR and PCR compress the data prior to performing the regression. However, unlike PCR, the PLSR algorithm integrates the compression and regression steps and it selects successive orthogonal factors that maximize the covariance between predictor and response variables. The number of factors to use in the models is selected by cross validation. By fitting a PLSR model, one hopes to find a few PLSR factors that explain most of the variation. PLSR is generally characterized by high computational and statistical efficiency and offers great flexibility and versatility in its handling of analysis problems (Boulesteix and Stimmer, 2007). It takes advantage of the correlation that exists between the spectra and the soil, thus the resulting spectral vectors are directly related to the soil attribute (Geladi and Kowalski, 1986). Further advantages of the PLSR are that it handles multicollinearity, robust in terms of data noise and missing values and it performs the decomposition and regression in a single step. Therefore, PLSR was chosen as multivariate statistical method for development of soil properties' calibration model in this study.

PLSR is a method to relate a matrix X (predictor variables) to a vector y (response variables). The x-variables (the 221 spectra data) are transformed into a set of a few latent variables or factors/components. These new variables are used for regression with a dependent variable y (the reference values from laboratory analysis). PLSR is linear method and therefore, the final latent variable that predicts the modeled property, y, is a linear combination of the original variables.

The goal of PLSR is to find a linear relation between x- and y-variables using an regression coefficient, b of and on error term or residual, e as follows;

$$y = Xb + e \quad (1)$$

Resulting model predicts a property y from the original dependent variables $x_1$ to $x_m$. The linear model contains regression coefficients b1 to bm and an intercept $b_0$.

The ability of the PLSR model to predict the soil properties is usually assessed using the coefficient of determination ($R^2_{val}$) of the linear regression of predicted against measured value and root mean square error of prediction or validation ($RMSE_{val}$). $R^2_{val}$ measures the proportion of the total variations accounted for by the model when using cross-validation. $RMSE_{val}$ is the standard deviation of the difference between the measured and the predicted values of soil properties. $RMSE_{val}$ is calculated from the validation dataset using the following equation (Brereton, 2003).

$$RMSE_{val} = \frac{\sqrt{\sum_{i=1}^{n}(y_m - y_{cv})^2}}{n} \quad (2)$$

Where $y_m$ is the measured laboratory value and $y_{cv}$ is the predicted value using cross-validation in PLSR and n is the number of samples. Another parameter that is commonly used to assess the model accuracy is ratio of prediction to deviation (RPD) which is the ratio of the standard deviation of measured values of soil properties to the $RMSE_{val}$ denoted as in following equation (Chang, et al. 2001; Cozzolino et al,. 2005; Mouazen et al., 2006)

$$\mathrm{RPD} = \frac{\mathrm{SD}(y_m)}{\mathrm{RMSE}_{val}} \quad (3)$$

Where $SD(y_m)$ is the standard deviation of measured values. As reported by Williams and Norris (2001), RPD is the most useful statistic when evaluating the analytical efficiency of calibration models. It is also the statistically least sensitive to an increase in range by a few large values (Malley et al., 2004). The best prediction model is shown by the highest $R^2_{val}$ and RPD with lowest $RMSE_{val}$ (Kusumo et al., 2008).

### 1.2.7 Soil Spatial Variability Mapping

The global positioning system (GPS) receivers, used to locate and navigate agricultural vehicles within a field, have become the most common sensor in precision agriculture. When a GPS receiver and a data logger are used to record the position of each soil sample and/or spectra measurement, a map can be generated and processed along with other layers of spatially variable information. This method is frequently called a “map-based” approach (Adamchuk et al., 2004).

The soil properties amount either measured by laboratory analysis (measured value) or predicted on the spectra collected using soil sensor (predicted value) are commonly presented in map as to clearly visualize the spatial variability of the field with the integration of GPS data. Growers would be able to make agronomic decision based on the distribution of the soil properties presented on the map. Furthermore, comparison of the temporal carbon map for a period of time (several years) could assist the carbon inventories proses in carbon farming practice.

A standard method for creating soil properties maps is to assign the measured or predicted values on the targeted location using a grid sampling scheme (Kravchenko and Bullock 1999). Then, the soil map can be made by interpolating the soil property either measured or predicted values. Interpolation is the procedure of predicting the value of attributes at unsampled sites from measurements made at point locations within the same area (Karydas et al., 2009). Interpolation is used to convert data from point observations to continuous fields so that the spatial patterns sampled by these measurements can be compared with spatial patterns of other spatial entities. The rationale behind spatial interpolation is the very common observation that, on average, values at points close together in space are more likely to be similar than points further apart (Karydas et al., 2009). Among spatial interpolation methods, one can find Radial Basis Functions (RBF), Inverse Distance Weighting (IDW), and Kriging techniques (Burrough and Macdonnell, 1998). The two latter interpolation methods are most commonly used for agriculture soil mapping (Franzen and Peck, 1995; Weisz et al., 1995). Many previous studies have evaluated and compared the performance of these two methods for mapping soil properties (Weber and Englund, 1992; Wollenhaupt et al., 1994; Gotway et al., 1996; Karydas et al., 2009). They found that IDW method to be more accurate than kriging method for mapping of soil P and K (Wollenhaupt et al., 1994), SOM and $NO_3$ (Gotway et al., 1996; Karydas et al., 2009). Both methods estimate values at unsamples locations based on the measurements from the surrounding locations with certain weights assigned to each of the measurements. IDW method is however easier to implement, while kriging method is more time-consuming and cumbersome (Kravchenko and Bullock 1999). Thus, IDW method was chosen for developing soil map in this study.

## 1.3 Aims and Objectives

Numerous techniques and approaches have been addressed in previous study of utilizing Vis-NIR spectroscopy for measurement of soil properties either lab-based spectra measurement or in real-time. However there are still many aspects that need to be improved as to optimize the used of Vis-NIR soil sensor for mapping of soil properties towards better agriculture management either in precision agriculture or precision carbon farming. Hence, in light of preceding background and literature reviews, the ultimate aim of this study is to recommend an improved techniques and function of agricultural soil mapping using Vis-NIR real-time soil sensor as to optimize the used of this state-of-the-art technology. The precision agriculture and precision carbon farming practices can implement this goal for better agriculture production with minimal unintended environmental effects. Basically, this study intended to achieve the following objectives;

1. To investigate the potential of a Vis-NIR real-time soil sensor for mapping of paddy soil properties at multiple soil depths
2. To demonstrate the potential of Vis-NIR real-time soil sensor for high-resolution mapping of up to 24 paddy soil properties.
3. To describe the feasibility of integrated calibration model developed from three agriculture fields and compare with local model for mapping of soil properties

## 1.4 Thesis Structure

This thesis is divided into five chapters. The first chapter is the Introduction which described the background issues, literature reviews and objectives of this study. This chapter also described the chronology of the soil sensing development, methods that crucial for measurement of soil properties by means of spectroscopy and basic knowledge

on chemometrics technique. The second chapter is on the mapping of multiple-depth soil properties using Vis-NIR real-time soil sensor and the importance of this multiple-depth map for making agronomic decisions. The third chapter discussed on the development of high-resolutions maps for 24 soil properties. The fourth chapter discussed the development of integrated calibration model for prediction of agriculture soil properties and its predictions performance. Finally, the fifth chapter is summary and conclusion which also addressed some suggestions for future research.

# Chapter 2

## Multiple-Depth Soil Mapping of a Paddy Field

**ABSTRACT**

In describing soil variability, information on the distribution of soil properties is required in both the horizontal and vertical directions. This study investigated the potential of a real-time soil sensor (RTSS) for mapping six soil properties at multiple soil depths of a paddy field. Soil spectra were acquired at three depths using RTSS. Three calibration models were developed. The first model (CM1) combined the dataset for depths of 10 and 15 cm, the second model (CM2) combined the dataset for depths of 15 and 20 cm, and the third model (CM3) combined all the three depths. CM3 produced highest coefficient of determination ($R^2_{val}$) and ratio prediction to deviation (RPD) with lowest root mean square error of validation ($RMSE_{val}$) was regarded as the best calibration model for all the soil properties. The generated maps exhibited variations in the distribution of all the soil properties at different depths.

## 2.1 Introduction

The conventional practice of soil quantification often results in under-sampling due to time-consuming, laborious, and costly sampling and analysis, making it impractical for mapping large field areas for precision agriculture purposes. Moreover, the capacity to detect temporal changes of these properties in soil using conventional sampling and analysis techniques is quite limited due to the large spatial variability and slow response of these properties in soil (Stevens et al., 2006). Therefore, an improved and efficient method is required for measuring spatial and temporal variability of soil attributes. One solution to overcome the limitation found in the conventional method of soil sampling and analysis is the adoption of a visible-near infrared (Vis-NIR) sensor that is real time, cost effective and can rapidly measure soil properties.

The real-time measurement of soil properties in many previous studies, however, was only conducted in the horizontal strata (a single depth) whilst ignoring the distribution of soil variability vertically (depth direction). Mouazen et al. (2007) and Kodaira and Shibusawa (2013) generated soil maps at the depth of 15 cm only while Christy (2008) estimated SOM at the depth of 7 cm only. As claimed by Donovan (2012), vertical distribution is important for describing the variability of soil carbon because it is likely to vary with depth. Most soil carbon sampling thus defines one or more layers of soil, usually by the distance in centimeters from the soil surface. Variation in soil compositions including SOM was also found at different depths as reported by Reeves et al. (2002). Even though there are several studies that considered several depths including depths of 10 to 20 cm (Yang et al., 2011), 0 to 20 cm (Viscarra Rossel et al., 2010) and 50 to 105 cm (Ge et al., 2011), the spectra measurements for calibration model development in these studies, however, were laboratory basis which is

again laborious, time consuming and expensive because the samples need to be crushed, sieved and dried prior to spectra scanning. Sarkhot et al. (2011) used a hydraulic soil probe to take soil cores and then separated the soil cores into five depths at increments of 0-10, 10-20, 20-30, 30-40 and 40-50 cm where the soil samples were oven dried before scanning the spectra in the laboratory. Only the map at the depth of 10 cm (single depth) is shown. In another study by Li (2013), the distribution of total carbon and total nitrogen are presented on maps at several depths but the maps were generated based on the laboratory analysis of a small number of samples. The resolutions of the maps were low because they were mapped using the laboratory analysis data only and no spectra were acquired to predict the value of total carbon and total nitrogen. Thus, the objectives of this study were to investigate the potential of a Vis-NIR real-time soil sensor for mapping moisture content (MC), organic matter (SOM), total carbon (C-t), total nitrogen (N-t), hot-water-extractable nitrogen (N-h), and available phosphorus (P-a) of paddy soil at multiple soil depths, and to describe the effect of sensing depth on the mapping of soil properties. The spatial distributions of these six soil properties were observed at three depths of paddy soil that were 10, 15 and 20 cm from the soil surface.

## 2.2 Materials and Methods

### 2.2.1 Experimental Site – organic paddy field in Matsuyama

The field experiment was conducted at an organic paddy field in Matsuyama City of Ehime Prefecture Japan (33º 8’N, 132º 8’E) as shown in Figure 2.1. This site comprises a number of small paddy fields and field no. 437 (58.3 m x 21.7 m) was selected for this study. The experiment was conducted after harvesting the paddy in autumn 2012. The average, maximum and minimum temperature of the day was 20.8,

26.3 and 14.5 ℃, respectively. The soil texture of the field was described according to three depths as follows: 52.82% sand, 24.71% silt and 22.47% clay at a depth of 10 cm, 54.55% sand, 21.02% silt and 24.43% clay at a depth of 15 cm, and 66.29% sand, 11.82% silt and 21.89% clay at a depth of 20 cm.

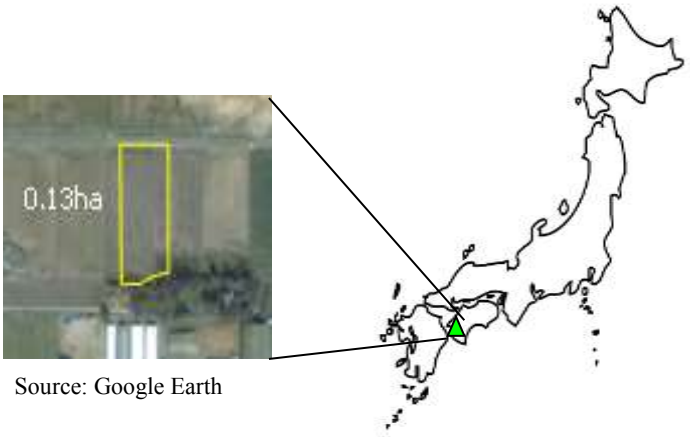


Fig. 2.1 Location of the Matsuyama experimental site.

### 2.2.2 Real-time Soil Sensor (RTSS) – SAS1000

The RTSS used for this study was SAS1000, SHIBUYA MACHINERY Co., Ltd as shown in Fig. 2.2. It is comprises of a sensor unit housing, a touch panel and a soil penetrator with a sensor probe housing. The sensor unit housing consists of a personal computer, Trimble DSM132 differential global positioning system (DGPS) receiver, 150-W Al-coated tungsten halogen lamp as a light source and two spectrophotometers. The one spectrophotometer which is for visible (Vis) spectra (310 to 1150 nm) has a 256-pixel linear diode array, while the other spectrophotometer which is for NIR spectra (900 to 1700 nm), has a 128-pixel linear diode array of multiplexed InGaAs. In the probe housing, two optical fibers were

used to guide the light from the light source (halogen lamp) and illuminate the underground soil surface with an area of about 50 mm in diameter. The underground soil Vis-NIR reflectance spectra were then collected through additional optical fiber probes to the two spectrophotometers. The probe housing is also equipped with a micro CCD camera to capture, record and display images of uniform soil surfaces while the RTSS running across the field. The saved images were then used to provide information for eliminating the dataset from the data analysis. By checking on the saved images, the spectra corresponding to the image that exhibited foreign objects such as stone, plant debris or larvae were identified as outliers for the calibration and prediction process. Next to the CCD camera is a laser distance sensor for monitoring distance variations between the soil surface and the micro optical devices.

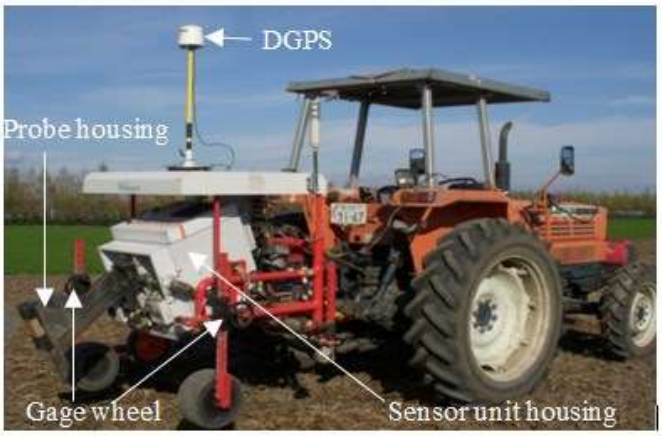


Fig. 2.2 Real-time Soil Sensor SAS1000.

### 2.2.3 Spectra Acquisition and Soil Sampling at Three Depths

The RTSS was designed with gage wheels on both sides that can be adjusted to spacings of 5 cm at depths from 5 cm to 35 cm (Fig. 2.2). In this experiment, the gage wheels were initially adjusted for acquiring spectra at a depth of 10 cm. The

tractor that attached with the RTSS was travelled on four transects at spacings of 5 m and a speed of 0.25 $ms^{-1}$. When the RTSS was running on the track, the soil penetrator tip with a flat plane edge ensured uniform soil cuts and the soil flattener following behind formed a trench with a uniform underground surface. The Vis-NIR reflectance spectra of the underground soil were acquired automatically from the bottom of the trench every 4 s, and this resulted in the Vis-NIR reflectance spectra being sampled at a distance of every 1 m. After the RTSS had completely travelled all four transects, the process was repeated for depths of 15 and 20 cm by adjusting the gage wheels.

While the RTSS was running on the track, a notification lamp was triggered at each data acquisition (every 1 m travelled). The number of spectra data were counted and displayed on the touch panel screen. When the RTSS acquired every $11^{th}$ spectra data (11 m), a wooden stick was inserted into the soil for marking the soil sampling points. Two sets of soil samples were subsequently collected at the trench bottom of twenty wooden sticks' positions and they were packed in sealable plastic bags. This procedure was conducted for depths of 10, 15 and 20 cm. In total, there were two sets of 60 soil samples collected. However, due to the RTSS encountering an obstacle at one point at a depth of 20 cm, invalid spectra were acquired at that particular point. Hence, a soil sample corresponding to that single point was omitted from each set. Finally, only 59 soil samples of each set were collected. Figure 2.3 illustrated the collected spectra scanning line (dotted line) and locations of the sampling point. The green, red and blue fulled circles corresponding to the sampling points locations at the depth of 10, 15 and 20 cm respectively

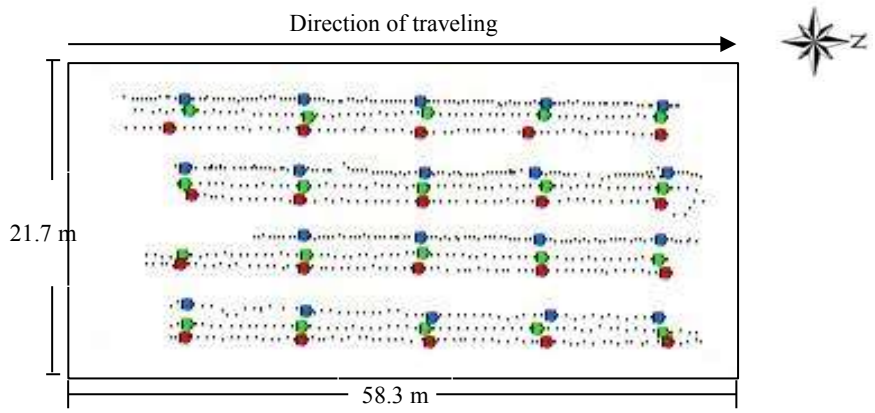


Fig. 2.3. RTSS Scanning line (dotted line) and soil sampling points' position (filled circle), green:10 cm; red:15 cm; blue:20 cm.

### 2.2.4 Soil Chemical Analysis

In order to measure the chemical amount in the soil samples collected at the three depths, one set of the soil samples was transported to the Tokyo University of Agriculture and Technology (TUAT) laboratory for MC and SOM analysis while the other set was transported to the Agricultural Product Chemical Research Laboratory (APCRL: Federation of Tokachi Agricultural Cooperative Association, Hokkaido, Japan) for analysis of C-t, N-t, N-h and P-a.

The first set of 59 fresh soil samples was crushed and sieved through a 2-mm sieve. Debris such as plant material and stones were removed. The samples were then stored in sealable plastic bags at 5 °C until the completion of the chemical analysis. MC was measured in fresh soil samples using the oven-dry method at 110 °C for 24 h while SOM was measured in dried soil samples that were sieved through a 1-mm sieve and burnt in a muffle furnace at 750 °C for 3 h. Each soil analysis was conducted three times, and the average values were adopted as a reference values for the multivariate statistical analysis.

The second set of 59 soil samples transported to APCRL were analyzed for C-t, N-t, N-h and P-a by APCRL using the standard procedures in the Hokkaido area in Japan (Souma and Kikuchi, 1992). This set of soil samples was also dried, crushed and sieved. The soil analysis methods and instruments that were used for analysis of the six chemical properties are given in Table 2.1.

Table 2.1 Soil analysis methods and instruments.

| Soil Properties | Analysis Method | Instrument |
|---|---|---|
| MC | Oven Dry | DK610Yamato |
| SOM | Ignition Combustion | FM28Yamato |
| C-t | Tyurin's Method | NC-220F, SUMIGRAPH |
| N-t | Kjeldahl Method | NC-220F, SUMIGRAPH |
| N-h | Absorptiometry | QUAATRO, BRAN+LUEBBE |
| P-a | Absorptiometry | QUAATRO, BRAN+LUEBBE |

### 2.2.5 Calibration Model Development and Three Depths Mapping

Prior to the development of calibration models, all collected underground Vis-NIR soil reflectance spectra using the RTSS in the organic paddy field were converted to absorbance with white reference spectra using the standard reflector (Spectralon, Labsphere Inc.) and dark reference due to light shielding, and using Beer-Lambert's law (William and Norris, 2001) as described in Equation 3,

$$\text{Absorbance spectra} = log_{10}(R_{white} - R_{dark}) - log_{10}(R - R_{dark}) \quad (3)$$

$R_{white}$ = white reflectance spectra using the standard reflector

$R_{dark}$ = dark reflectance spectra due to light shielding

R = reflectance spectra of underground soil surface

The absorbance spectra were then converted to 5-nm-interval data by the interpolation method using Data Monitor Software (Shibuya Seiki Co., Ltd.). The spectra of original absorbance ranged from 350 to 1700 nm. To enhance weak signals and remove noise due to diffuse reflection, the absorbance spectra were pre-treated using the second-derivative Savitzky and Golay method. Moreover, both edges of the spectra were removed as these parts of the spectra were unstable and rich in noise. The calibration models were subsequently developed by applying the partial least-square regression (PLSR) technique coupled with full cross-validation to establish the relationship between the amount of soil properties obtained by chemical analysis (reference values) with the pretreated Vis-NIR soil absorbance spectra from the corresponding locations. The spectra pretreatment and calibration model development were done using Unscrambler X10.2 software.

For each soil property, three calibration models were developed. The first model (CM1) combined the dataset (spectra and reference values) for depths of 10 cm and 15 cm, the second model (CM2) combined the dataset for depths of 15 cm and 20 cm, and the third model (CM3) combined the dataset for all three depths. In the PLSR analysis, sample outliers were detected by checking the residual sample variance plot after the PLSR. Individual sample outliers located far from the zero line of residual variance were considered to be outliers and excluded from the analysis. In this study, one sample was selected as a sample outlier at one time up to four times for CM1 and CM2, and six times for CM3. In total, four sample outliers were removed for CM1 and CM2, and six outliers for CM3.

The performance of the three calibration models for each soil property was assessed based on the value of the coefficient of determination ($R^2_{val}$), root mean

square error of prediction ($RMSE_{val}$) and residual prediction deviation (RPD) produced from the PLSR analysis. In this study, RPD was classified according to category, which means the properties of the full cross-validation ability of PLSR in this study. Values of RPD larger than 2.0 were considered as excellent, between 1.4 and 2.0 were good and below 1.4 were unreliable (Chang et al., 2001). The best calibration model that possesses maximum $R^2_{val}$ and RPD but minimum $RMSE_{val}$ in the regression analysis for each soil property was then used to provide quantitative prediction and mapping of the respective soil properties at three depths using ArcGIS Ver. 10.0 software. The soil maps were interpolated using the inverse-distance weighting (IDW) method.

## 2.3 Results and Discussions

### 2.3.1 Performance of the Calibration Models on Different Depths

The raw absorbance Vis-NIR spectra and pretreated with $2^{nd}$ derivative Savitzky-Golay spectra were depicted in Figure 2.4. Both edges of the raw absorbance Vis-NIR were removed as these parts of spectra were unstable and rich in noise. Therefore, the wavelength of the Vis-NIR spectra that used for developing the calibration models were at range of 500 to 1600 nm. In order to obtain the best calibration model for each of the soil property, the PLSR were performed on spectra that were pretreated with second derivative Savitzky-Golay method with several number of smoothing points. These pretreated spectra were regressed with the reference values obtained from the laboratory soil analysis to generate several calibration models. The calibration models that produced the highest $R^2_{val}$ with

lowest $RMSE_{val}$ were chosen as the best calibration models for each of the soil property.

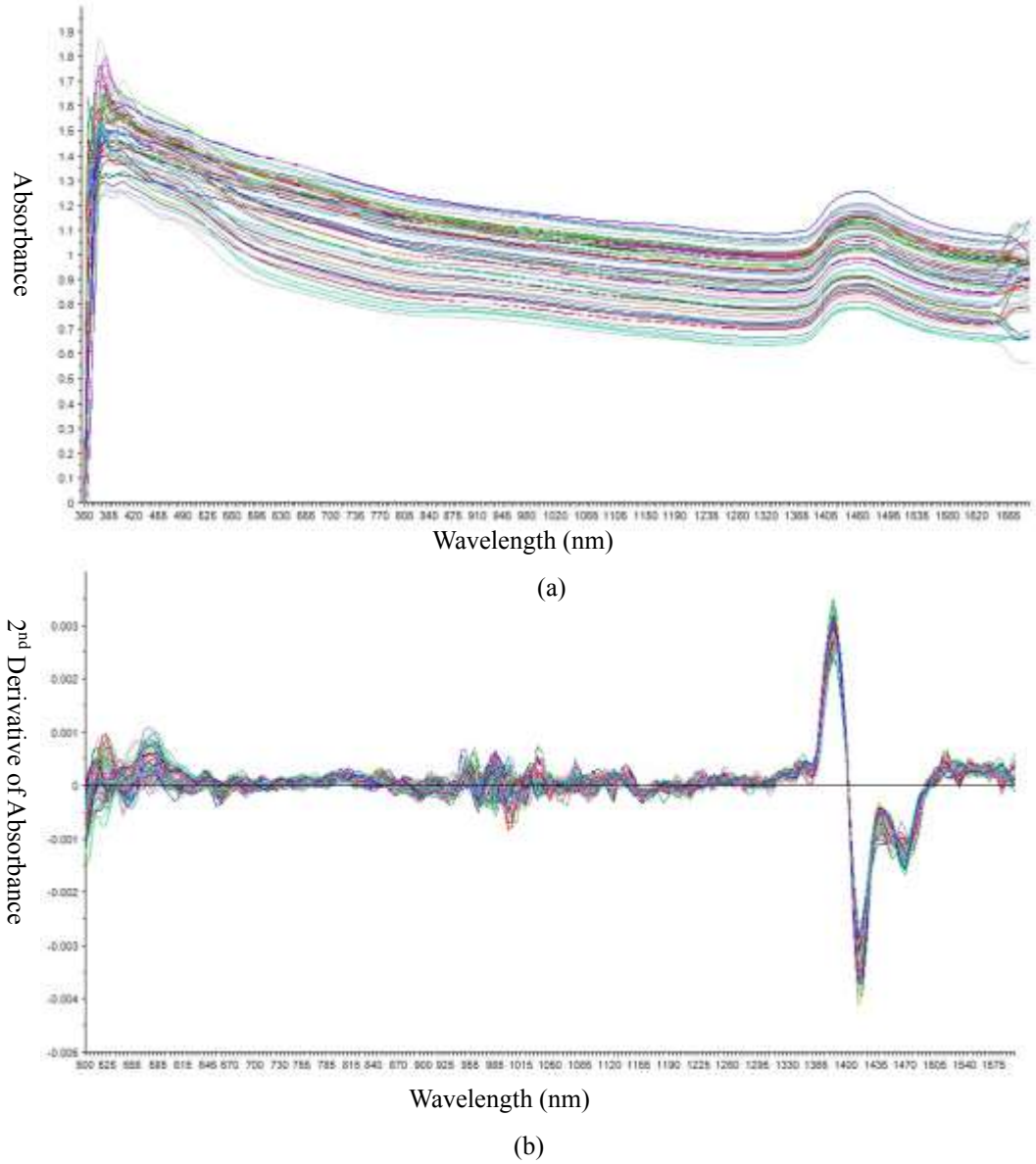


Fig. 2.4 Absorbance spectra for developing the calibration model (a) original absorbance spectra, (b) pretreated using 2nd derivative absorbance spectra.

PLSR results of the calibration and validation were obtained as shown in Table 2.2. Based on the determination of coefficient ($R^2_{val}$) and root mean square

error of validation ($RMSE_{val}$), CM3 that combined datasets of all three depths resulted in the highest accuracy for MC, SOM, C-t, N-t and N-h with $R^2_{val}$ and $RMSE_{val}$ of 0.88 and 1.38 for MC, 0.83 and 0.26 for SOM, 0.88 and 0.15 for C-t, 0.85 and 0.01 for N-t, and 0.87 and 0.43 for N-h. For P-a, however, both CM2 and CM3 showed the same level of accuracy with both $R^2_{val}$ being 0.72, but the $RMSE_{val}$ for CM3 (4.53) was lower than CM2 (4.74). CM1 produced the lowest accuracy amongst the three calibration models of all the six soil properties.

Table 2.2 Summary of PLSR results for three calibration models of each soil property.

| Soil Properties | Calibration Dataset[a] | N[b] | Calibration | | Validation | | SD | RPD |
|---|---|---|---|---|---|---|---|---|
| | | | $R^2_{cal}$ | $RMSE_{cal}$ | $R^2_{val}$ | $RMSE_{val}$ | | |
| MC [%] | CM1 | 35 | 0.76 | 1.28 | 0.64 | 1.62 | 2.66 | 1.6 |
| | CM2 | 36 | 0.85 | 1.08 | 0.75 | 1.47 | 2.88 | 2.0 |
| | CM3 | 53 | 0.95 | 0.85 | 0.88 | 1.38 | 3.95 | 2.9 |
| SOM [%] | CM1 | 35 | 0.70 | 0.19 | 0.51 | 0.25 | 0.36 | 1.4 |
| | CM2 | 36 | 0.83 | 0.20 | 0.71 | 0.27 | 0.50 | 1.9 |
| | CM3 | 53 | 0.87 | 0.23 | 0.83 | 0.26 | 0.63 | 2.4 |
| C-t [%] | CM1 | 35 | 0.52 | 0.12 | 0.39 | 0.13 | 0.17 | 1.3 |
| | CM2 | 36 | 0.94 | 0.10 | 0.87 | 0.14 | 0.39 | 2.8 |
| | CM3 | 53 | 0.91 | 0.13 | 0.88 | 0.15 | 0.43 | 2.9 |
| N-t [%] | CM1 | 35 | 0.46 | 0.01 | 0.33 | 0.01 | 0.01 | 1.0 |
| | CM2 | 36 | 0.91 | 0.01 | 0.80 | 0.01 | 0.03 | 3.0 |
| | CM3 | 53 | 0.88 | 0.01 | 0.85 | 0.01 | 0.03 | 3.0 |
| N-h [mg $(100g)^{-1}$] | CM1 | 35 | 0.55 | 0.44 | 0.44 | 0.50 | 0.66 | 1.3 |
| | CM2 | 36 | 0.88 | 0.30 | 0.81 | 0.39 | 0.89 | 2.3 |
| | CM3 | 53 | 0.90 | 0.38 | 0.87 | 0.43 | 1.17 | 2.7 |
| P-a [ mg $(100g)^{-1}$] | CM1 | 35 | 0.66 | 2.69 | 0.40 | 3.66 | 4.67 | 1.3 |
| | CM2 | 36 | 0.80 | 3.90 | 0.72 | 4.74 | 8.87 | 1.9 |
| | CM3 | 53 | 0.87 | 3.02 | 0.72 | 4.53 | 8.50 | 1.9 |

[a]Combination datasets. CM1: 10 and 15 cm depths, CM2: 15 and 20 cm depths, CM3: 10, 15 and 20 cm depths

[b]Number of samples used in the model.

Referring to the accuracy classification by Chang et al. (2001), CM2 and CM3 proved to be excellent calibration models for MC, C-t, N-t and N-h with all of the RPD for these soil properties above 2.0. For SOM, only CM3 is regarded as excellent while CM2 is classified as good (1.4 < RPD < 2.0). CM2 and CM3 for P-a

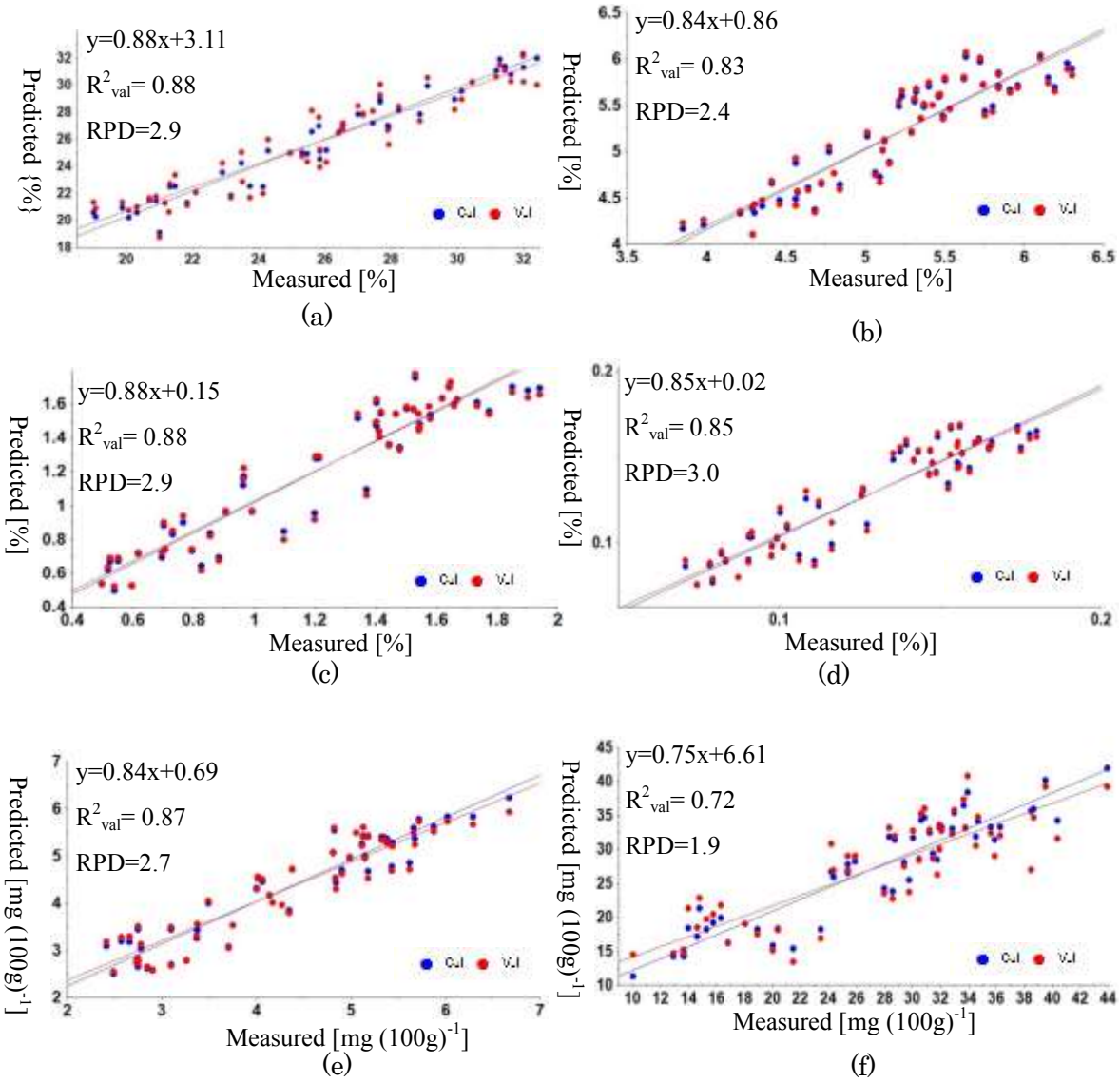


Fig 2.5 Scatter plot of measured value versus Vis-NIR predicted values of CM3 datasets using PLSR for (a) MC, (b) SOM, (c) C-t, (d) N-t, (e) N-h and (f) P-a

are also classified as good calibration models. CM1 for MC and SOM showed good models while for the other four properties are classified as unreliable (RPD < 1.4). The results of this study indicated that the combination of the calibration dataset for three depths gave a wider range of dataset and resulted in better prediction accuracy of MC, SOM, C-t, N-t, N-h and P-a. Hence, CM3 of each soil property was used to provide quantitative prediction and mapping of the respective soil properties. Scatter plots of the CM3 models are depicted in Figure 2.5.

### 2.3.2 Three Depths Soil Maps

The values of soil properties for 265 spectral collected at a depth of 10 cm, 270 spectral at a depth of 15 cm and 377 spectral at a depth of 20 cm were predicted using calibration model CM3 of the respective soil properties. These predicted values were used to draw prediction maps at three depths as illustrated in Figure 2.6. The generated maps clearly show that the distribution of all six soil properties varied both horizontally and also in depth. At the depth of 10 cm exhibited the highest concentration of all six soil properties, followed by a diminishing pattern at deeper soil depths. The results of C-t, N-t and SOM qualitatively agreed with a previous study using laboratory analysis (Li et al., 2012) and using lab-based spectra acquisition on dried soil (Reeves et al., 2002; Xie et al., 2011).

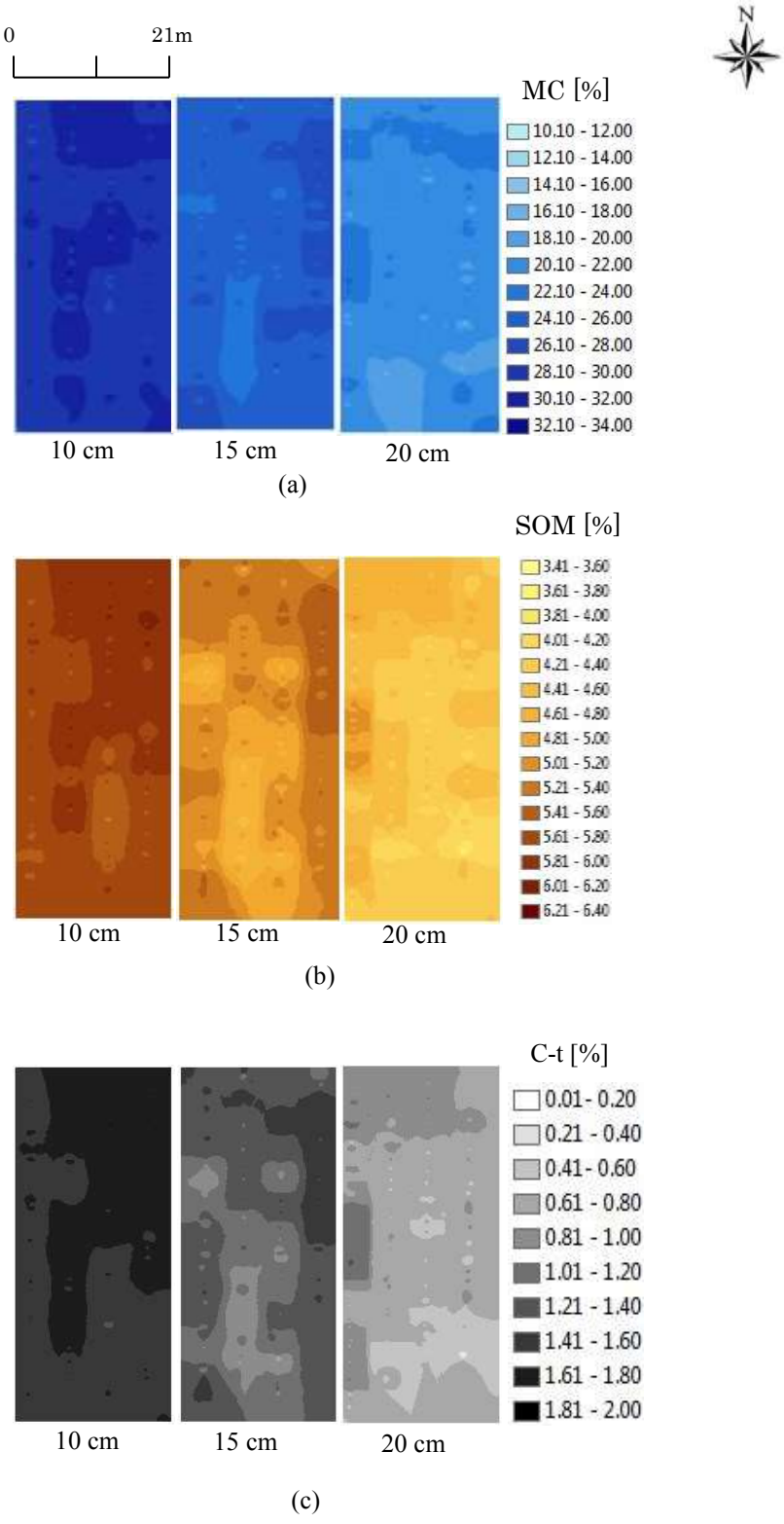


Fig. 2.6. Soil maps for three depths predicted using CM3 for (a) MC, (b) SOM, (c) C-t, (d) N-t, (e) N-h and (f) P-a

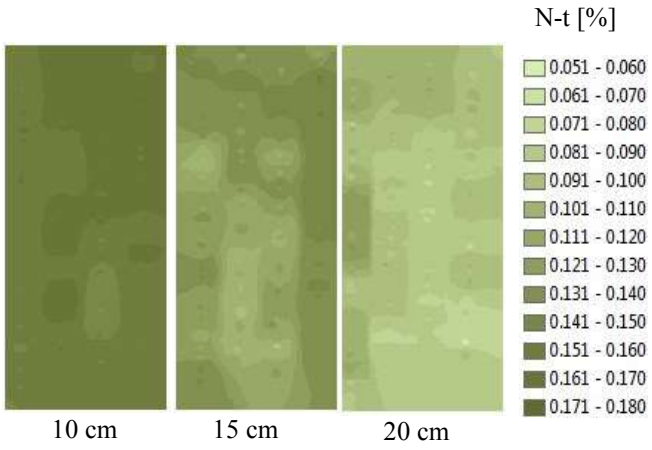


(d)

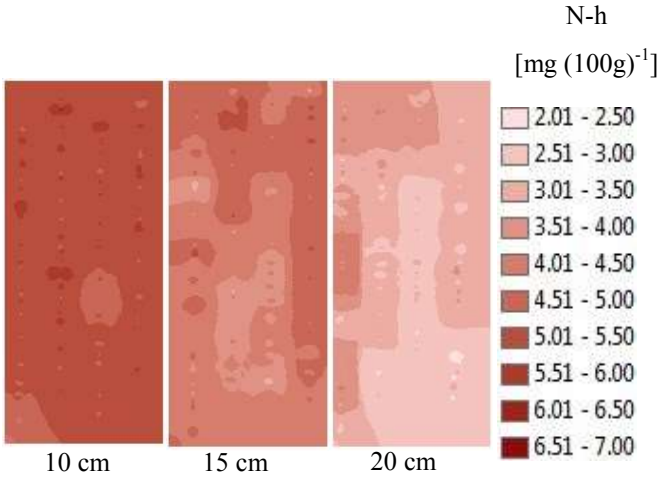


(e)

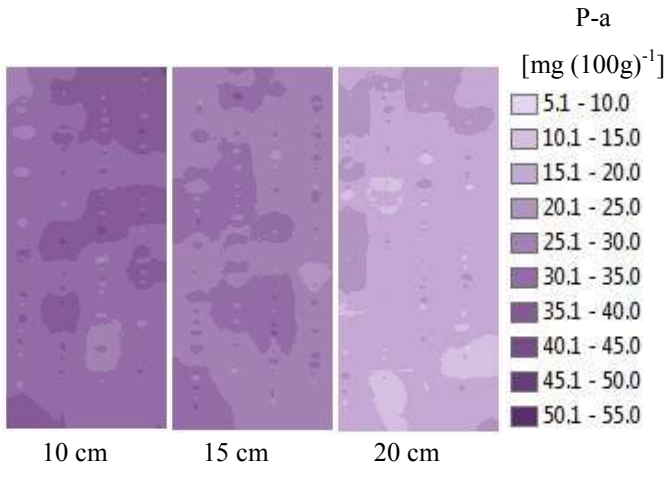


(f)

Fig. 2.6. (Continued)

### 2.3.3 Importance of Multiple-depth Soil Mapping

Since it was found that the distribution of the soil properties also varied at different soil depths, the effect may differ if the distribution of the soil properties was just considered at a single depth. For example, by referring to the N-t map in Figure 2.6 (d), it can be seen there are some areas with low nitrogen content at a depth of 15 cm but high nitrogen content at a depth of 10 cm. If a grower makes an observation at a depth of 15 cm only, he might tend to put more fertilizer on the area of paddy field that contains low or insufficient nitrogen. This inadvertently leads to excessive nitrogen application if that particular area with less nitrogen at a depth of 15 cm was actually contains high or sufficient nitrogen at a depth of 10 cm. Therefore, from this study, it can be suggested that several depths of soil variability observation need to be considered and growers need to determine at what depth (optimum depth) should be observed for specific soil management in precision agriculture practice. Besides its potential for producing high-resolution soil distribution maps at multiple depths, the use of Vis-NIR RTSS could constantly maintain the observation depth by adjusting the gage wheel. This may eliminate poor reproducibility due to inconsistency of soil sampling by manual labor at several depths as mentioned by Kanda (2011).

## 2.4 Summary and Conclusion

Three spectroscopic calibration models have been developed for MC, SOM, C-t, N-t, N-h and P-a using Vis-NIR spectra acquired at three depths by the RTSS. The CM3 produced the highest accuracy of all the examined soil properties and hence, it was used to predict the amounts of soil properties at three depths. The generated maps

exhibited variation in the distribution of MC, SOM, C-t, N-t, N-h and P-a not only horizontally but also at different depths. Furthermore, the incorporation of multiple soil depths maps for MC, SOM, C-t, N-t, N-h and P-a provided comprehensive information on soil variability for making precisions agronomic decisions. Hence, the Vis-NIR real-time soil sensor has great potential for determining the soil properties at multiple soil depth.

# Chapter 3

# Mapping of Twenty-Four Paddy Soil Properties

**ABSTRACT**

This chapter describes the potential of a visible-near infrared (Vis-NIR) real-time soil sensor (RTSS) to predict and map 24 paddy soil properties. The Vis-NIR reflectance spectra of fresh soil were acquired at four fields using the RTSS SAS2500. Fresh soil samples were also collected at each field along the RTSS's tramline for analysis of moisture content (MC), soil organic matter (SOM), pH, electrical conductivity (EC), cation exchange capacity (CEC), total carbon (C-t), total nitrogen (N-t), ammonium nitrogen (N-a), hot water extractable nitrogen (N-h), nitrate nitrogen (N-n), available phosphorus (P-a), exchangeable calcium (Ca), exchangeable potassium (K), exchangeable magnesium (Mg), hot water soluble soil boron (B), soluble copper (Cu), easily reducible manganese (Mn), soluble zinc (Zn), phosphate absorption coefficient (PAC), calcium saturation percentage (CSP), base saturation percentage (BSP), bulk density (BD), ratio of magnesium to potassium (Mg/K) and ratio of calcium

to magnesium (Ca/Mg) in the laboratory. Calibration models were then developed for each soil property using the partial least square regression (PLSR) technique coupled with full cross-validation to establish the relationship between the Vis-NIR soil spectra and the reference values obtained by the laboratory analysis. The 24 calibration models were then used to provide quantitative predictions and mapping of the 24 soil properties respectively. The coefficient of determination ($R^2_{val}$) ranged from 0.43 to 0.90. Of these 24 soil properties, 8 soil properties' models were categorized as excellent, 14 as good and 2 as unreliable based on their residual prediction deviation (RPD) values. Reasonable similarity exhibited between the measured and predicted maps is sufficient to declare that the Vis-NIR real-time soil sensor measurement system has potential to be used for the real-time measurement of numerous soil properties.

## 3.1 Introduction

There is wide spread interest for using visible–near infrared (Vis–NIR) diffuse reflectance spectroscopy for soil analysis and to provide data for digital soil mapping. The technique is rapid, cost effective, requires minimal sample preparation, can be used in situ (Viscarra Rossel et al., 2009), is non-destructive, no hazardous chemicals are used, and importantly, several soil properties can be measured from a single scan (Viscarra Rossel et al., 2006b). This multi-parameter feature of diffuse reflectance spectroscopy implies that one spectrum holds information about various soil constituents and indeed, vis–NIR spectra are sensitive to both organic and inorganic soil composition (Viscarra Rossel and Behren, 2010).

The soil properties that can be determined based on a single scan action using a single instrument system in previous studies are limited to just several numbers of soil

properties. The study by Kodaira and Shibusawa (2014a, 2014b, 2014c) reported on mapping up to 25 soil properties for upland agriculture fields. To the best of knowledge at the time of writing, it was found that this is the largest number of soil properties that can be measured from a single scan of Vis-NIR spectra, using a single sensor system. However, the performances of those calibration models and comparison between measured and predicted maps in this previous study were not discussed in detail. The objective of this study is therefore to demonstrate the potential of Vis-NIR RTSS for the mapping of up to 24 soil properties for a paddy field. The investigated soil properties were moisture content (MC), soil organic matter (SOM), pH, electrical conductivity (EC), cation exchange capacity (CEC), total carbon (C-t), total nitrogen (N-t), ammonium nitrogen (N-a), hot water extractable nitrogen (N-h), nitrate nitrogen (N-n), available phosphorus (P-a), exchangeable calcium (Ca), exchangeable potassium (K), exchangeable magnesium (Mg), hot water soluble soil boron (B), soluble copper (Cu), easily reducible manganese (Mn), soluble zinc (Zn), phosphate absorption coefficient (PAC), calcium saturation percentage (CSP), base saturation percentage (BSP), bulk density (BD), ratio of magnesium to potassium (Mg/K) and ratio of calcium to magnesium (Ca/Mg). Our aimed in this study was to provide as much information as possible on paddy soil properties that can be derived from a single scan of Vis-NIR spectra in real-time.

## 3.2 Materials and Methods

### 3.2.1 Experimental Site – inorganic paddy field Yamatsuri

The field experiment was conducted at an inorganic paddy farm in Yamatsuri City of Fukushima Prefecture in Honshu Island (36°52’ N, 140°25’ E)

(Figure 3.1). The average, maximum and minimum temperatures of the day were 7.9, 10.9 and 4.9 ℃, respectively. The experiment was conducted after the paddy harvesting season in early winter 2013. Four fields selected for this study were Field 1 (0.26 ha, 26.0 x 101.5m), Field 2 (0.29 ha, 29.0 x 100.0 m), Field 3 (0.18 ha, 28.0 x 62.8 m) and Field 5 (0.41 ha, 42.0 x 97.1 m). The soil texture of the four fields is described as follows: 71.4% sand, 9.3% silt and 19.3 % clay for Field 1, 66.0% sand, 13.6% silt and 20.4% clay for Field 2, 63.7% sand, 14.4% silt and 21.9% clay for Field 3, 62.1% sand, 16.2% silt and 21.7% clay for Field 5.

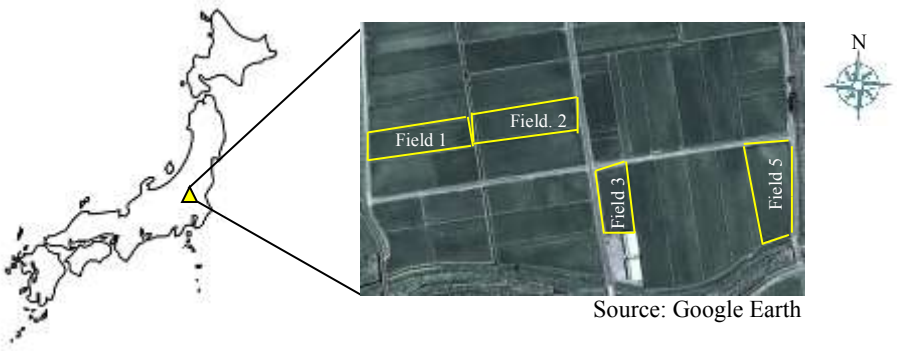

Source: Google Earth

Fig. 3.1 Location of the Yamatsuri experimental site.

### 3.2.2 Real-time Soil Sensor – SAS25000

The RTSS used for this study was SAS2500, SHIBUYA MACHINERY Co., Ltd. as shown in Figure 3.2. It is comprised of a sensor unit, a touch panel and a soil penetrator with a sensor probe housing. The sensor unit consists of a personal computer, Trimble DSM132 single global positioning system (DGPS) receiver, 150-W Al-coated tungsten halogen lamp as a light source and two mini spectrophotometers by Hamamatsu. The first mini spectrophotometer is C10083CAH, a high resolution (2048-pixels) spectrophotometer for visible (Vis) spectra (320 to 1000 nm) with back-thinned type CCD image sensor as a detector, while the second

mini spectrophotometer is C9406GC with 512-pixels which used InGaAs linear image sensor for NIR (900 to 1700 nm) detection. In the probe housing, two optical fibers were used to guide the light from the light source (tungsten halogen lamp) and illuminate the underground soil surface with an area of about 50 mm in diameter. The underground soil Vis-NIR reflectance spectra were then collected through additional optical fiber probes to the two mini spectrophotometers. The probe housing is also equipped with a micro video camera to capture and record the video of the uniform soil surfaces while the RTSS runs across the field. Next to the video camera is a laser distance sensor for monitoring distance variations between the soil surface and the micro optical devices.

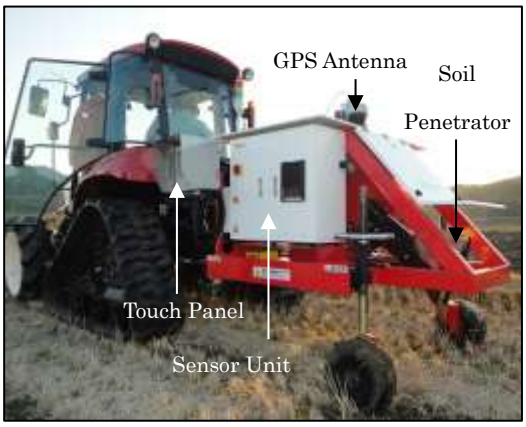


Fig. 3.2 Real-time Soil Sensor SAS2500.

### 3.2.3 Spectra Acquisition and Soil Sampling

The Vis-NIR spectra were acquired at six transects on Field 1, seven transects on Field 2 and 3, and 20 transects on Field 5. When the tractor attached with the RTSS running on the transects, the soil penetrator tip with a flat plane edge

ensured uniform soil cuts and the soil flattener following behind produced a trench with uniform underground surface at a depth of 0.10 m. The underground soil Vis-NIR reflectance spectra at the range of 320 to 1700 nm were then collected through an additional optical fiber probe to the two spectrophotometers. Each spectrum data was acquired from the bottom of the trench every 3 s with the traveling speed of 0.28 $ms^{-1}$. This resulted in the Vis-NIR reflectance spectra being sampled at approximately every 0.84 m.

While the RTSS was running on the transects, a notification lamp with alarm was triggered at each data acquisition (every 0.84 m travelled). When the RTSS acquired every $25^{th}$ spectra data (21 m) on Field 1, $11^{th}$ spectra data (9 m) on Field 2, $20^{th}$ spectra data (17 m) on Field 3 and $8^{th}$ spectra data (7 m) on Field 5, a wooden stick was inserted into the soil for marking the soil sampling points. Two sets of 24, 63, 21 and 80 fresh soil samples were then collected from Field 1, Field 2, Field 3 and Field 5 respectively, at the trench bottom of the wooden sticks' position along the RTSS's tracks. In total, there were two sets of 188 soil samples collected and packed in sealable plastic bags. Figure 3.3 illustrates the collected spectra scanning line (dotted line) and locations of the sampling point (black circles) on Field 2 as an example.

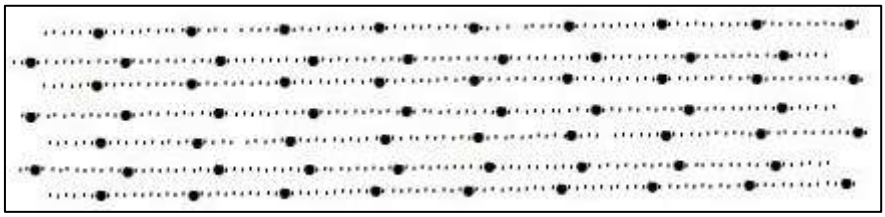

Fig. 3.3. RTSS Scanning line (small dotted lines) and soil sampling points' position (large dotted points) of Field 2.

### 3.2.4 Laboratory Soil Chemical Analysis of Twenty-four Soil Properties

In order to measure the chemical amount in the soil samples collected at the four fields, one set of the soil samples was transported to Tokyo University of Agriculture and Technology (TUAT) laboratory for analysis of MC, SOM, pH and EC while the other set was transported to the Agricultural Product Chemical Research Laboratory (APCRL: Federation of Tokachi Agricultural Cooperative Association, Hokkaido, Japan) for analysis of CEC, P-a, PAC, C-t, N-t, N-h, N-n, N-a, Ca, K, Mg, B, Cu, Mn, Zn, BD, BSP, CSP, Ca/Mg and Mg/K. Both sets were transported by a refrigerator car at a temperature below 10 °C.

Soil chemical analyses for MC, SOM, pH and EC were conducted on the first set of 188 soil samples at TUAT. The fresh soil samples were crushed and sieved through a 2-mm sieve. Debris such as plant material and stones were removed. The samples were then stored in sealable plastic bags at 5 °C until the completion of the chemical analysis. MC, pH and EC were measured in fresh soil samples. MC was measured using the oven-dry method at 110 °C for 24 h. Soil pH was measured by glass electrode (F-74, HORIBA) using a soil:distilled-water weight ratio of 1:2.5. Soil EC was measured by the AC bipolar method (F-74, HORIBA) using a soil to distilled-water weight ratio of 1:5. After shaking for 2 h and equilibration, pH and EC were measured in the supernatant liquid. The soil to distilled-water mass ratios for pH and EC were calculated using each MC result of soil samples. SOM was measured on dried soil samples that were sieved through a 1-mm sieve and burnt in a muffle furnace at 750 °C for 3 hours. Each soil analysis was conducted three times, and the average values were adopted as reference values for the multivariate statistical analysis.

Table 3.1 Twenty-four Soil analysis methods, instruments and locations.

| | Soil Properties | Analysis Method | Instrument | Location |
|---|---|---|---|---|
| 1. | MC (%) | Oven Dry | DK610Yamato | TUAT |
| 2. | SOM (%) | Loss on Ignition | Muffle Furnace FM28 Yamato | TUAT |
| 3 | pH | Glass Electrode | F-74 HORIBA | TUAT |
| 4. | EC (μS/cm) | AC Bipolar | F-74 HORIBA | TUAT |
| 5. | CEC (me/100g) | Absorptiometry | BRAN+LUEBBE, QUAATRO | APCRL |
| 6. | C-t (%) | Tyurin's Method | NC-220F, SUMIGRAPH | APCRL |
| 7. | N-t (%) | Kjeldahl Method | NC-220F, SUMIGRAPH | APCRL |
| 8. | N-h (mg/100g) | Absorptiometry | BRAN+LUEBBE, QUAATRO | APCRL |
| 9. | N-n (mg/100g) | Absorptiometry | BRAN+LUEBBE, QUAATRO | APCRL |
| 10. | N-a (mg/100g) | Absorptiometry | BRAN+LUEBBE, QUAATRO | APCRL |
| 11. | P-a (mg/100g) | Absorptiometry | BRAN+LUEBBE, QUAATRO | APCRL |
| 12. | PAC (non) | Absorptiometry | BRAN+LUEBBE, QUAATRO | APCRL |
| 13. | Ca (mg/100g) | Absorptiometry | VARIAN, SpectrAA-280F | APCRL |
| 14. | K (mg/100g) | Absorptiometry | VARIAN, SpectrAA-280FS | APCRL |
| 15. | Mg (mg/100g) | Absorptiometry | VARIAN, SpectrAA-280FS | APCRL |
| 16. | B (ppm) | Absorptiometry | VARIAN, SpectrAA-220 | APCRL |
| 17. | Cu (ppm) | Absorptiometry | VARIAN, SpectrAA-220 | APCRL |
| 18. | Mn (ppm) | Absorptiometry | VARIAN, SpectrAA-220 | APCRL |
| 19. | Zn (ppm) | Absorptiometry | VARIAN, SpectrAA-220 | APCRL |
| 20. | CSP (%) | - | - | APCRL |
| 21. | BSP (%) | - | - | APCRL |
| 22. | BD | - | - | APCRL |
| 23. | Mg/K | - | - | APCRL |
| 24. | Ca/Mg | - | - | APCRL |

The second set of 188 soil samples transported to APCRL was analyzed for CEC, C-t, N-t, N-h, N-n, N-a, P-a, Ca, K, Mg, B, Cu, Mn, Zn, PAC, BD, BSP, CSP, Ca/Mg and Mg/K by APCRL using the standard procedures in the Hokkaido area in Japan (Souma and Kikuchi, 1992). This set of soil samples was also dried, crushed and sieved. The soil analysis methods and instruments that were used for analysis of the 24 chemical properties are listed in Table 3.1.

### 3.2.5 Spectra Pretreatment and Calibration Model Development for Twenty-four Soil Properties

Prior to the development of calibration models, all collected underground Vis-NIR soil reflectance spectra were converted to absorbance using Beer-Lambert's law as in Equation (3) of Chapter 2. The absorbance spectra were then converted to 5-nm-interval data by the interpolation method using Data Monitor Software (Shibuya Seiki Co., Ltd.). The spectra of original absorbance ranged from 350 to 1700 nm. To enhance weak signals and remove noise due to diffuse reflection, the absorbance spectra were pre-treated using the second-derivative Savitzky and Golay method. Moreover, both edges of the spectra were removed as these parts of the spectra were unstable and rich in noise. This resulted in a final spectra wavelength range of 500 to 1600 nm. The calibration models were subsequently developed by applying the partial least-square regression (PLSR) technique coupled with full cross-validation to establish the relationship between the amount of soil properties obtained by chemical analysis (reference values) with the pretreated Vis-NIR soil absorbance spectra from the corresponding locations. These were performed using Unscrambler X10.2 software. In the PLSR analysis, up to 20 principal components

(PC) were used in the regression calculations and the number of PC was selected to give the highest coefficient of determination ($R^2_{val}$) close to one and the smallest root mean square error of full cross-validation ($RMSE_{val}$). Sample outliers were also detected by checking the residual sample variance plot on the validation views after the PLSR. Individual sample outliers located far from the zero line of residual variance were considered to be outliers and excluded from the analysis. In this study, the calculation for generating the model was performed seven times. Three samples were selected as sample outliers at one time of calculation up to six times of re-calculation and one final sample was removed as an outlier at the seventh time of re-calculation. In total, 19 samples were removed as outliers in the PLSR for each soil property.

In order to obtain the best calibration model for each of the 24 soil properties, the PLSR analyses were performed on the Vis-NIR spectra that were pretreated with 11 different numbers of smoothing points. Therefore, there were 11 calibration models developed for each of the 24 soil properties. Among of these calibration models, the model that produced the highest $R^2_{val}$ close to one and smallest $RMSE_{val}$ was selected as the best calibration model for each of the 24 soil properties. The performance of the calibration models was also assessed based on the value of residual prediction deviation (RPD) produced from the PLSR analysis.

The performance of the calibration models was classified based on the value of RPD where RPD larger than 2.0 was considered excellent, between 1.4 and 2.0 was good and below 1.4 was unreliable (Chang et al., 2001). Hence, the best calibration model that possesses the largest $R^2_{val}$ and RPD but minimum $RMSE_{val}$ in

the regression analysis for each soil property was then used to provide quantitative prediction and mapping of the respective soil properties.

### 3.2.6 Development of Twenty-four Soil Properties Maps

In order to obtain higher resolution soil maps, the Vis-NIR spectra that were acquired in between the sampling points along transects of the four fields were then predicted using the best calibration model of each soil property. These quantitative prediction values were then used to generate high-resolution prediction maps of 24 soil properties using ArcGIS Ver. 10.0 software (ESRI Inc. USA). As a comparison, the reference values obtained from the chemical analysis were also used to generate measured maps. Both soil maps were interpolated using the inverse-distance weighting (IDW) method.

## 3.3 Results and Discussions

### 3.3.1 Performance of the Twenty-four Soil Properties Calibration Models

The raw absorbance Vis-NIR spectra and pretreated with second-derivative Savitzky-Golay spectra were depicted in Figure 3.4. Both edges of the raw absorbance Vis-NIR were removed as these parts of spectra were unstable and rich in noise. The PLSR results of the calibration and full cross-validation were obtained as listed in Table 3.2. The number of samples used in the model was 169 after excluded 19 outliers. The highest accuracy of calibration model obtained was for Mn with the $R^2_{val}$ is 0.90 and the lowest calibration model accuracy was for N-a with the $R^2_{val}$ is 0.43. Even though Mn and some other soil properties such as Mg, CEC, pH, and Ca

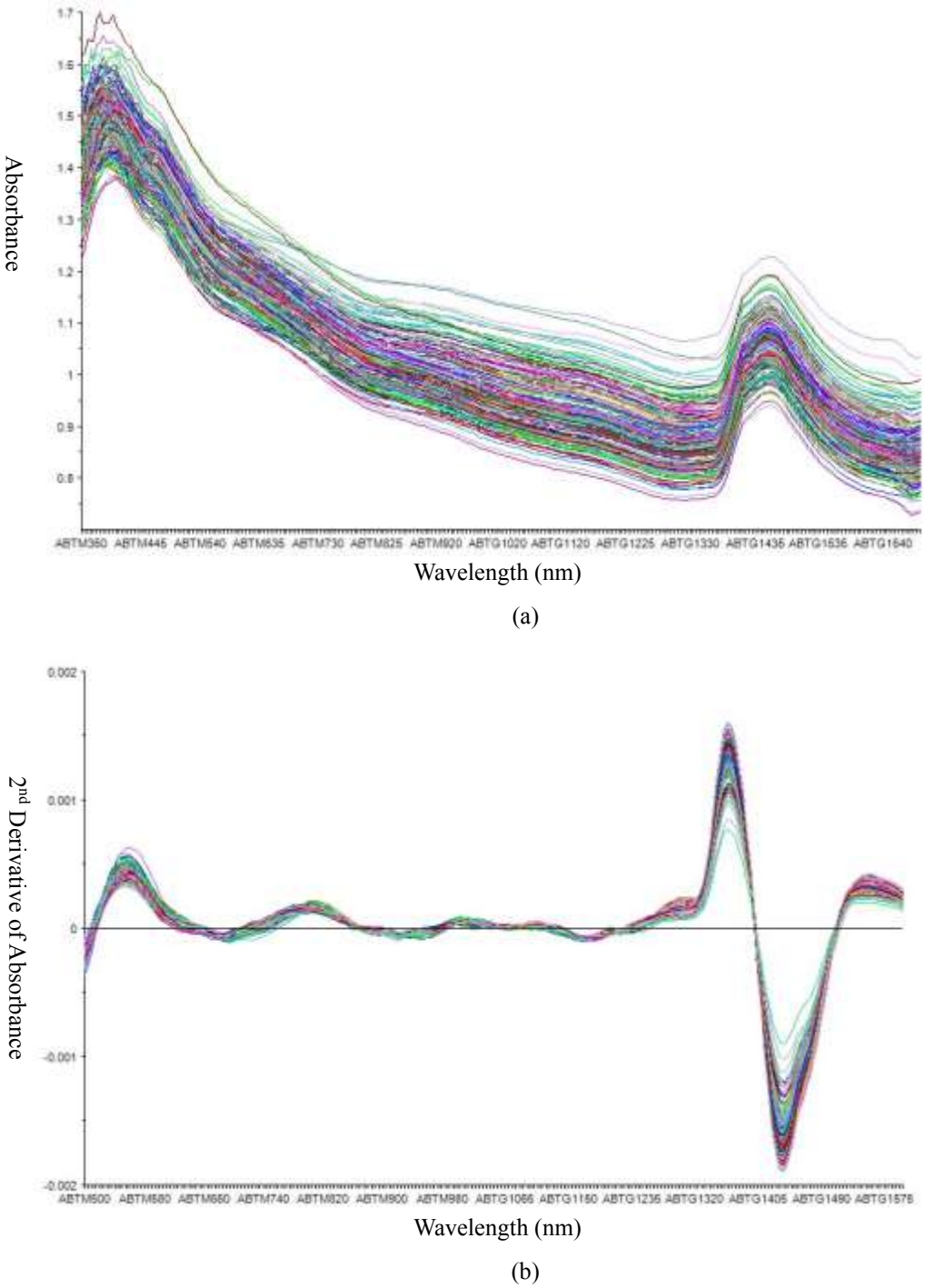


Fig. 3.4 Absorbance spectra collected by RTSS SAS2500 for developing the calibration model (a) original absorbance spectra, (b) pretreated using 2nd derivative absorbance spectra

do not have direct response to Vis-NIR spectra, the correlation analyses between Vis-NIR spectra and these soil properties concentration have yielded inconclusive results to date, suggesting that these soil properties concentration may belong to a class of "tertiary" soil parameters, linked to Vis-NIR spectra through "surrogate", or indirect, correlations, involving some other primary or secondary parameter like soil organic matter content, to which Vis-NIR spectra are very sensitive (Wu et al., 2010). Thus, these tertiary soil properties can be measured with good accuracy due to co-variation with one or more primary or secondary properties (Stenberg et al., 2010).

Referring to the classification by Chang et al. (2001), calibration models that fall in the excellent category are those for Mn, Ca/Mg, SOM, Mg, C-t, pH, N-t and BD due to the values of RPD are 3.19, 2.46, 2.33, 2.21, 2.13, 2.11, 2.10 and 2.00 respectively. Calibration models for EC, CEC, N-h, P-a, Ca, K, B, Cu, Zn, PAC, CSP, BSP and Mg/K showed good levels of accuracy with RPD values between 1.41 and 1.93. Two models categorized as unreliable were the models for N-a and N-n due to their RPD values were 1.33 and 1.22 respectively. This result is consistent with the study by Islam et al. (2004) and Kodaira and Shibusawa (2013) who also obtained unreliable model accuracy for N-a and N-n respectively. Another study by Ehsani et al. (1999) also found that it was possible to use the NIR spectrum of the soil in the range of 1800 – 2300 nm to determine the soil nitrate content whereas the spectrophotometer used in this study was just up to 1700 nm (1600 nm after removing noise). The scatter plots of the models for the 24 soil properties are depicted in Fig. 3.5. Also shown in this figure are the primary regression equations of the respective soil properties

Table 3.2 Summary of Partial Least Square Regression (PLSR) for the Twenty-four Soil Properties.

| | **Soil Properties** | **[a]N** | **PC[c]** | **$R^2_{cal}$** | **$R^2_{val}$** | **$RMSE_{val}$** | **SD** | **RPD** | **[d]Category** |
|---|---|---|---|---|---|---|---|---|---|
| 1. | MC (%) | 169 | 8 | 0.78 | 0.70 | 1.82 | 3.29 | 1.81 | B |
| 2. | SOM (%) | 169 | 10 | 0.88 | 0.82 | 0.22 | 0.52 | 2.33 | A |
| 3. | pH | 169 | 8 | 0.84 | 0.78 | 0.09 | 0.19 | 2.11 | A |
| 4. | EC (μS/cm) | 169 | 7 | 0.62 | 0.50 | 5.01 | 7.07 | 1.41 | B |
| 5. | CEC (me/100g) | 169 | 8 | 0.80 | 0.73 | 0.58 | 1.10 | 1.90 | B |
| 6. | C-t (%) | 169 | 5 | 0.80 | 0.77 | 0.11 | 0.23 | 2.13 | A |
| 7. | N-t (%) | 169 | 5 | 0.78 | 0.74 | 0.01 | 0.02 | 2.10 | A |
| 8. | N-a (mg/100g) | 169 | 2 | 0.53 | 0.43 | 0.15 | 0.20 | 1.33 | C |
| 9. | N-h (mg/100g) | 169 | 5 | 0.75 | 0.54 | 0.52 | 0.76 | 1.46 | B |
| 10. | N-n (mg/100g) | 169 | 7 | 0.54 | 0.45 | 0.09 | 0.11 | 1.22 | C |
| 11. | P-a (mg/100g) | 169 | 8 | 0.65 | 0.50 | 2.22 | 3.18 | 1.43 | B |
| 12. | PAC (non) | 169 | 6 | 0.81 | 0.66 | 24.99 | 42.64 | 1.71 | B |
| 13. | Ca (mg/100g) | 169 | 8 | 0.79 | 0.72 | 10.52 | 19.70 | 1.87 | B |
| 14 | K (mg/100g) | 169 | 6 | 0.83 | 0.66 | 1.03 | 1.78 | 1.73 | B |
| 15. | Mg (mg/100g) | 169 | 9 | 0.87 | 0.80 | 1.49 | 3.30 | 2.21 | A |
| 16. | B (ppm) | 169 | 5 | 0.76 | 0.70 | 0.06 | 0.10 | 1.67 | B |
| 17. | Cu (ppm) | 169 | 5 | 0.70 | 0.65 | 0.35 | 0.59 | 1.69 | B |
| 18. | Mn (ppm) | 169 | 9 | 0.94 | 0.90 | 3.51 | 11.20 | 3.19 | A |
| 19. | Zn (ppm) | 169 | 7 | 0.66 | 0.55 | 0.40 | 0.60 | 1.50 | B |
| 20. | CSP (%) | 169 | 6 | 0.87 | 0.73 | 3.82 | 7.38 | 1.93 | B |
| 21. | BSP (%) | 169 | 5 | 0.83 | 0.67 | 4.43 | 7.70 | 1.74 | B |
| 22. | BD | 169 | 8 | 0.77 | 0.70 | 0.02 | 0.04 | 2.00 | A |
| 23. | Mg/K | 169 | 5 | 0.57 | 0.49 | 0.54 | 0.76 | 1.41 | B |
| 24. | Ca/Mg | 169 | 13 | 0.92 | 0.83 | 0.28 | 0.69 | 2.46 | A |

[a]Number of samples used in the model,

[b]Number of principal component,

[c] Number of PLSR factors used in the model.,

[d]Category of prediction (full cross-validation) ability of PLSR for parameters. A: Excellent (RPD>2.0); B: Good 1.4<RPD<2.0); C: Unreliable (1.4<RPD) (Chang et al., 2001).

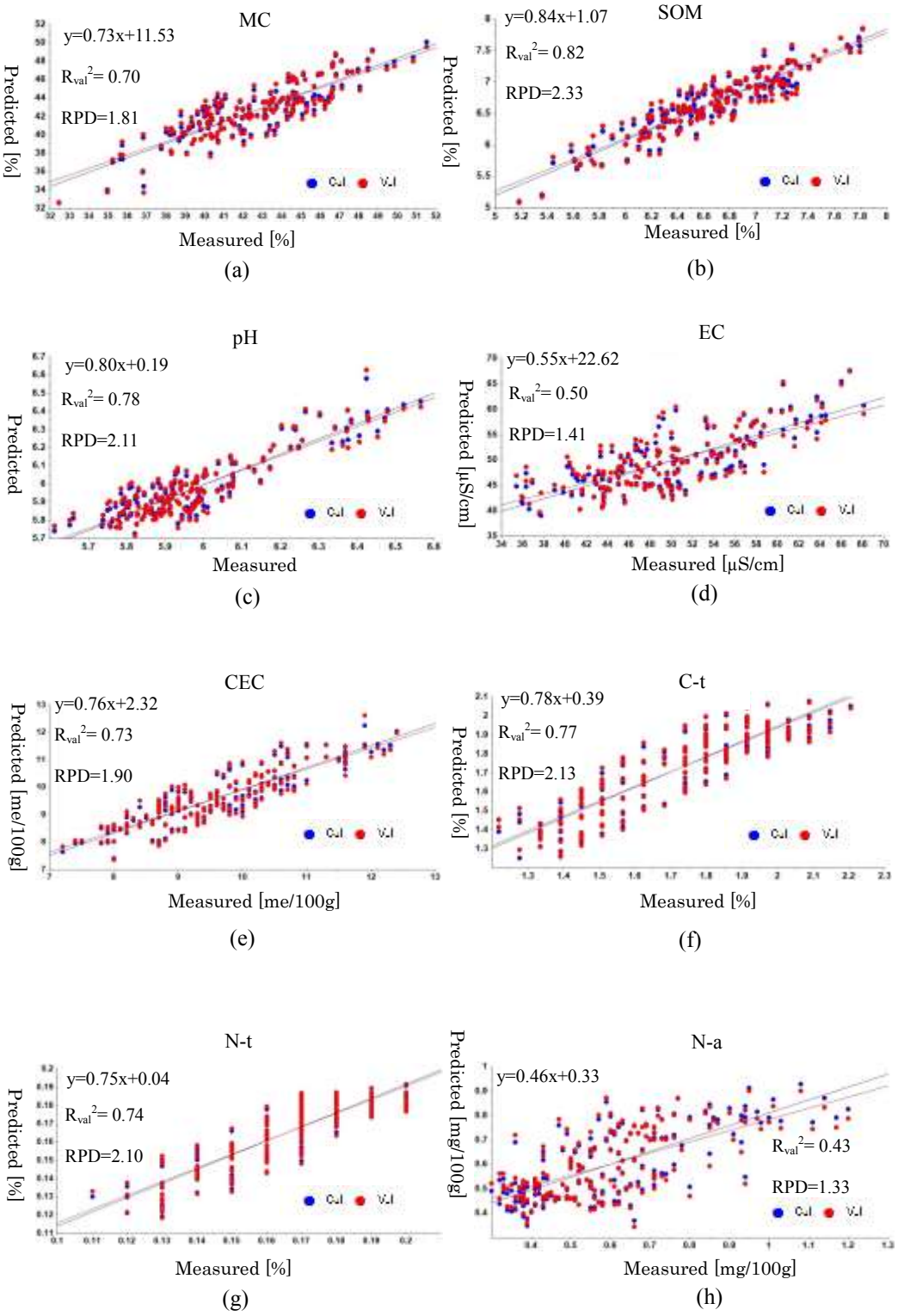


Fig. 3.5 Scatter plot of measured values versus Vis–NIR predicted values using partial least squares regression (PLSR) coupled with full cross-validation datasets for 24 soil properties.

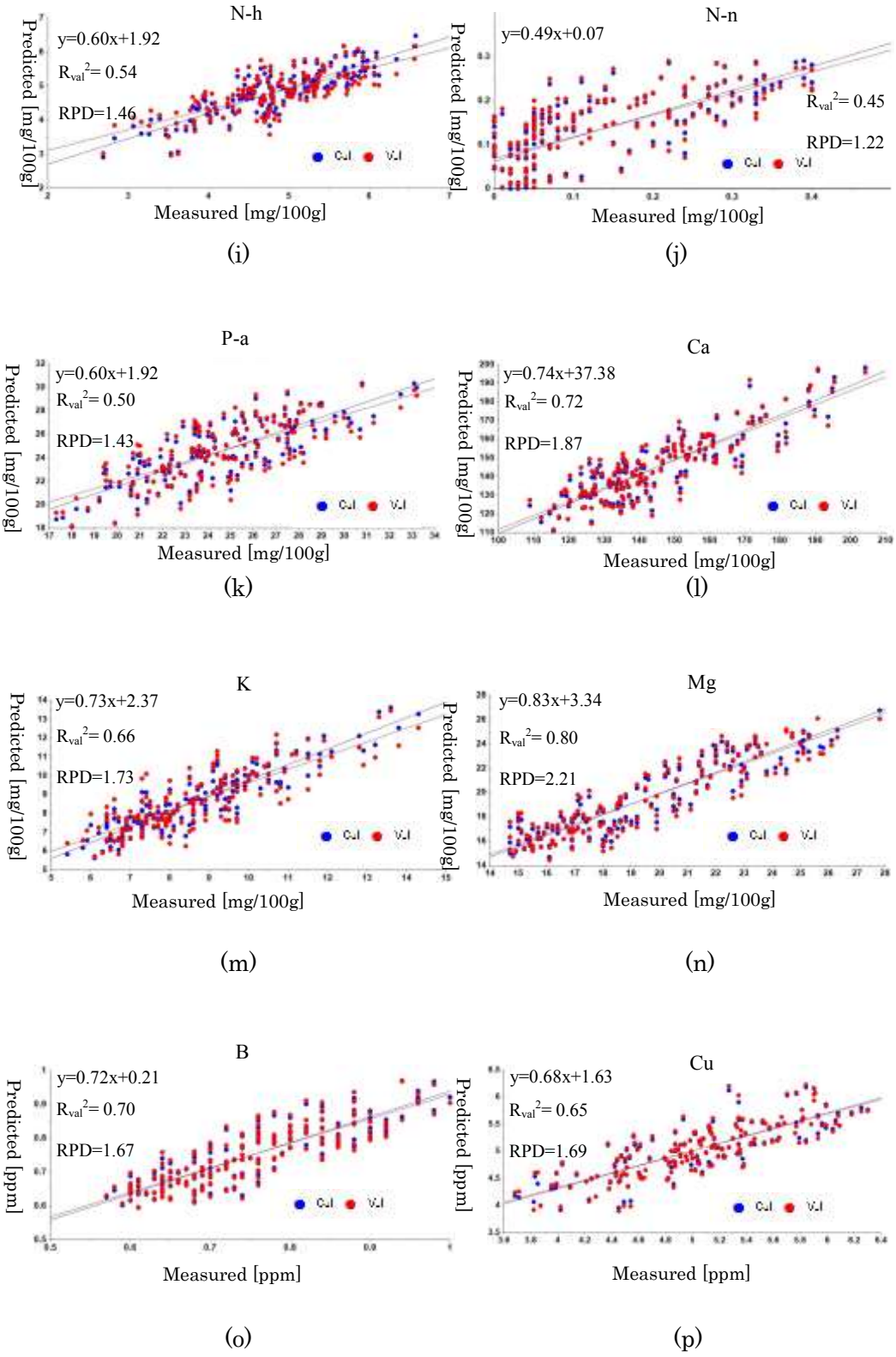


Fig. 3.5 (continued)

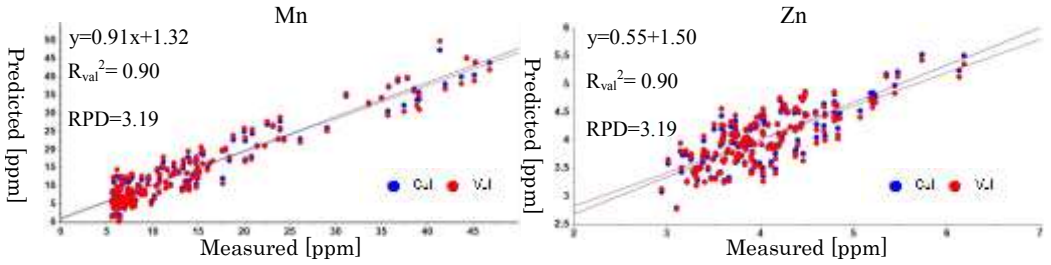


(q)




(r)

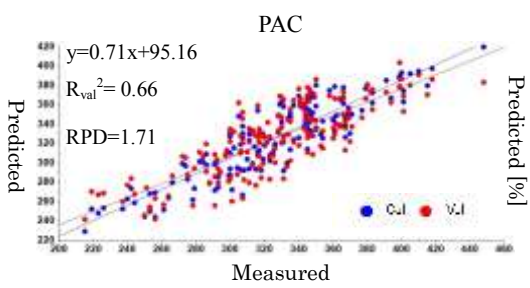


(s)

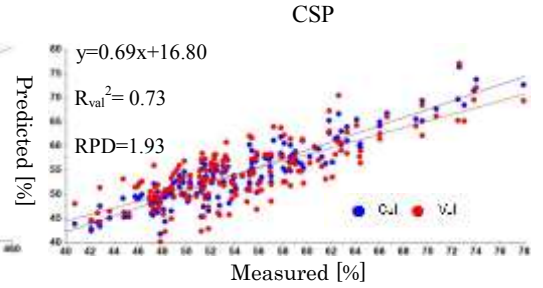


(t)

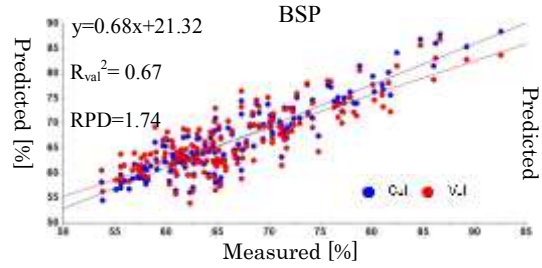


(u)

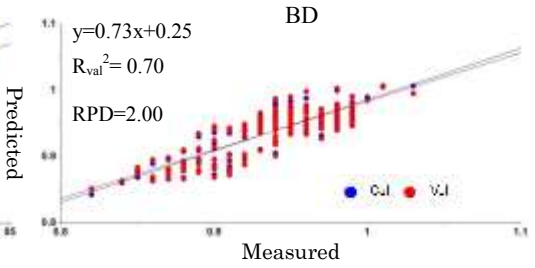


(v)

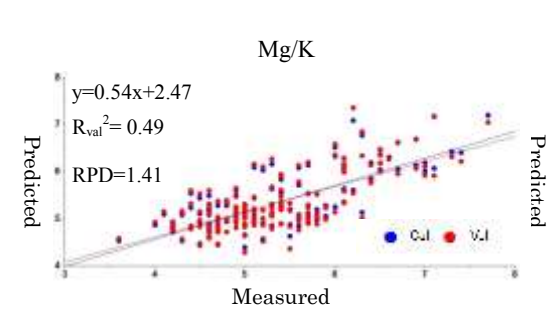


(w)

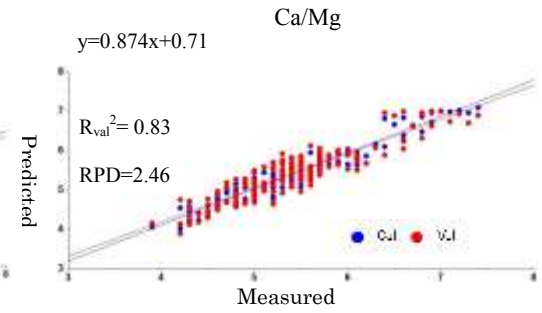


(x)

Fig. 3.5 (continued)

### 3.3.2 Twenty-four Soil Properties Maps

The RTSS also acquired other spectra for prediction in between the sampling points along transects of the four fields. The number of spectra acquired was 588 at Field 1, 678 at Field 2, 408 at Field 3 and 1460 spectra at Field 5. All these spectra were predicted using the best 24 soil properties' calibration models to determine the amount of the respective soil properties. The predicted values were then used to generate the predicted soil maps. The measured maps were also developed using the reference values obtained from soil analysis in the laboratory. In order to allow useful comparisons between measured and predicted maps, the same number of classes for both measured and predicted maps was used for every soil property. Moreover, the range (minimum and maximum) of each class was made identical for the pair of measured and predicted maps. Figure 3.6 compares the maps of the laboratory measured and predicted of 24 soil properties for the four fields. Both maps show a spatial similarity at most area especially maps for Field 2 and Field 5. However, less similarity exhibited for Field 1 and Field 3. This is because the number of datasets (reference values and spectra) from Field 1 and Field 3 that were used to develop the calibration models was just 24% (45 out of 188 datasets) whereas the majority of the datasets that were used to develop the calibration model were from Field 2 and Field 5 (145 out of 188 dataset). This is attributed to the developed models being more influenced from Field 2 and Field 5. Hence, the accuracies of the developed calibration models were higher and the maps generated were more representative for predicting Field 2 and Field 5 than Field 1 and Field 3.

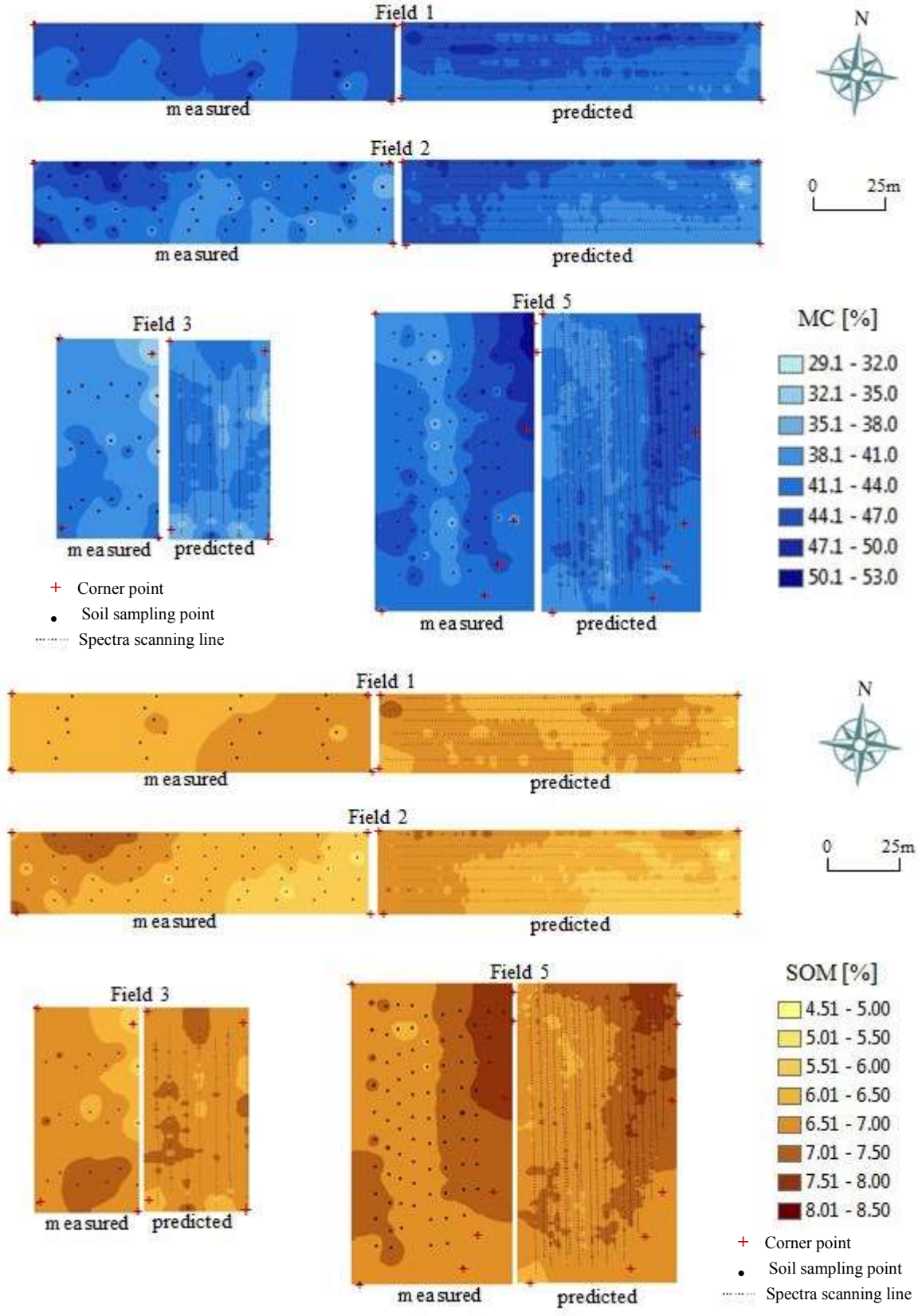


Fig 3.6 Comparison of measured and predicted map of 24 soil properties for the four fields

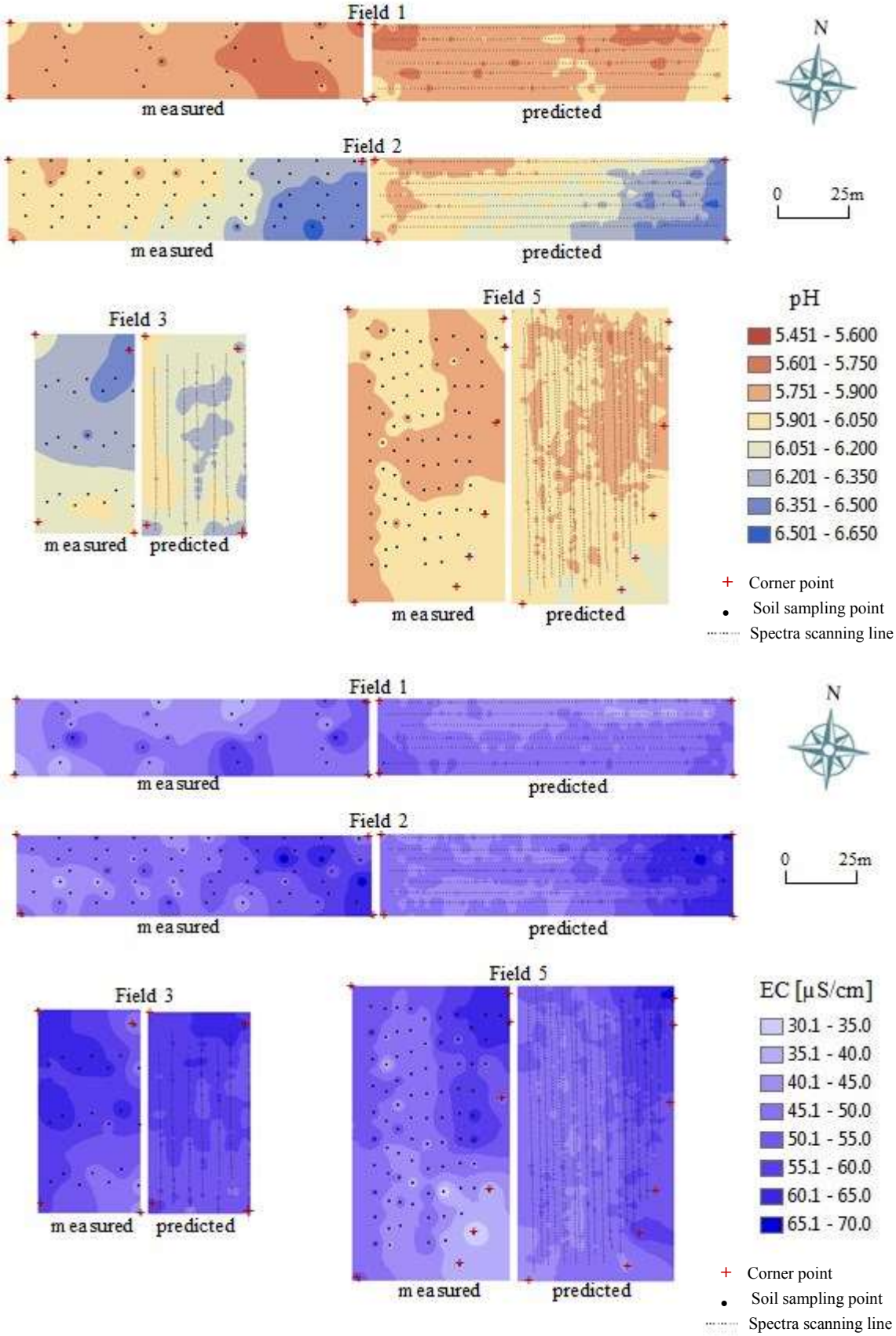


Fig 3.6 (Continued)

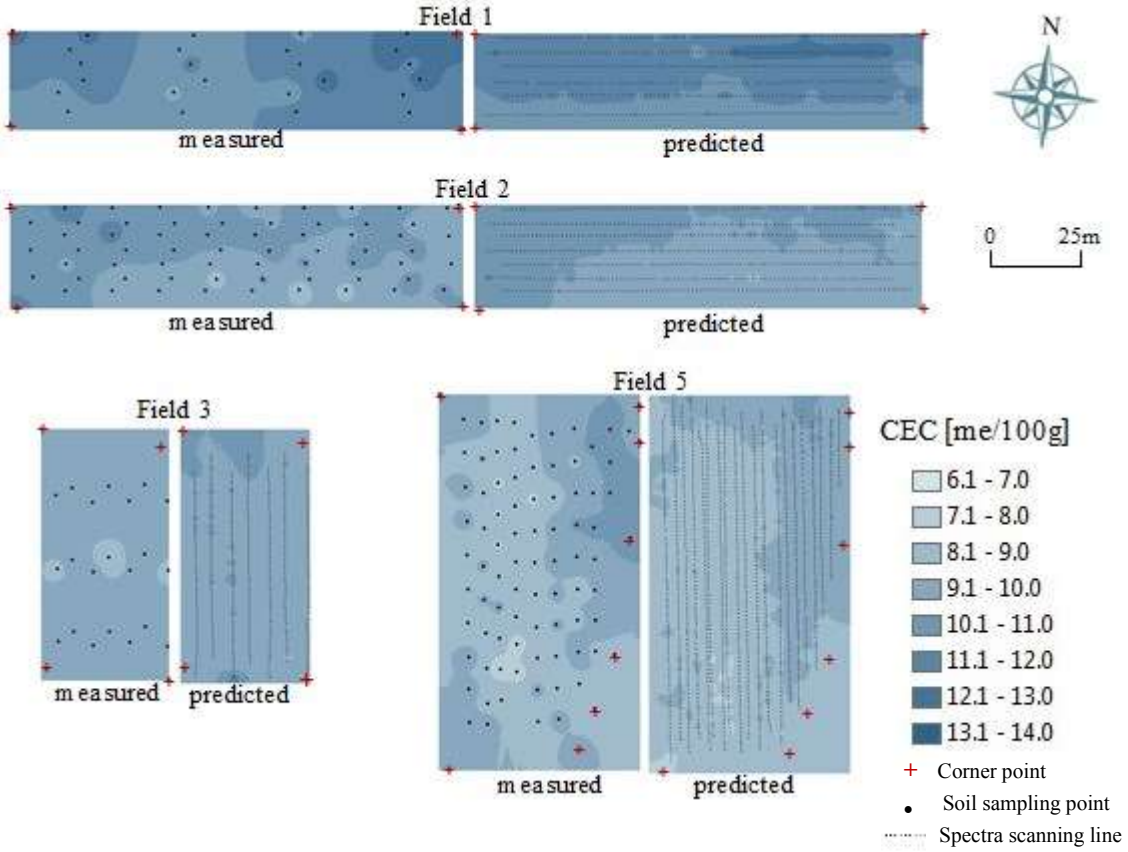


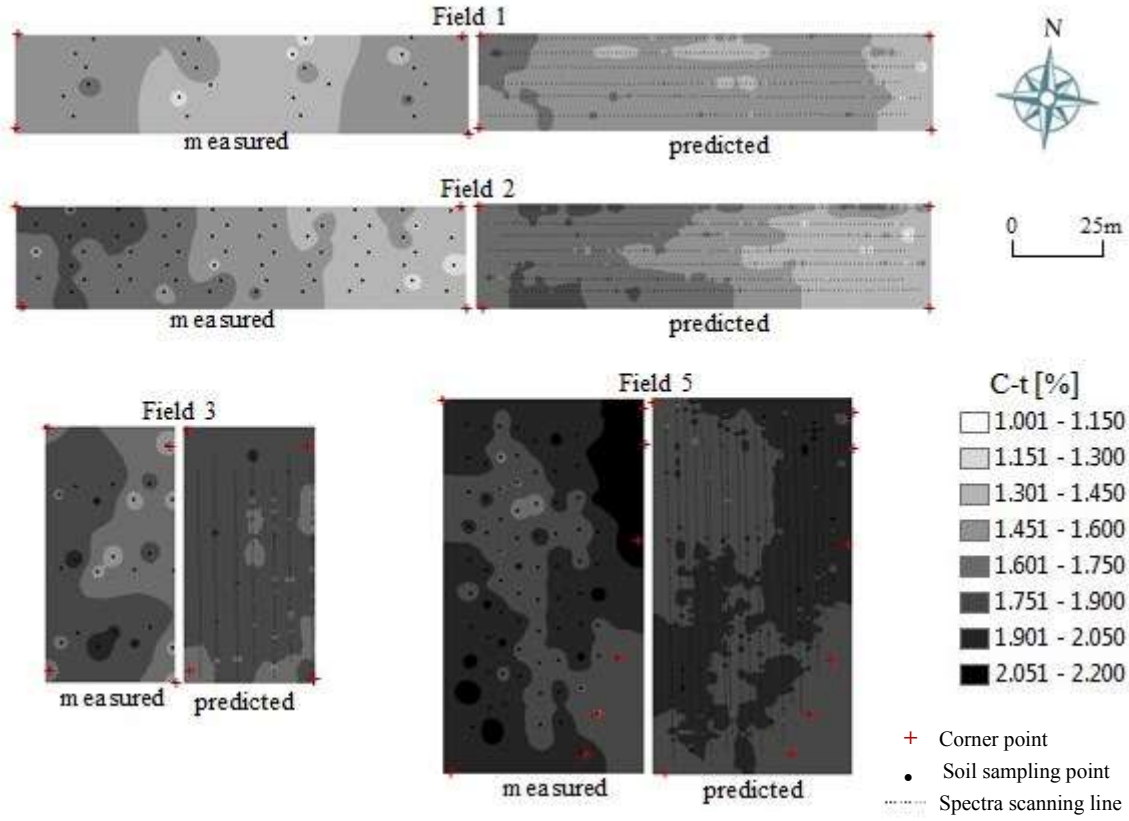


Fig 3.6 (Continued)

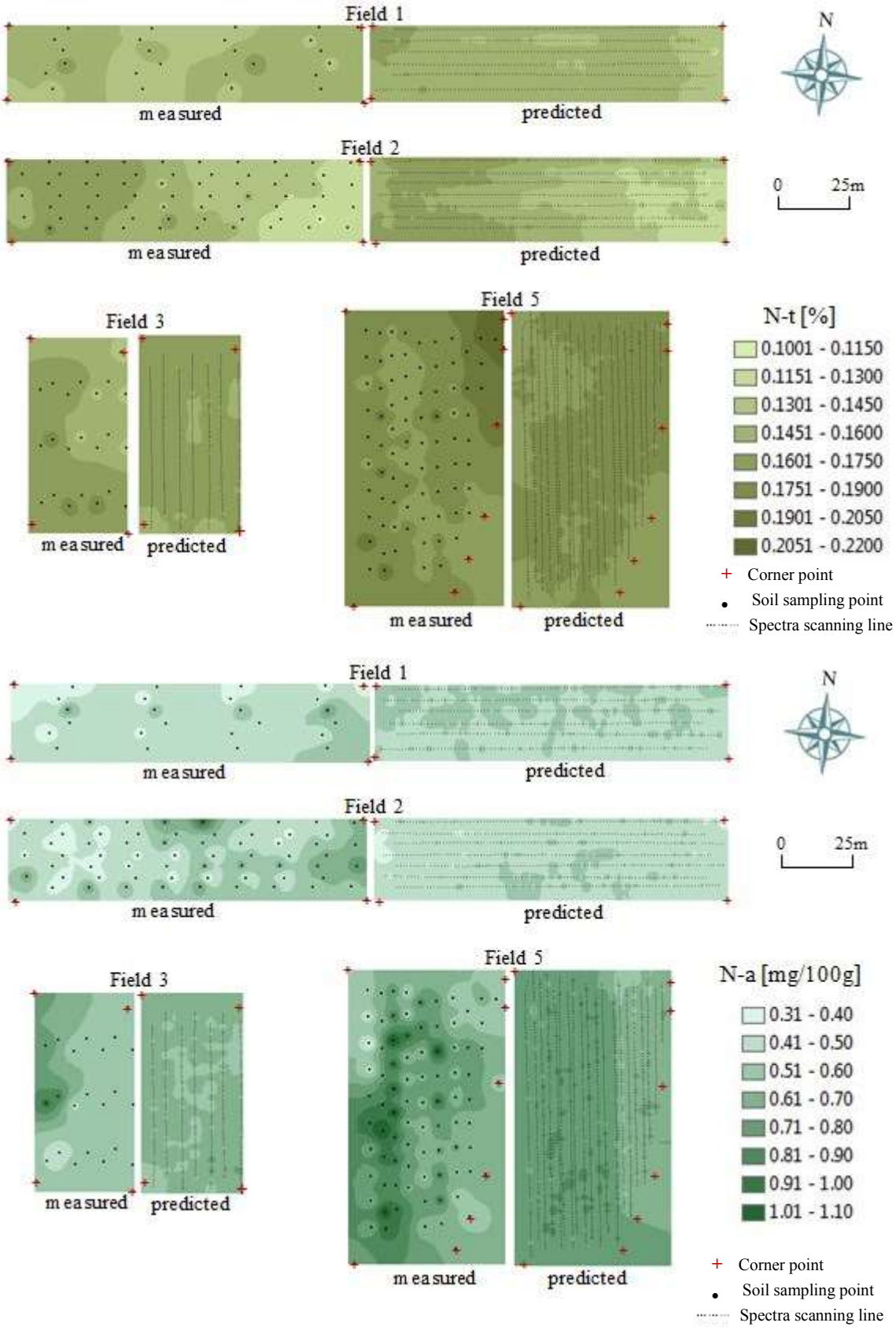


Fig 3.6 (Continued)

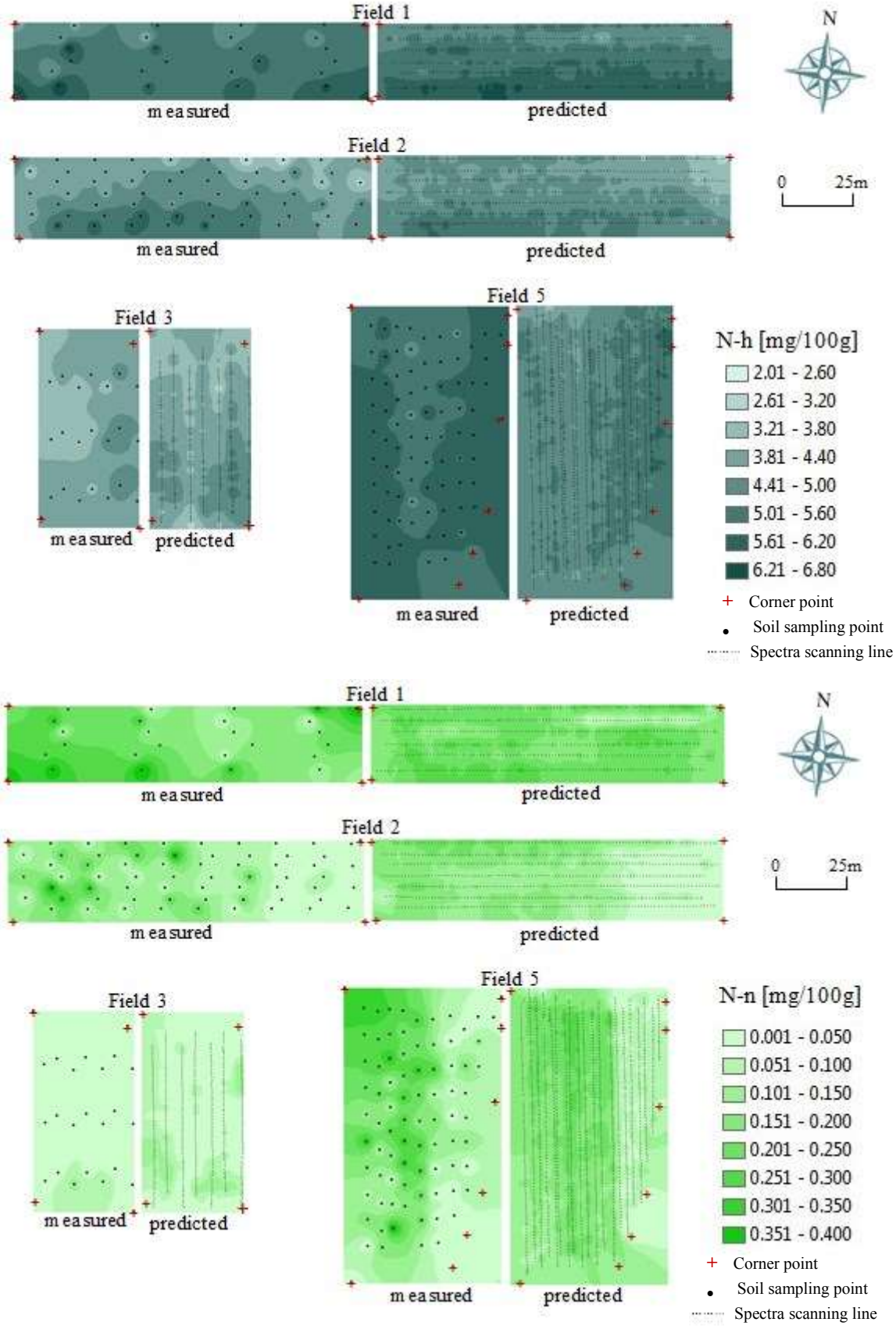


Fig 3.6 (Continued)

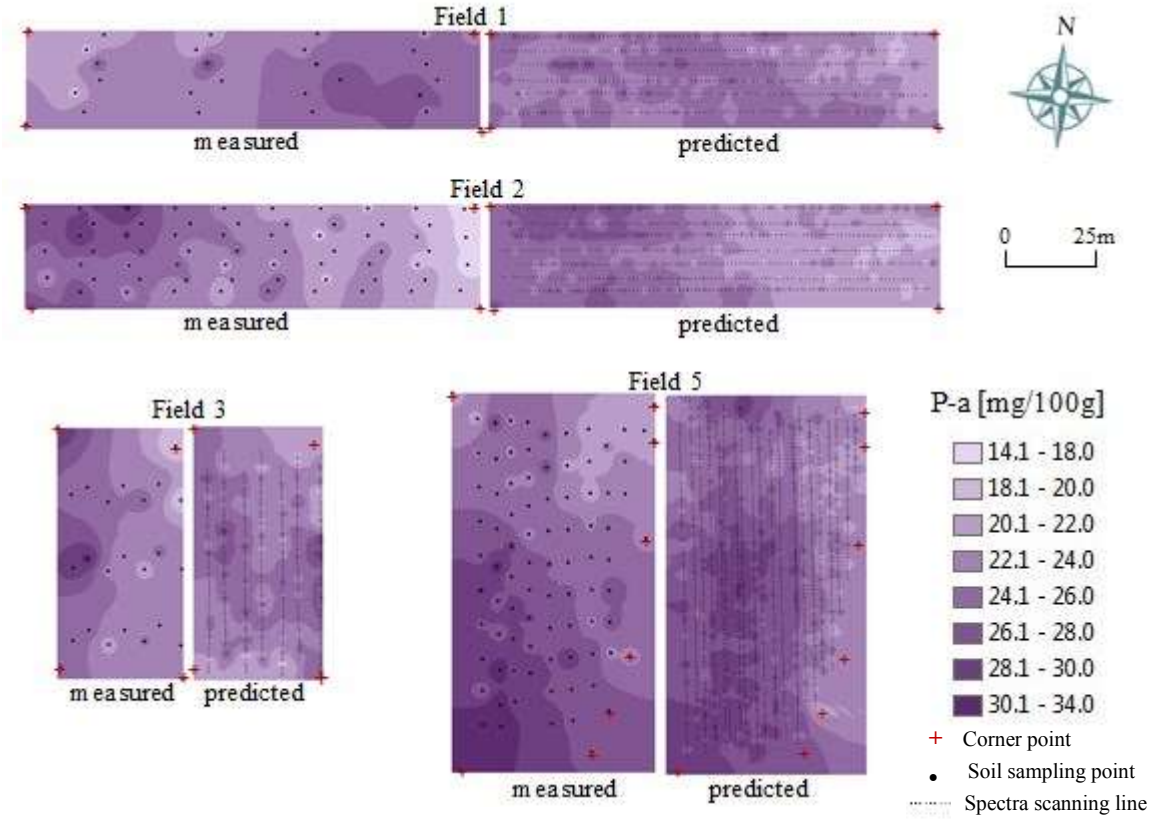


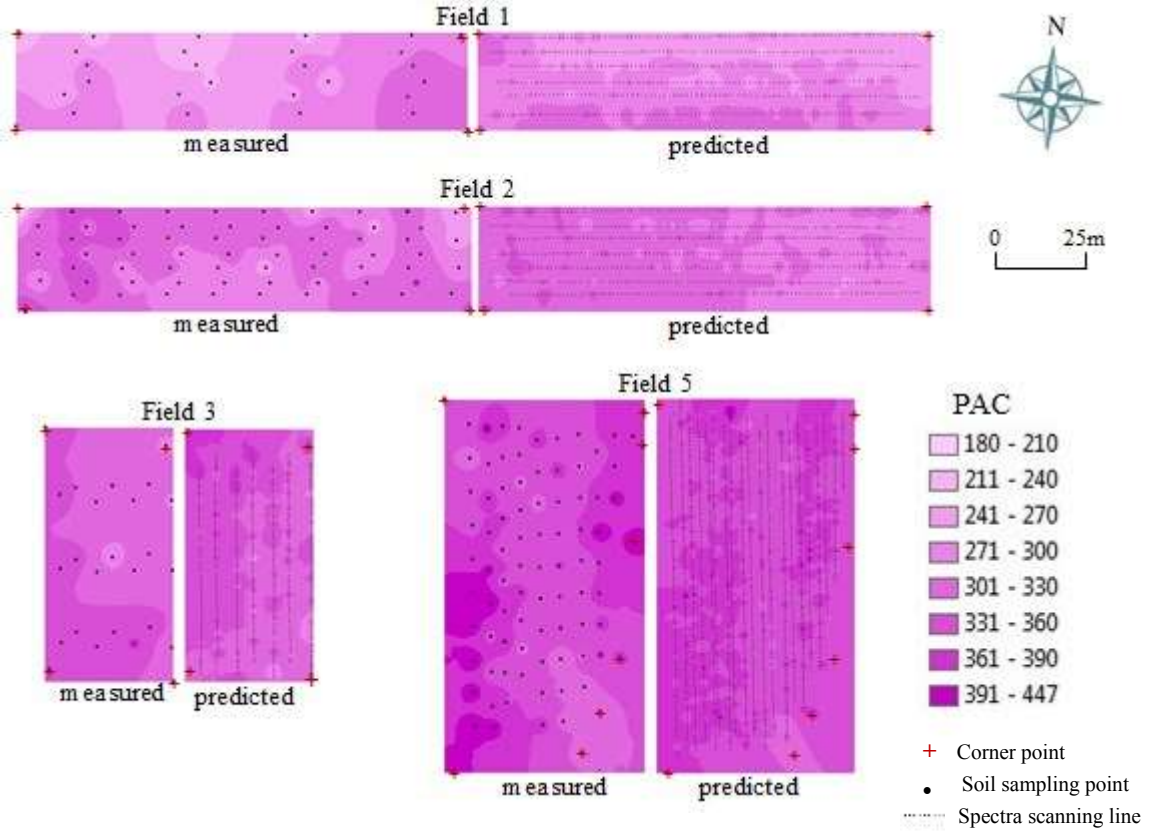


Fig 3.6 (Continued)

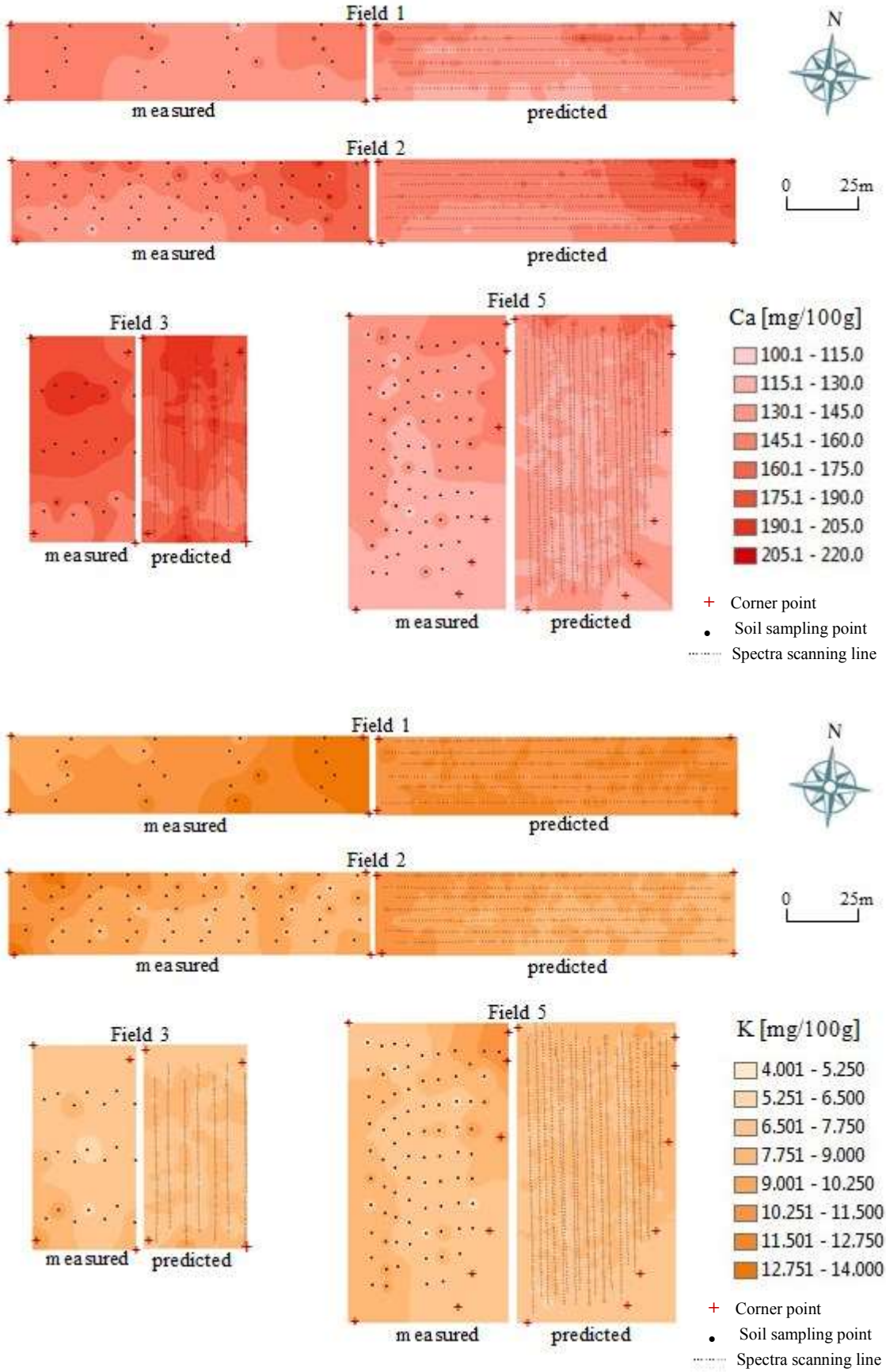


Fig 3.6 (Continued)

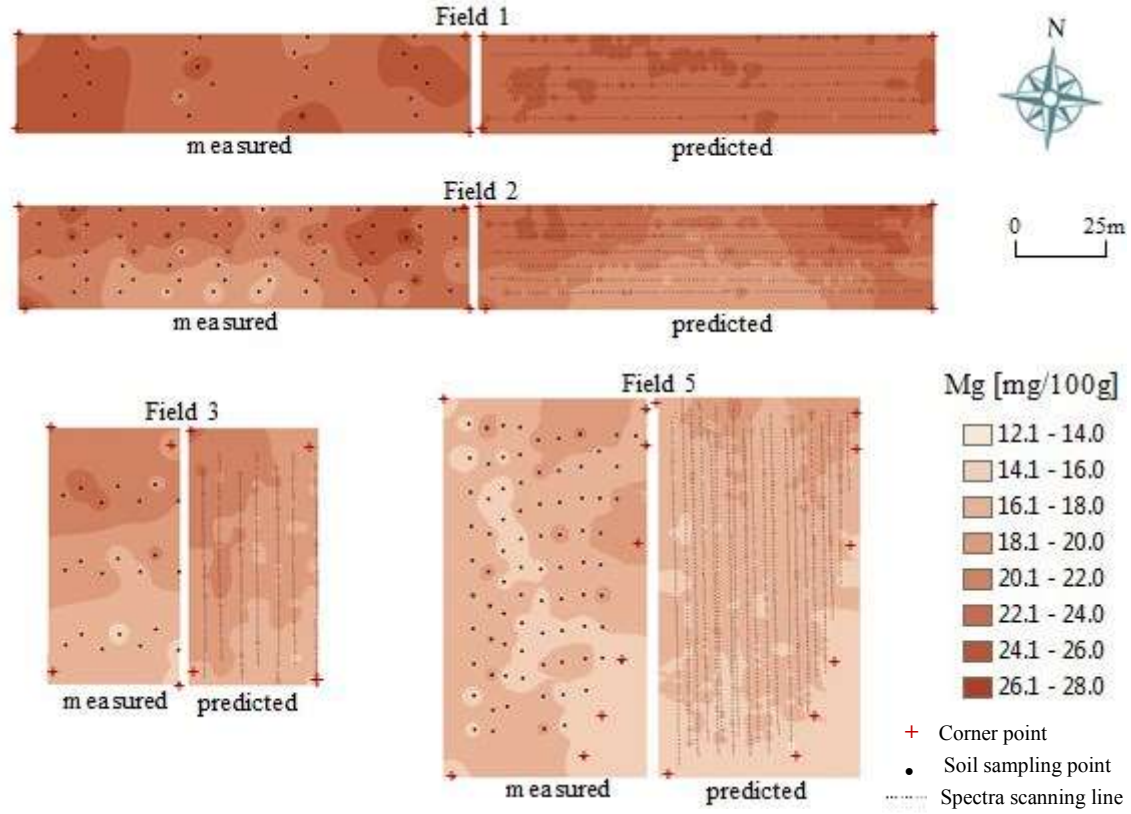


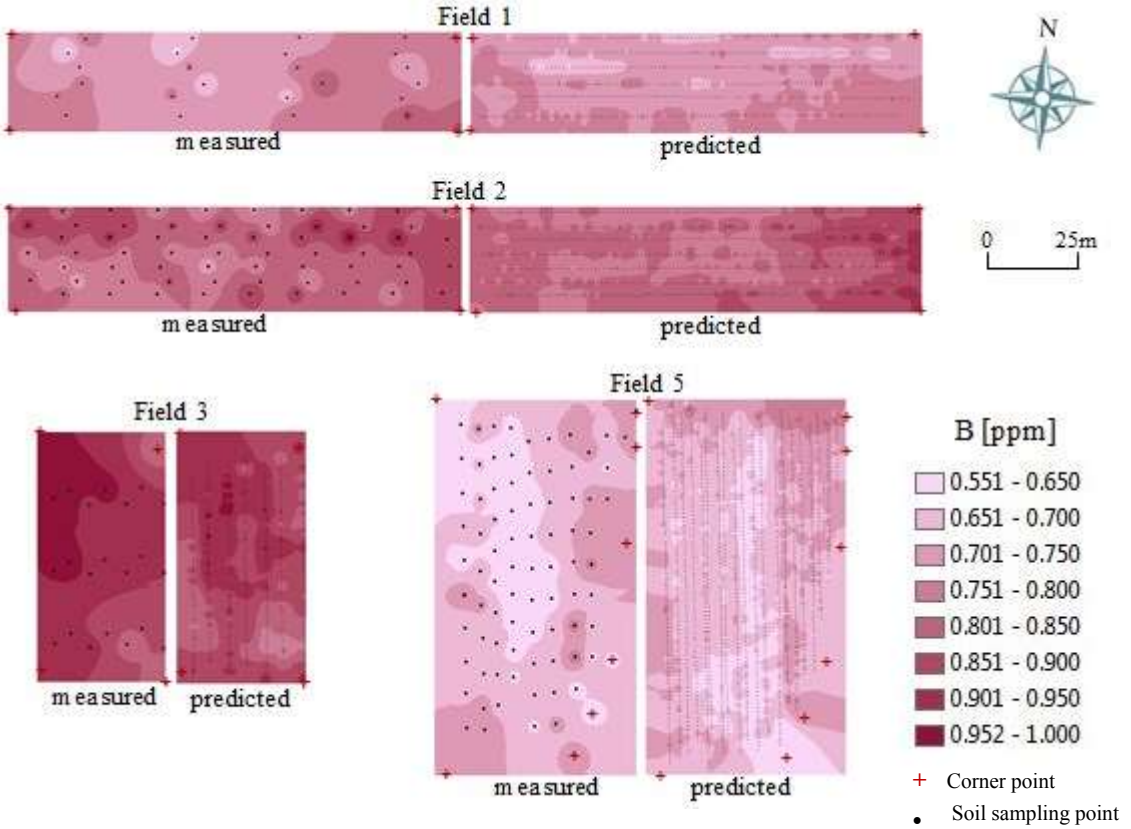


Fig 3.6 (Continued)

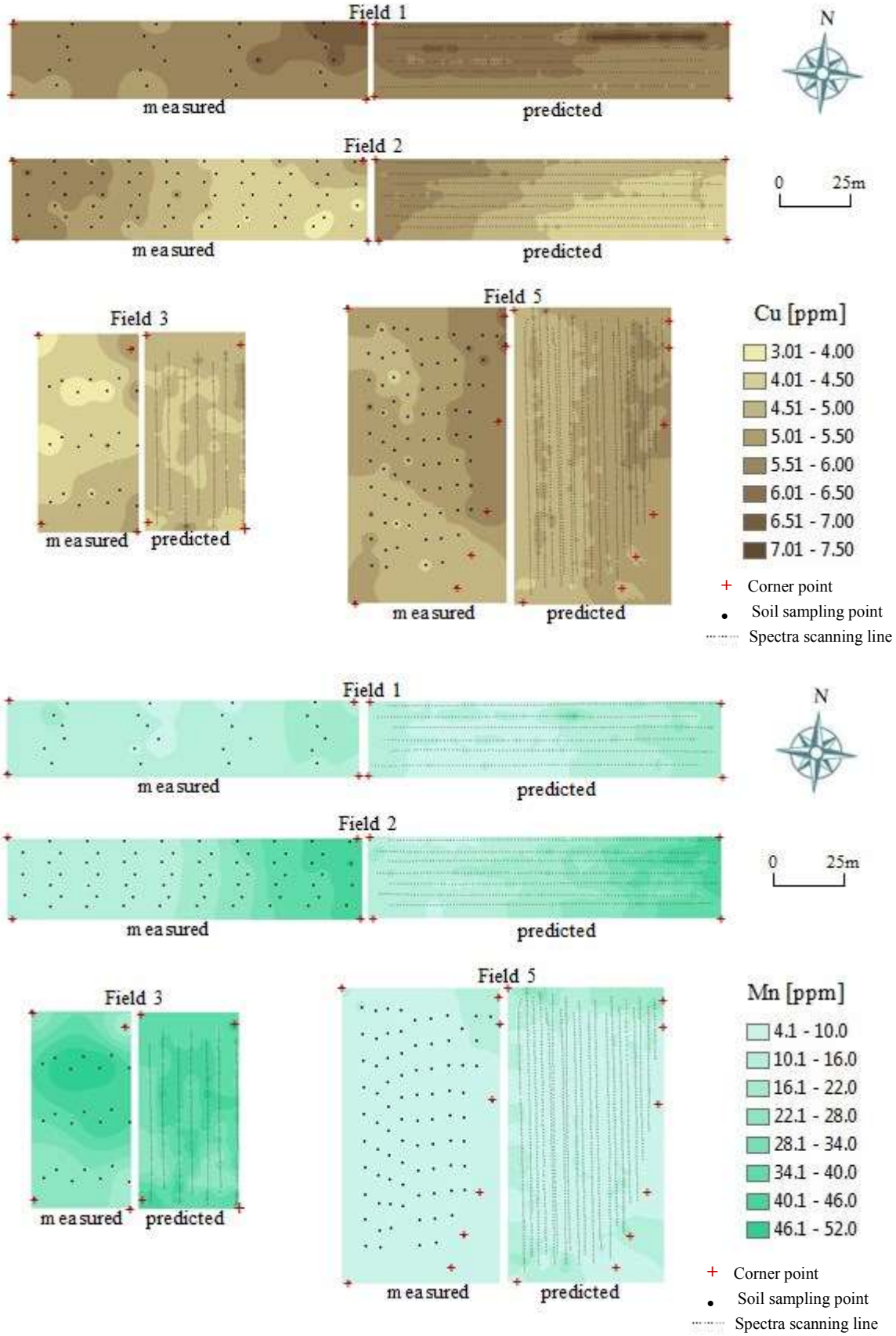


Fig 3.6 (Continued)

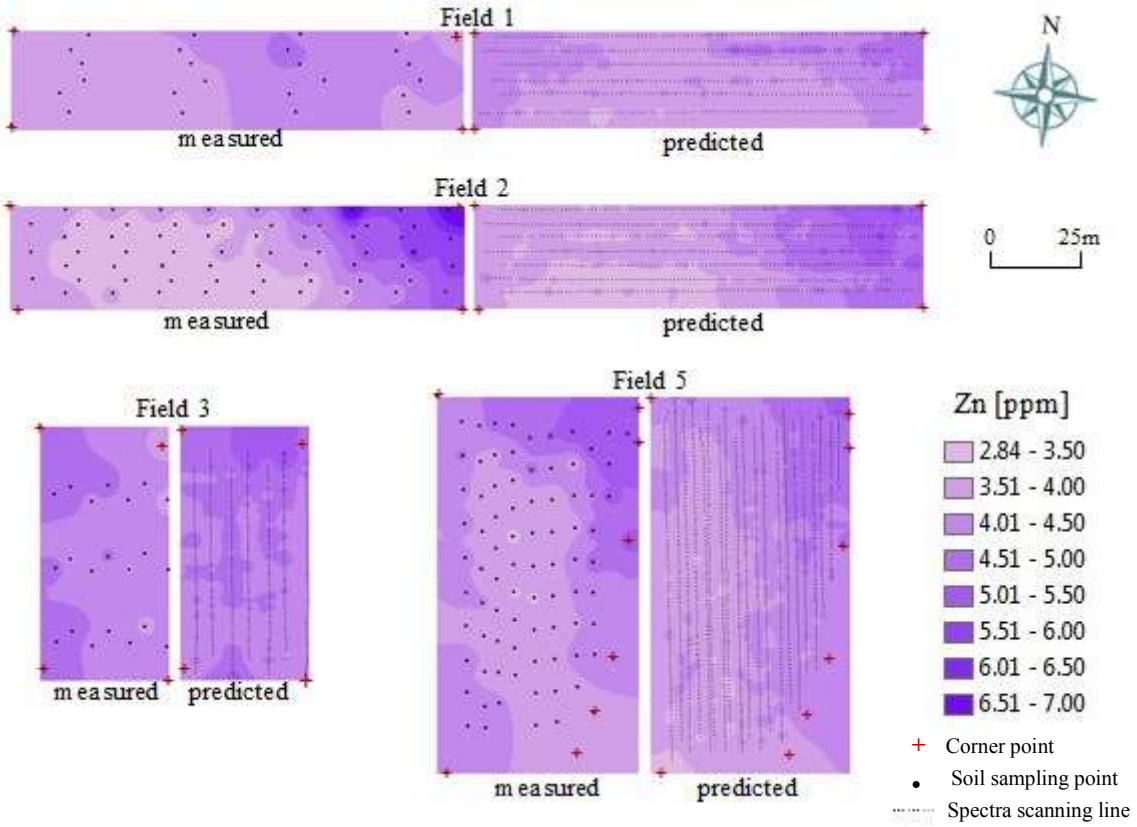


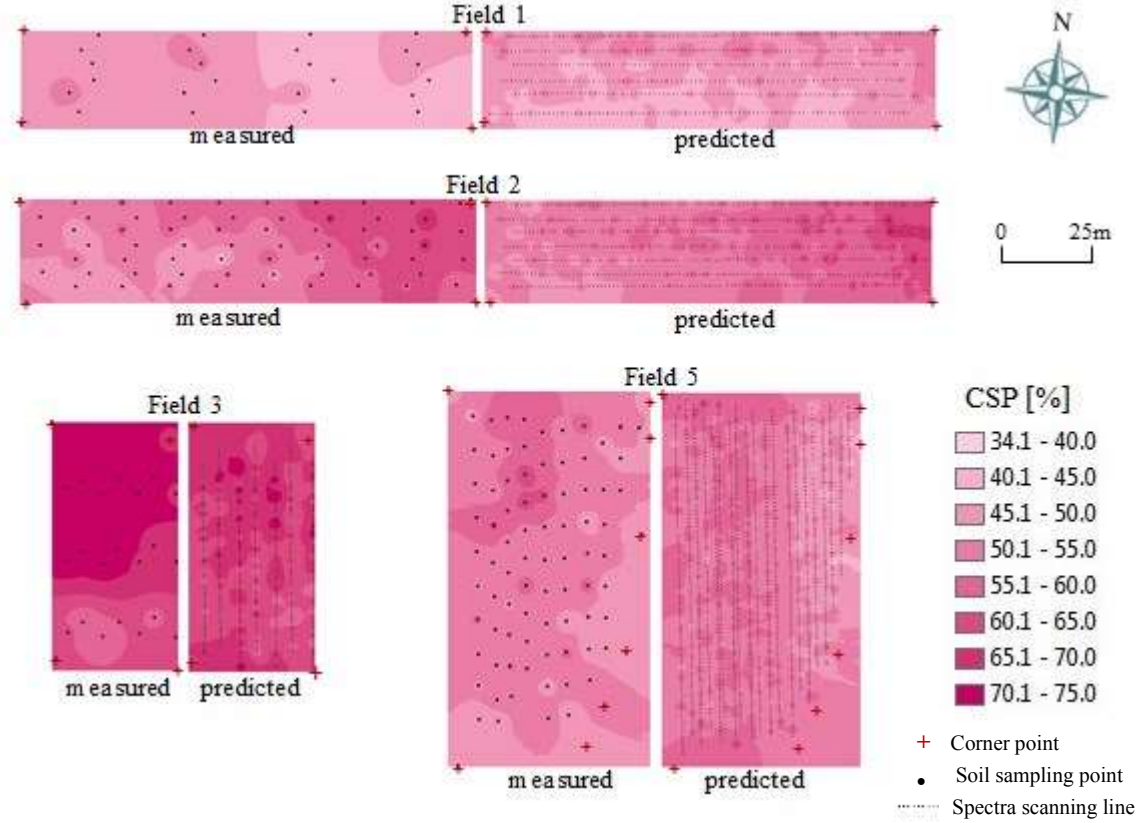


Fig 3.6 (Continued)

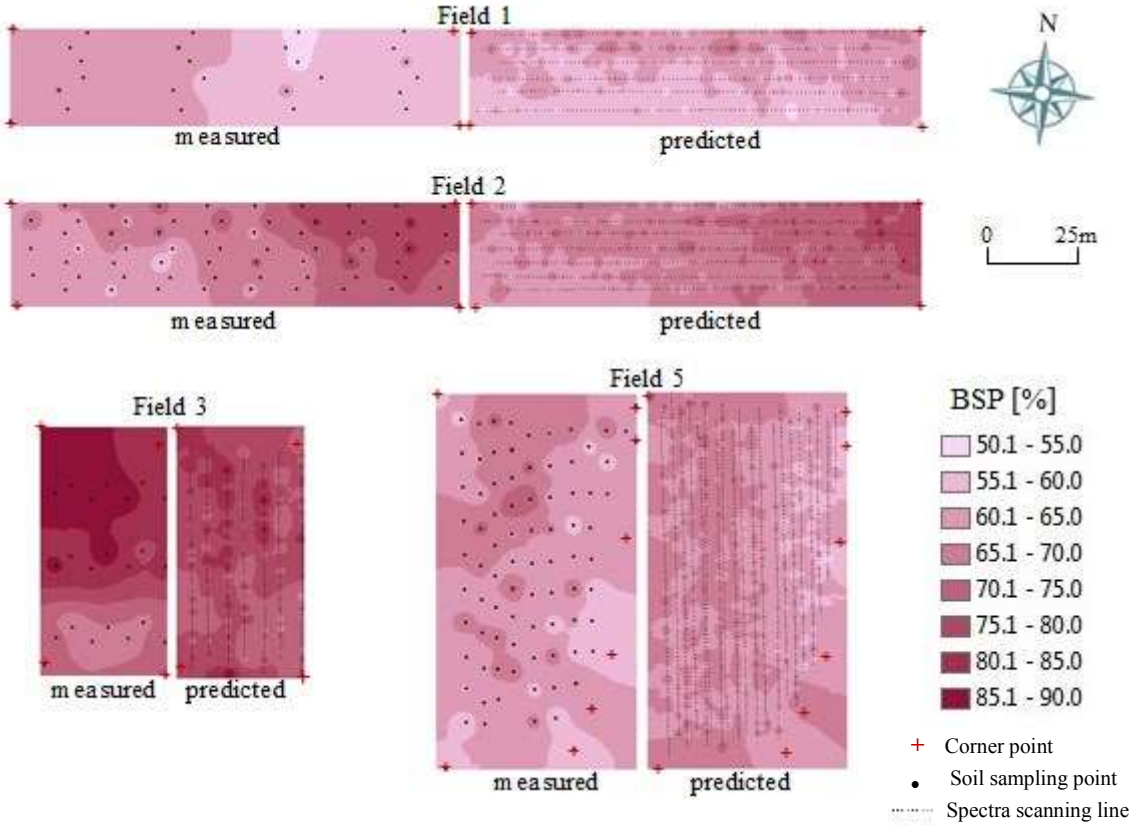


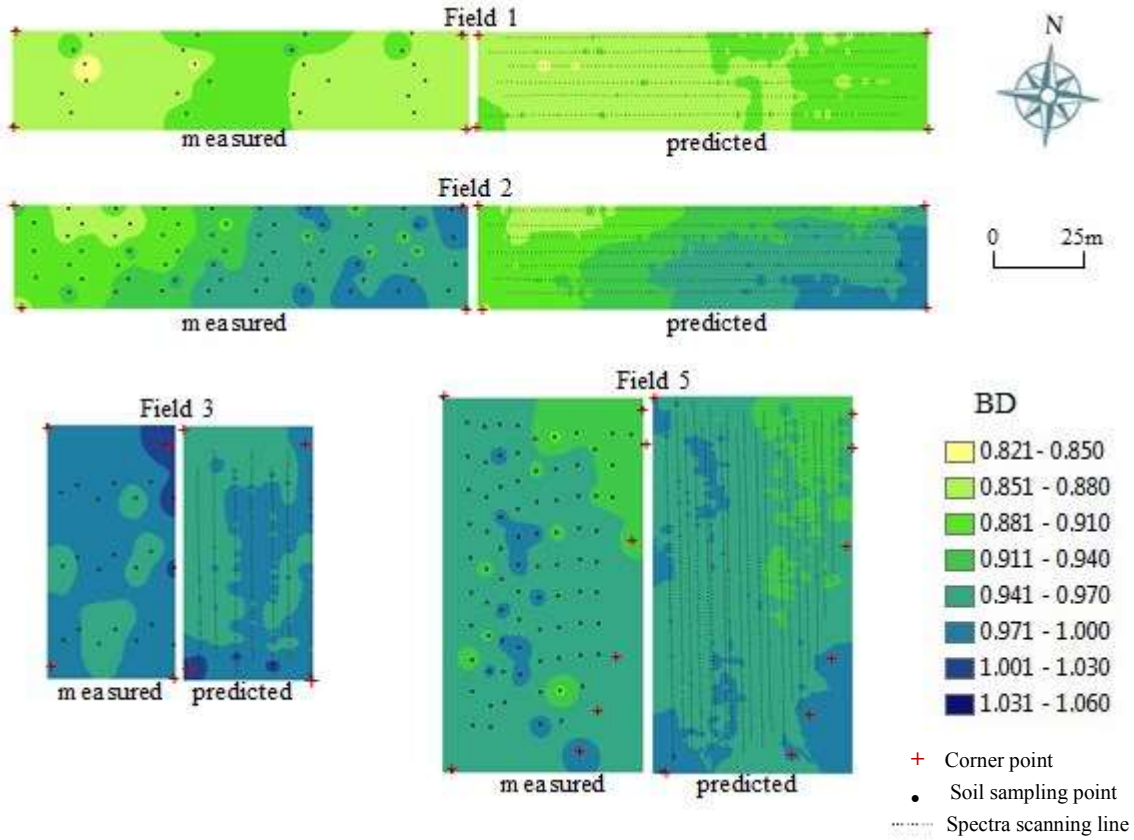


Fig 3.6 (Continued)

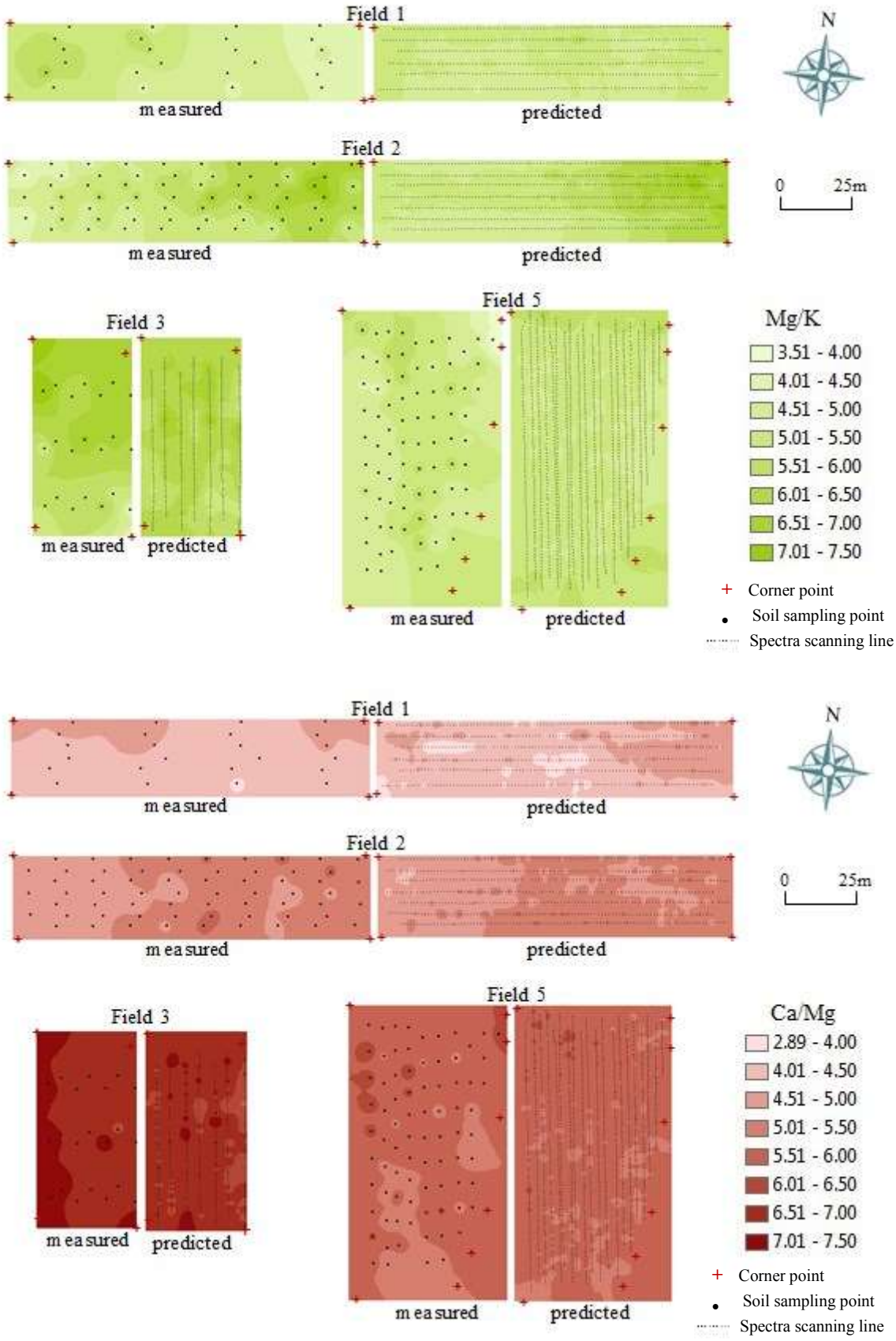


Fig 3.6 (continued)

Table 3.3 Comparison between mean of measured and predicted values of soil properties.

| Soil Properties | Mean Measured (188 samples) | Mean Predicted (188 spectra) | Mean Error (%) |
|---|---|---|---|
| MC (%) | 42.435 | 42.473 | 0.090 |
| SOM (%) | 6.643 | 6.656 | 0.196 |
| pH | 6.005 | 5.985 | 0.333 |
| EC (μS/cm) | 49.691 | 50.057 | 0.737 |
| CEC (me/100g) | 9.700 | 9.626 | 0.763 |
| C-t (%) | 1.737 | 1.726 | 0.633 |
| N-t (%) | 0.163 | 0.162 | 0.613 |
| N-a (mg/100g) | 0.668 | 0.601 | 10.030 |
| N-h (mg/100g) | 4.817 | 4.776 | 0.851 |
| N-n (mg/100g) | 0.116 | 0.142 | 22.731 |
| P-a (mg/100g) | 24.684 | 24.452 | 0.940 |
| PAC (non) | 320.223 | 323.747 | 1.100 |
| Ca (mg/100g) | 147.067 | 146.484 | 0.396 |
| K (mg/100g) | 8.874 | 8.745 | 1.454 |
| Mg (mg/100g) | 19.725 | 19.476 | 1.262 |
| B (ppm) | 0.752 | 0.756 | 0.532 |
| Cu (ppm) | 4.990 | 5.068 | 1.563 |
| Mn (ppm) | 17.279 | 16.305 | 5.637 |
| Zn (ppm) | 4.571 | 4.067 | 11.026 |
| CSP (%) | 54.447 | 54.618 | 0.314 |
| BSP (%) | 66.452 | 66.798 | 0.521 |
| BD | 0.938 | 0.939 | 0.107 |
| Mg/K | 5.316 | 5.330 | 0.263 |
| Ca/Mg | 5.407 | 5.410 | 0.055 |

The evaluation of the accuracy of the prediction model developed from the Vis-NIR spectra was performed by visual comparison between the spatial variation of reference (laboratory) and real-time measurement. On the other hand, the statistical evaluation of map similarity could be performed by considering the mean

error between the two techniques of measurement as listed in Table 3.3. The prediction error for each soil property ranged from 0.055% to 22.731% with the smallest and largest prediction errors were Ca/Mg and N-n respectively.

### 3.3.3 Comparison with Previous Study

Table 3.4 shows the result of comparison between this study and a previous study by Kodaira and Shibusawa (2014c). The previous study was conducted on an upland agriculture fields and the Vis-NIR RTSS model used was SAS1000 whereas our study used the SAS2500 model for spectra acquisition at a paddy field. The tractor speed in previous study was 0.56 $ms^{-1}$ and the spectra was acquired at the depth of 15 cm. To the best of our knowledge, this previous study has the most number of soil properties (25 soil properties) investigated for their potential in predicting and mapping based on a single scan of Vis-NIR spectra acquired using a single real-time sensor system. Hence, this previous study was selected as a comparison for our study.

As shown in Table 3.4, the category of RPD for pH, Mg, Mn, BD and Ca/Mg on the prediction models of this study is better than the previous study while MC, N-a, N-n, P-a and PAC are slightly poorer than previous study. The RPD categories of other 15 soil properties and are the same as in both studies. The accuracies of $R^2_{val}$ for Vis-NIR modeling compared with the previous study are better for SOM, pH, Ca, K, Mg, B, Cu, Mn, CSP, BSP, and Ca/Mg. The other 13 soil properties show slightly poorer accuracies than in the previous study. As reported by Bricklemyer (2011), field moisture content is one of the factors that can reduce the accuracy of Vis-NIR method. Chang et al. (2005) showed that small increases in

Table 3.4. Comparison of quantitative predictions for the soil properties with previous study.

| Soil Properties | $R^2_{val}$ | | RPD | | [d]Category | |
|---|---|---|---|---|---|---|
| | S | K | S | K | S | K |
| MC (%) | 0.70 | 0.84 | 1.81 | 2.52 | B | A |
| SOM (%) | 0.82 | 0.71 | 2.33 | 13.47 | A | A |
| pH | 0.78 | 0.65 | 2.11 | 1.68 | A | B |
| EC (μS/cm) | 0.50 | 0.65 | 1.41 | 1.69 | B | B |
| CEC (me/100g) | 0.73 | 0.74 | 1.90 | 1.95 | B | B |
| C-t (%) | 0.77 | 0.82 | 2.13 | 2.36 | A | A |
| N-t (%) | 0.75 | 0.80 | 2.10 | 2.22 | A | A |
| N-a (mg/100g) | 0.43 | 0.69 | 1.33 | 1.79 | C | B |
| N-h (mg/100g) | 0.54 | 0.74 | 1.46 | 1.94 | B | B |
| N-n (mg/100g) | 0.45 | 0.80 | 1.22 | 2.25 | C | A |
| P-a (mg/100g) | 0.50 | 0.78 | 1.43 | 2.12 | B | A |
| PAC (non) | 0.66 | 0.79 | 1.71 | 2.20 | B | A |
| Ca (mg/100g) | 0.72 | 0.64 | 1.87 | 1.67 | B | B |
| K (mg/100g) | 0.66 | 0.64 | 1.73 | 1.67 | B | B |
| Mg (mg/100g) | 0.80 | 0.64 | 2.21 | 1.67 | A | B |
| B (ppm) | 0.70 | 0.64 | 1.67 | 1.67 | B | B |
| Cu (ppm) | 0.65 | 0.64 | 1.69 | 1.67 | B | B |
| Mn (ppm) | 0.90 | 0.64 | 3.19 | 1.67 | A | B |
| Zn (ppm) | 0.55 | 0.64 | 1.50 | 1.67 | B | B |
| CSP (%) | 0.73 | 0.64 | 1.93 | 1.67 | B | B |
| BSP (%) | 0.67 | 0.64 | 1.74 | 1.67 | B | B |
| BD | 0.70 | 0.73 | 2.00 | 1.93 | A | B |
| Mg/K | 0.49 | 0.65 | 1.41 | 1.68 | B | B |
| Ca/Mg | 0.83 | 0.64 | 2.46 | 1.67 | A | B |

S = This study,

K = Study by Kodaira and Shibusawa (2014c),

[d]Category of prediction (full cross-validation) ability of PLSR for parameters. A: Excellent (RPD>2.0);

B: Good (1.4<RPD<2.0); C: Unreliable (1.4<RPD) (Chang et al., 2001).

moisture content can considerably change the reflectance baseline and increase the peak intensities at 1400 nm. This probably the reason for low accuracy of some soil properties' models in this study as the mean soil moisture content measured in the laboratory for this study is higher (42.44%) than in the previous study (21.87%). Although the accuracy of these 13 soil properties models is better in the previous study, this study however, has demonstrated some improvement on the accuracies of other 11 soil properties' calibration models.

## 3.4 Summary and Conclusion

Twenty-four spectroscopic calibration models for 24 soil properties were developed based on Vis-NIR underground reflectance spectra collected by the RTSS on a commercial paddy field. The 24 soil properties investigated in this study were MC, SOM, pH, EC, CEC, C-t, N-t, N-h, N-n, N-a, P-a, Ca, K, Mg, B, Cu, Mn, Zn, PAC, BD, BSP, CSP, Ca/Mg and Mg/K. This study showed that 22 out of 24 soil properties can be predicted (RPD>1.4) by just a single scan of Vis-NIR using a single soil sensor in real-time with different levels of model accuracy. Only two soil properties' models are unreliable which were N-a and N-n (RPD<1.4).

Improvement of the reliability and robustness of the calibration models which then improves the quality of the developed maps is necessary in future. One of the suggestions in further studies is to incorporate more soil samples from various types of cultivation fields at other regions of Japan in order to have large variability of soil properties. Using a wider spectra range probably up to 2500 nm also need to be taken into account as there are perhaps important absorption features available between 1700 and 2500 nm especially for N-a and N-n. However, the efficiency of using wider range

of NIR need to be investigated as Mouazen et al., 2006b, claimed that a full range NIR spectrometer was less advantageous for real-time measurement. Further research need to be carried out to determine the basis of the calibration for soil properties that do not have direct spectra response. The correlation between the primary/secondary soil properties (have direct spectra response) with tertiary properties (do not have direct spectra response) need to be elucidated for better understanding of the surrogate calibration. The validation of the model on independent validation set need to be also carried out as to examine whether it will be robust or limited to the conditions under which the calibration samples were obtained. Although the on-line developed predicted maps did not perfectly match the corresponding measured maps for all the 24 soil properties especially for Field 1 and Field 3, the similar pattern of distribution that existed between the two map groups is sufficient to declare that the Vis-NIR real-time soil sensor measurement system is a promising technique for real-time measurement of numerous soil properties.

# Chapter 4

# Integrated Calibration Modelling Approach for Soil Mapping

**ABSTRACT**

The visible-near infrared (Vis-NIR) based real-time soil sensor (RTSS) is found to be a great tool for determining distribution of various soil properties for precision agriculture purposes. However, the developed calibration models applied on the collected spectra for prediction of soil properties were site-specific (local). This is found to be less practical since the RTSS needs to be calibrated separately for every field. Integrated calibration approach is expected to minimize this limitation. This chapter describes the feasibility of integrated calibration model developed from three types of agriculture fields and to compare the performance of this model with the local models. For this purpose, the datasets (reference value and spectra) collected from previous study were used to develop 3 local calibration models, 1 calibration model for paddy field and 1 integrated calibration, model using partial least square regression (PLSR) technique coupled with full cross-validation for MC, SOM, C-t, N-t and P-a.

The first two local models (M and Y) were developed using dataset from organic and inorganic paddy field respectively while the third local model (Ob) used the datasets from upland field. The fourth model (MY) was combination of organic and inorganic paddy field (paddy model) and the fifth model (IM – integrated model) was developed from combination of dataset from all the three fields. Results showed for MC, C-t and P-a, the IM produced the highest prediction accuracy with the $R^2_{val}$ are 0.94, 0.91 and 0.86 respectively. The Y local model produced the lowest accuracy for all the soil properties. From this result, it can also be noted that the calibration model which combined datasets from all the three sites (IM model) resulted in the highest RPD for MC, C-t and P-a with the RPD values were 4.1, 3.3 and 2.7 respectively. The maps generated through prediction on the independent validation set using the IM model showed spatial similarity for the 4 soil properties except P-a. This result could be used as a step towards establishment a robust calibration model for agriculture soil in Japan.

## 4.1 Introduction

The visible-near infrared based real-time soil sensor (Vis-NIR RTSS) is found to be a great tool for describing distribution of various soil properties for precision agriculture purpose. It has been proven to be a rapid, inexpensive and relatively accurate tool for measuring soil properties. Furthermore, this sensing technology offers on-line measurement of multiple soil properties as have been described in Chapter 3. The information on the distribution of these multiple soil properties can be derived from the high-resolution soil map which then can be used for making agronomic decisions and environmental monitoring.

One of the huge advantages of Vis-NIR soil sensor can be that they can replace the need for time-consuming and expensive methods. However, if calibrations need to be developed for many different fields, then the cost of the calibrations may still be too great to make the method practical and a less perfect, but less expensive method may need to be used (Reeves III, 2010). In previous studies including the study described in Chapter 2 and 3 of this thesis, researchers tended to develop local calibration model for each field they measured with Vis-NIR spectroscopy (Imade Anom et al., 2001; Mouazen et al., 2005; Kodaira and Shibusawa, 2013; Tekin et al., 2013). In other words, the developed calibration models applied on the collected spectra for prediction of soil properties were site-specific (local). This found to be less practical since the RTSS needs to be calibrated separately for every field. As consequences, the employment of RTSS for describing soil variability would become less time and cost effective because soil sampling and soil laboratory analysis need to be carried out every time when developing calibration model for every different fields. Shonk et al. (1991) developed an online soil organic matter sensor that was calibrated for each soil landscape rather than a larger geographic area. Mouazen et al. (2005) reported that the calibration of the online sensor to predict MC was limited to one single field, for which the calibration model was developed. From practical point of view, the calibration model of real-time soil sensors should facilitate measurement over a large geographic area. To achieve this requirement, integrated calibration approach is expected to minimize the drawback in the previous real-time soil sensing even though the accuracy of the model might less accurate but still good enough to be acceptable for farm management in precision agriculture application.

In order to establish a robust integrated calibration model, the Vis-NIR spectra and soil samples need to be collected from a wide geographic range. Malley et al. (2004), Viscarra Rossel et al. (2006b), and Stenberg et al. (2010) have drawn soils from a wide geographic range and thus do not directly address the use of reflectance spectroscopy to determine the soil properties for specific field. Estimation of soil properties in these studies has had varying degrees of success. Furthermore, the performance of multi-farm (integrated) models in predicting key soil properties compared with the corresponding models for individual farms with different sample number and statistics has not been explored so far. The objective of this study was therefore to describe the feasibility of integrated calibration model developed from three agriculture fields that have different geographical area, soil texture and soil nutrient management (organic, inorganic and combination). This chapter also compares the results of local models (individual farm) with that of an integrated (multi-farm) model using samples from three farms across three Japan Island. This study can be a preliminary step towards developing a prediction models that could be applied to all Japan agriculture field with whatever the agricultural management history.

## 4.2 Materials and Methods

### 4.2.1 Data Mining

Japan country consists of four main islands which are Honshu, Hokkaido, Kyushu and Shikoku. The soil reference values and Vis-NIR spectra used in this research were not obtained specifically for this work. They are the datasets collected for three different studies. These datasets were obtained from experiments

at three different experimental sites in three different islands of Japan. The first datasets (59 reference values and Vis-NIR spectra) used for this study were originated from Shikoku Island (Figure 4.1) which these datasets were collected for the study in Chapter 2. The details on the procedure of Vis-NIR spectra acquisition, soil sampling and analysis are as explained in Chapter 2, section 2.2.

For the second datasets, a field experiment was conducted at the same experimental site with the study explained in Chapter 4. This experimental site located at Honshu Island (Figure 4.1) and the field experiment was carried out on spring 2013. However, for this study, only Field 2 and Field 5 were involved and numbers of soil samples collected from these two fields were 63 and 67 respectively. The Vis-NIR spectra were also acquired from only these fields. The similar procedure of Vis-NIR spectra acquisition, soil sampling and soil analysis as described in Chapter 3, session 3.2 were performed for this field experiment and soil analysis.

The third datasets utilized in this research was the datasets for the study that was conducted by Kodaira and Shibusawa (2013) who demonstrated the used of Vis-NIR real-time soil sensor for high resolution mapping of soil properties. The collection of the Vis-NIR spectra and soil sample in this study were conducted at a commercial upland field at Obihiro city of Tokachi sub-prefecture in Hokkaido island Japan (Figure 4.1). The crop rotation system used at the site was five crops for 5 years: winter wheat–sugar beet–soy bean–potato–green manure (Kodaira and Shibusawa, 2013). The Vis-NIR spectra acquisition the soil sampling for development of calibration model were performed on Field A (4.43 ha, 303.0×146.2 m; 42°50′55.32″ N and 143°00′13.68″ E) and Field B (4.51 ha,

303.0×148.8 m; 42°50′52.85″ N and 143° 00′19.86″ E) after harvesting winter wheat in August 2008. Soil samples and Vis-NIR spectra were also collected at Field A after harvesting soy bean in October 2009. Details on the procedure of Vis-NIR spectra acquisition, soil sampling, soil analysis and calibration model developement were described by Kodaira and Shibusawa (2013). Figure 4.1 shows the location of the three different experimental sites for three different studies and Table 4.1 listed the characteristic of these three different sites.

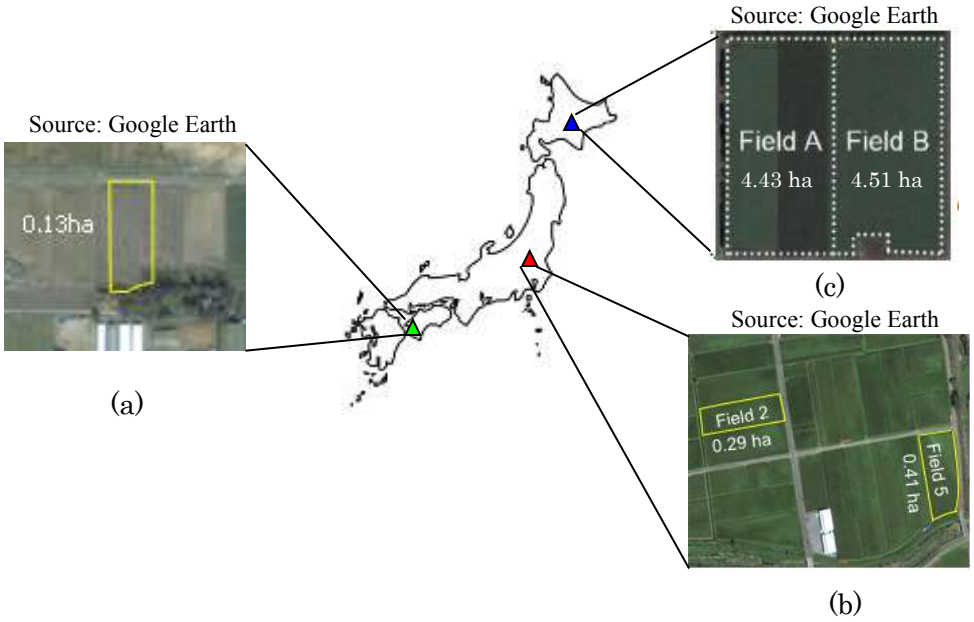


Fig 4.1 Location of the experimental site of three different studies (a) Matsuyama in Shikoku Island (b) Yamatsuri in Honshu Island and (c) Obihiro in Hokkaido Island.

Table 4.1 Characteristic of three sites.

| Site Location | | Matsuyama | Yamatsuri | Obihiro |
|---|---|---|---|---|
| Field Type | | Paddy Field | Paddy Field | Upland Field |
| Soil Nutrient Management | | Organic | Inorganic | Organic + inorganic |
| Soil Composition (%) | sand | 57.89 | 64.05 | 81.41 |
| | silt | 19.18 | 14.90 | 11.32 |
| | clay | 22.90 | 21.05 | 7.27 |
| Soil texture | | Sandy-clay-loam | Sandy-clay-loam | Loamy-sand |
| Model of RTSS used for Vis-NIR spectra acquisition | | SAS1000 | SAS1000 | SAS1000 |

### 4.2.2 Development of Local and Integrated Calibration Model

The soil properties investigated in this study were MC, SOM. C-t, N-t and P-a. For each of the soil property, five calibration models were developed. The first model (M model) is a local model which was developed as in Chapter 2 (using dataset spectra and reference values from Matsuyama field), the second model (Y model) was developed using the 130 dataset from Yamatsuri field and the third model (Ob model) was developed by Kodaira and Shibusawa (2013) using 144 dataset from Obihiro field. These three models were classified as local model as these models were developed from a single site datasets. The fourth calibration model (MY model) was developed by combining the datasets from Matsuyama (59 dataset) and Yamatsuri field (130 datasets) where these two fields were organic and inorganic paddy fields. The fifth model which is regarded as integrated calibration model (IM) was a model that developed by incorporation of all the three sites datasets (333 datasets). All of the calibration models were subjected to a PLSR with full cross-validation using the Unscramber X10.2 software (Camo Inc.; Oslo,

Norway). The number of factors for a model was determined by examining the plot of full cross-validation residual variance against the number of factors obtained from PLSR. Furthermore, outliers were then detected by checking the residual sample variance plot after the PLSR. Samples located far from the zero line of residual variance on the validation views were considered to be outliers and excluded from the analysis. The number of sample outliers was determined as 10 percent of the total samples calculated in the PLSR. Therefore, 6, 13 and 14 datasets were removed as outliers for the M, Y and Ob model respectively. For MY model, 19 sample outliers were removed whereas 33 sample outliers were removed for IM model. The performance of the five calibration models for each of the soil property were then assessed based on the value of $R^2_{val}$ and RPD produced from the PLSR analysis.

### 4.2.3 Preparation of Soil Properties Maps

The integrated models of each soil property were then used to provide quantitative prediction on Vis-NIR soil spectra that was collected from Field A in the year 2009 (independent set). These prediction values were then mapped using ArcGIS Ver10.0 software and interpolated using the inverse distance weighing (IDW) method. The measured values which were obtained from the laboratory soil analysis on the soil samples collected at Field A in 2009 were also mapped as to allow useful comparison of these measured maps with the predicted maps.

## 4.3 Results and Discussions

### 4.3.1 Soil Compositions and Spectra Properties

The statistic result (Table 4.2) of the laboratory soil chemical analysis shows that the Yamatsuri site possesses the highest content of MC, SOM, N-t and P-a while Obihiro site possessed the highest content of C-t. However, the variability of Matsuyama field is the highest for C-t, N-t and P-a while the variability of Obihiro Field is the highest for MC and SOM based on the coefficient of variations (CV) of all the fields. Yamatsuri Field possessed the lowest variability of all the soil properties. Merging of datasets of the two paddy fields (Matsuyama and Yamatsuri) increased the variability of MC and SOM while the variability of datasets from Matsuyama Field for other three soil properties remains highest. Integration of all the three fields data, increased the variability for only MC and P-a.

The mean $2^{nd}$ derivatives of absorbance Vis-NIR spectra for the three fields are depicted in Figure 4.2. The spectral data were analyzed by principal component analysis (PCA). The two-dimensional scatter plot of PCA gives information about patterns among the spectra samples (Figure 4.3). The closer together samples were in the scatter plot, the more similar they were in composition as reflected in their spectra. The spectra of Matsuyama group tended to separate between spectra of Yamatsuri and Obihiro group along the PC-1 axis. From this scatter plot also, the discrimination on the spectra for different depths of Matsuyama field (10, 15, and 10 cm) and different plots (Field 2 and Field 5; Field A and Field B) of Yamatsuri and Obihiro field can be observed along the PC-2 axis.

Table 4.2 Statistical results of soil chemical analysis on soil properties in calibration dataset

| Calibration Dataset | [a]SP | [b]n | Mean | Min | Max | [c]SD | [d]CV |
|---|---|---|---|---|---|---|---|
| Matsuyama | MC (%) | 59 | 18.25 | 11.77 | 23.63 | 2.47 | 13.53 |
| | SOM (%) | 59 | 5.21 | 3.85 | 6.30 | 0.61 | 11.71 |
| | C-t (%) | 59 | 1.23 | 0.50 | 1.94 | 0.42 | 34.15 |
| | N-t (%) | 59 | 0.13 | 0.07 | 0.18 | 0.03 | 23.08 |
| | P-a (%) | 59 | 28.39 | 10.04 | 53.99 | 9.63 | 33.92 |
| Yamatsuri | MC (%) | 130 | 32.94 | 26.36 | 40.12 | 3.06 | 9.29 |
| | SOM (%) | 130 | 7.65 | 6.11 | 9.13 | 0.61 | 7.97 |
| | C-t (%) | 130 | 1.65 | 1.13 | 2.10 | 0.23 | 13.94 |
| | N-t (%) | 130 | 0.15 | 0.11 | 0.19 | 0.02 | 13.33 |
| | P-a (%) | 130 | 22.49 | 14.69 | 28.43 | 3.51 | 15.61 |
| Obihiro* | MC (%) | 144 | 21.87 | 11.32 | 34.36 | 5.30 | 24.23 |
| | SOM (%) | 144 | 6.59 | 3.88 | 10.22 | 1.14 | 17.30 |
| | C-t (%) | 144 | 1.88 | 0.81 | 3.13 | 0.47 | 25.00 |
| | N-t (%) | 144 | 0.14 | 0.07 | 0.24 | 0.03 | 21.43 |
| | P-a (%) | 144 | 54.23 | 25.20 | 114.73 | 17.29 | 31.88 |
| Matsuyama and Yamatsuri | MC (%) | 189 | 28.35 | 11.77 | 40.12 | 7.40 | 26.10 |
| | SOM (%) | 189 | 6.89 | 3.85 | 9.13 | 1.29 | 18.72 |
| | C-t (%) | 189 | 1.52 | 0.50 | 2.10 | 0.35 | 23.03 |
| | N-t (%) | 189 | 0.15 | 0.07 | 0.19 | 0.03 | 20.00 |
| | P-a (%) | 189 | 24.33 | 10.04 | 53.99 | 6.67 | 27.42 |
| Matsuyama + Yamatsuri + Obihiro | MC (%) | 333 | 25.55 | 11.32 | 40.12 | 7.31 | 28.61 |
| | SOM (%) | 333 | 6.76 | 3.85 | 10.22 | 1.23 | 18.20 |
| | C-t (%) | 333 | 1.67 | 0.50 | 3.13 | 0.44 | 26.35 |
| | N-t (%) | 333 | 0.14 | 0.07 | 0.24 | 0.03 | 21.43 |
| | P-a (%) | 333 | 37.26 | 10.04 | 114.73 | 19.34 | 51.91 |

[a]Soil Properties

[b]number of samples

[c]standard deviation

[d]coefficient of variation

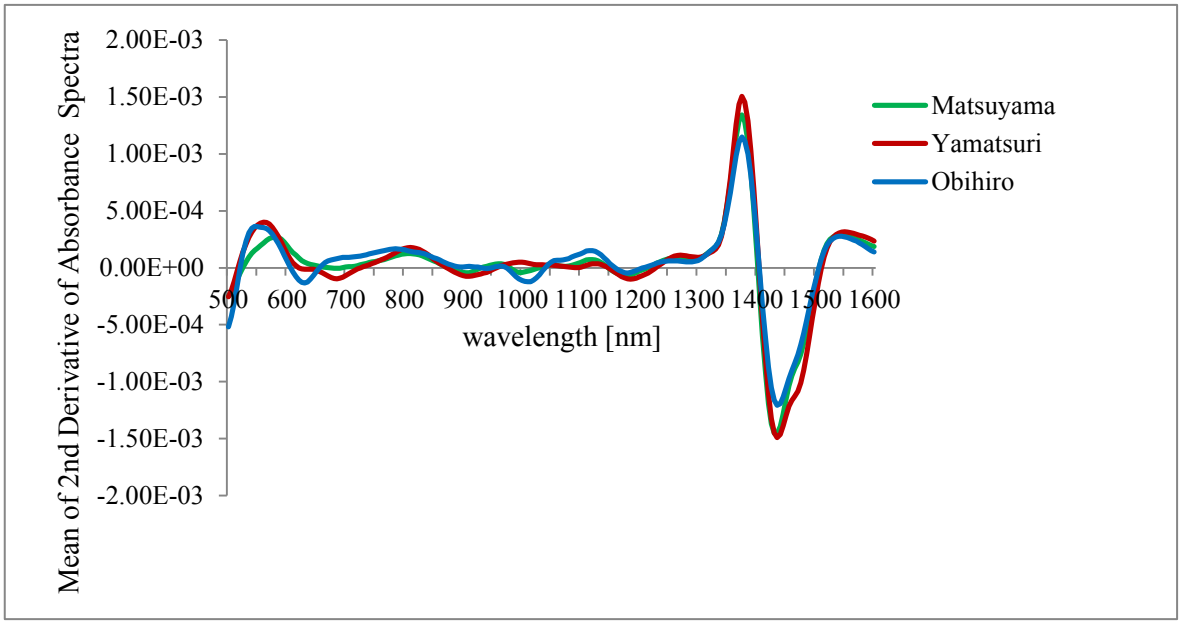


Fig. 4.2 The mean of 2nd Derivative of absorbance spectra of Matsuyama and Yamatsuri and Obihiro soil

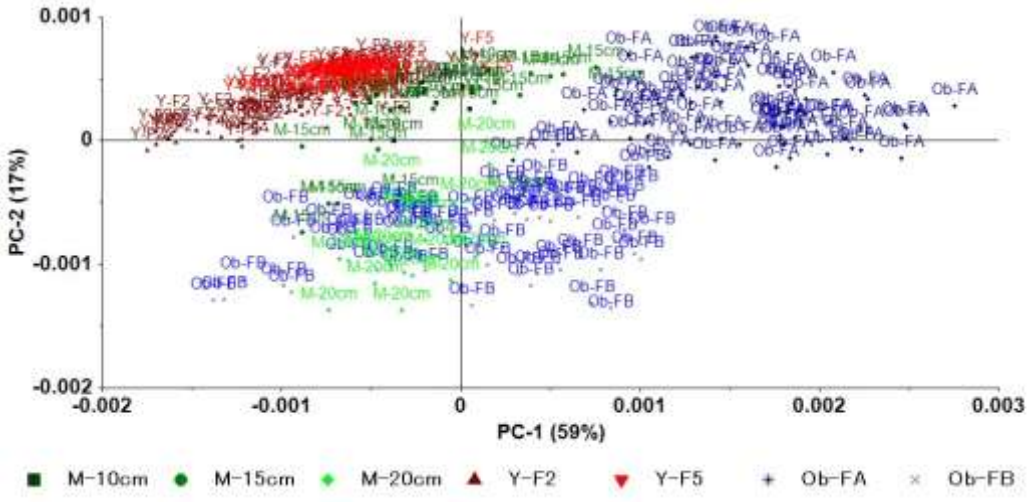


M-10cm : Matsuyama at depth of 10cm, M-15cm : Matsuyama at depth of 15cm, M-20cm : Matsuyama at depth of 20cm Y-2 : Yamatsuri Field 2, Y-5 : Yamatsuri Field 5, Ob-FA : Obihiro Field A, Ob-FB : Obihiro Field B

Fig. 4.3 Score plot of the 333 samples on the first two principal components explaining the variance in the Vis-NIR spectral data.

### 4.3.2 Comparison of Calibration Models

The PLSR results of the calibration and validation were obtained as shown in Table 4.3. Based on the $R^2_{val}$, IM model that combined datasets of soil from all fields resulted in the highest accuracy for MC, C-t and P-a due to the $R^2_{val}$ are 0.94, 0.91 and 0.86 respectively. For SOM, the accuracy of MY calibration model was the highest ($R^2_{val}$ = 0.95) while the Ob calibration model was the highest for N-t ($R^2_{val}$ = 0.87). The lowest model accuracy for all the soil properties was Y model.

Referring to the classification by Chang et al. (2001), all of the calibration models fall in excellent category (RPD>2.0) except Y model for MC and three local models (M, Y, and Ob) for P-a where their models fall in good category (2.0<RPD<1.4). From this result, it can also be noted that the calibration model which combined datasets from all the three sites (IM model) resulted in the highest RPD for MC, C-t and P-a with the RPD values were 4.1, 3.1 and 2.7 respectively. For SOM, the MY model obtained the highest RPD value (4.6) and for N-t, four models (M, Ob, MY and IM) has similar RPD value (3.0). The scatter plots of the IM models are depicted in Figure 4.4.

Table 4.3 Summary of Partial Least Square Regression (PLSR)

| Calibration Model | [a]SP | [b]n | calibration | | validation | | SD | RPD |
|---|---|---|---|---|---|---|---|---|
| | | | $R^2_{cal}$ | $RMSE_{cal}$ | $R^2_{val}$ | $RMSE_{val}$ | | |
| M (Matsuyama) | MC | 53 | 0.95 | 0.85 | 0.88 | 1.38 | 3.95 | 2.9 |
| | SOM | 53 | 0.87 | 0.23 | 0.83 | 0.26 | 0.63 | 2.4 |
| | C-t | 53 | 0.91 | 0.13 | 0.88 | 0.15 | 0.43 | 2.9 |
| | N-t | 53 | 0.88 | 0.01 | 0.85 | 0.01 | 0.03 | 3.0 |
| | P-a | 53 | 0.87 | 3.02 | 0.72 | 4.53 | 8.50 | 1.9 |
| Y (Yamatsuri) | MC | 117 | 0.77 | 0.14 | 0.73 | 1.52 | 2.89 | 1.9 |
| | SOM | 117 | 0.85 | 0.21 | 0.79 | 0.26 | 0.56 | 2.2 |
| | C-t | 117 | 0.77 | 0.10 | 0.74 | 0.11 | 0.22 | 2.0 |
| | N-t | 117 | 0.77 | 0.01 | 0.74 | 0.01 | 0.02 | 2.0 |
| | P-a | 117 | 0.84 | 1.97 | 0.65 | 1.97 | 3.31 | 1.7 |
| Ob (Obihiro) (Kodaira and Shibusawa, 2013) | MC | 130 | 0.95 | 1.23 | 0.93 | 1.42 | 5.11 | 3.6 |
| | SOM | 130 | 0.92 | 0.30 | 0.90 | 0.35 | 1.02 | 2.9 |
| | C-t | 130 | 0.91 | 0.13 | 0.89 | 0.15 | 0.42 | 2.8 |
| | N-t | 130 | 0.89 | 0.01 | 0.87 | 0.01 | 0.03 | 3.0 |
| | P-a | 130 | 0.76 | 7.46 | 0.72 | 8.00 | 14.35 | 1.8 |
| MY (Matsuyama + Yamatsuri) | MC | 170 | 0.93 | 1.30 | 0.90 | 1.55 | 4.77 | 3.1 |
| | SOM | 170 | 0.97 | 0.22 | 0.95 | 0.28 | 1.28 | 4.6 |
| | C-t | 170 | 0.90 | 0.11 | 0.87 | 0.13 | 0.36 | 2.8 |
| | N-t | 170 | 0.87 | 0.01 | 0.84 | 0.01 | 0.03 | 3.0 |
| | P-a | 170 | 0.81 | 2.40 | 0.77 | 2.64 | 5.53 | 2.1 |
| IM (Matsuyama + Yamatsuri + Obihiro) | MC | 303 | 0.96 | 1.51 | 0.94 | 1.77 | 7.29 | 4.1 |
| | SOM | 303 | 0.91 | 0.35 | 0.90 | 0.38 | 1.18 | 3.1 |
| | C-t | 303 | 0.93 | 0.12 | 0.91 | 0.14 | 0.44 | 3.1 |
| | N-t | 303 | 0.88 | 0.01 | 0.85 | 0.01 | 0.03 | 3.0 |
| | P-a | 303 | 0.87 | 5.74 | 0.86 | 5.94 | 15.94 | 2.7 |

[a]Soil Properties

[b]Number of samples used in the model

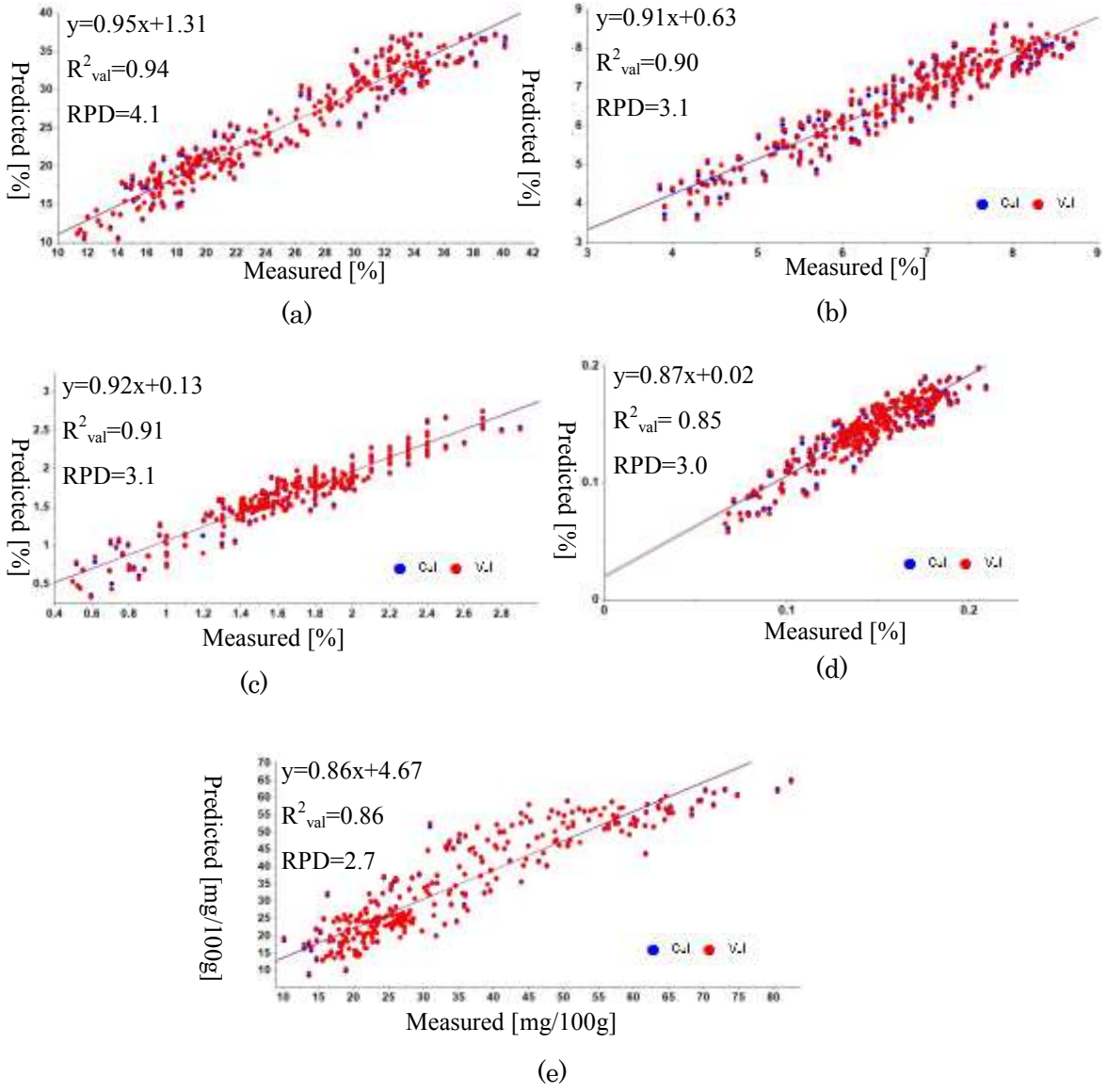


Fig. 4.4 Scatter plot of measured values versus Vis–NIR predicted values of IM model using partial least squares regression (PLSR) coupled with full cross-validation datasets for: (a) MC, (b) SOM, (c) C-t (d) N-t and (e) P-a.

Results from this study show that the combination of the calibration dataset from two or more fields of different soil management has provided a wider range of dataset (reference values and spectra responses), a wider variety sample types and large constituent range which resulted in improvement of model accuracy

for MC, C-t and P-a. The difference model performance between local and integrated model caused by different sample size is attributed to sample statistics, including the coefficient of variation (CV) of the samples in the model and standard deviation (SD). As indicated in Table 4.2, the combination of three sites data increased the CVs for MC, and P-a which resulted on highest $R^2_{val}$ values of these soil properties. The larger value of SD in the IM model also improved the RPD values of this model (Table 4.3) except for SOM where the YM model possessed highest SD and hence highest RPD. The low accuracy of Y model is expected due to the small variability (CV) of Yamatsuri soil properties (Table 4.2). This is consistent with studies by Sudduth et al. (2010) and Udelhoven et al. (2003) who found that when variability in the parameter of interest was small, generally poor estimations of the soil properties was obtained at the field scale. Furthermore, as reported by Bricklemyer (2011), field moisture content is one of the factors that can reduce the accuracy of Vis-NIR method. Chang et al. (2005) showed that small increases in moisture content can considerably change the reflectance baseline and increase the peak intensities at 1400 nm. This might be another reason for the low accuracy of Y model as the soil from Yamatsuri site was high in moisture content than other sites (Table 4.2).

### 4.3.3 Analysis of Prediction Error and Soil Properties Maps.

In order to assess the robustness of the integrated calibration model (IM model), the 72 spectra collected from Field A at Obihiro site on 2009 (independent validation datasets) were used to predict the amount of the five soil properties using the IM model. These prediction values were compared with the measured values obtained from the laboratory analysis on the 72 soil samples collected from

Field A on 2009. Table 4.4 shows the minimum, maximum and mean of the measured and predicted values for all the five soil properties. Also shows in the table are the percentage of error between measured and predicted values. The result from this error analysis showed that the prediction for P-a resulted in the largest error (30.60%) with a large difference in the range (minimum and maximum) between the measured and predicted values. Higher prediction error for P-a than MC, SOM, C-t and N-t can be attributed to that P-a does not has direct spectral responses in the Vis-NIR range (Maleki et al., 2006). This is in line with most studies reporting on the use of Vis-NIR spectroscopy for P-a estimation (Krischenko et al., 1991; Chang et. al, 2001: Williams, 2003). The ranges for other soil properties were just slightly different. The scatter plots of measured values versus the prediction values that were predicted using IM on spectra collected from Field A in year 2009 is depicted in Figure 4.5.

To allow visual comparison, the 72 measured and prediction values of Field A for year 2009 were mapped as illustrated in Figure 4.6. Maps of MC, SOM, C-t and N-t showed a spatial similarity between measured and predicted at most area. The spatial variation for P-a however, showed less distribution similarity. The similar distribution pattern of the two maps provides confidence in the used of IM model for the prediction of MC, SOM, C-t and N-t in fields of loamy-sand soils.

The mean prediction errors were compared with the mean prediction errors from the previous study by Kodaira and Shibusawa (2013) who predicted the amount of the soil properties using the calibration model developed using datasets collected from the same site (local calibration model). In this previous study, Kodaira and Shibusawa (2013) used the local calibration model that was developed

using the datasets collected on Field A in year 2008 to predict and validate the local model on spectra collected at the same field (Field A) in year 2009. The mean error comparison between the integrated model (IM) with the local calibration model (Ob) showed that the error of integrated IM model is smaller than the local Ob model for all the examined soil properties except for P-a. This result indicates that the integrated calibration model is considerably robust for prediction of the soil properties particularly for MC, SOM, C-t and N-t.

Table 4.4 Comparison between measured and predicted values of Field A (independent validation) and mean error percentage between this study (integrated model) and pervious study (local model).

| SP | Min | | Max | | Mean | | Mean error (%) | |
|---|---|---|---|---|---|---|---|---|
| | [a]Meas | [b]Pred | [a]Meas | [b]Pred | [a]Meas | [b]Pred | this study | [c]K&S |
| MC | 20.90 | 23.13 | 36.60 | 36.58 | 29.37 | 29.68 | 1.06 | 1.6 |
| SOM | 4.70 | 4.64 | 8.30 | 8.31 | 6.62 | 6.71 | 1.39 | 9.91 |
| C-t | 1.00 | 1.47 | 2.70 | 2.79 | 1.89 | 2.23 | 18.14 | 19.95 |
| N-t | 0.10 | 0.09 | 0.20 | 0.18 | 0.15 | 0.14 | 6.74 | 7.72 |
| P-a | 40.69 | 28.58 | 114.75 | 56.56 | 64.36 | 44.66 | 30.6 | 18.7 |

[a] Measured, [b] Predicted, [c] Kodaira and Shibusawa (2013)

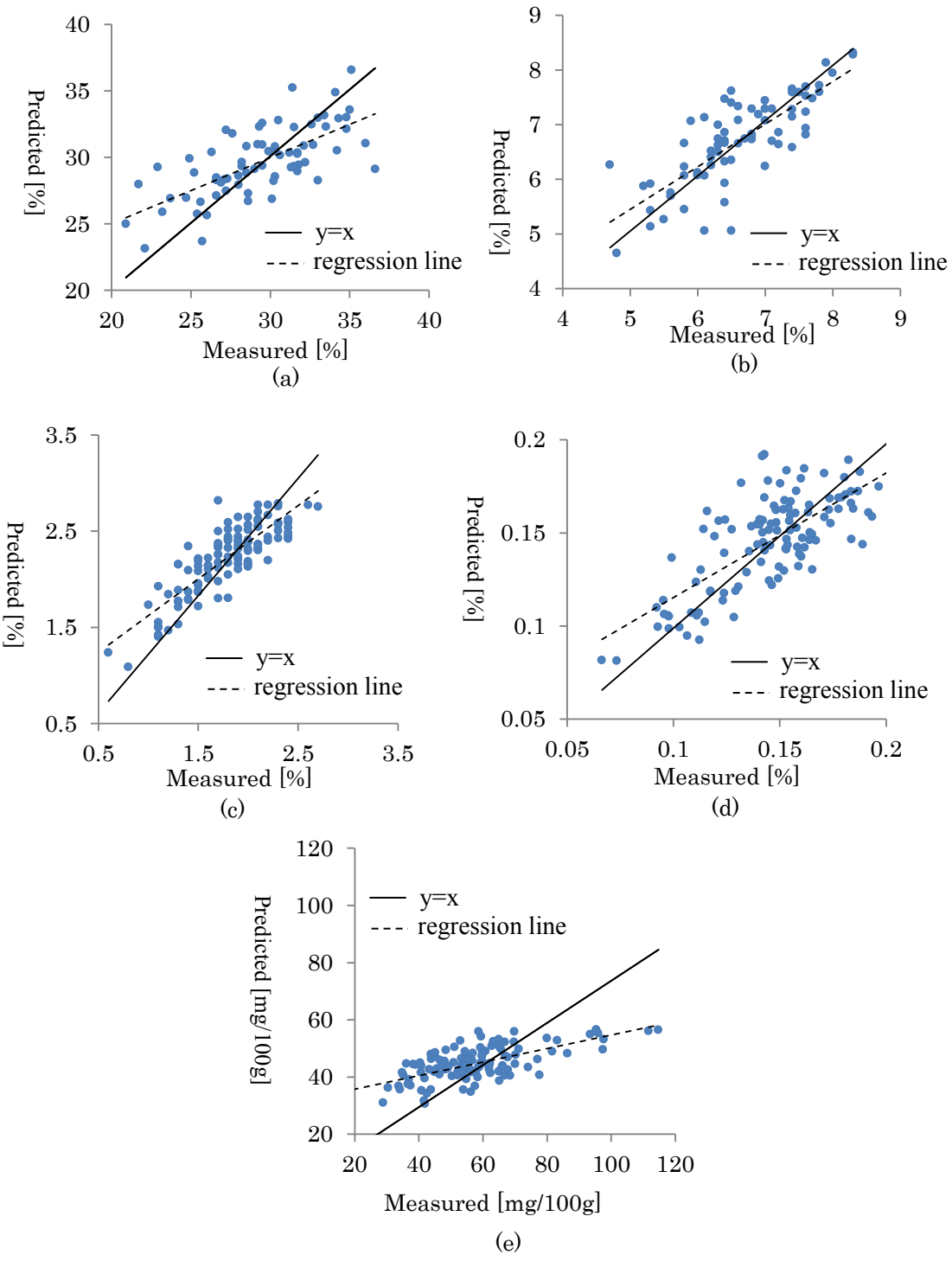


Fig. 4.5 Scatter plot of linear correlation between measured and predicted using IM model on 72 validation Vis–NIR spectra (of Field A collected in year 2009 for: (a) MC, (b) SOM, (c) C-t (d) N-t and (e) P-a.

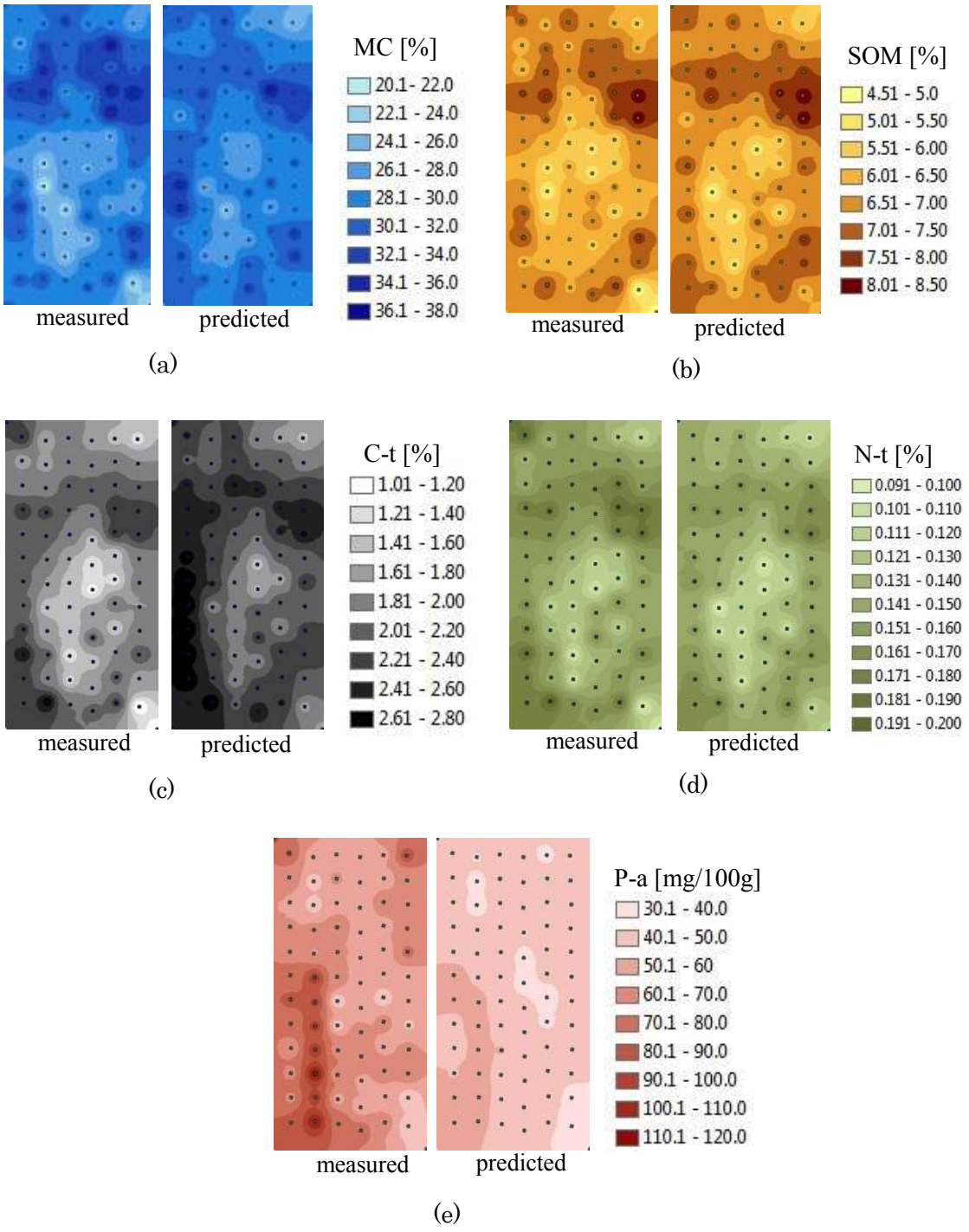


Figure 4.6 Comparison of measured and predicted soil maps of Field A (Obihiro) (predicted using IM) for (a) MC, (b) OM, (c) C-t, (d) N-t and (e) P-a.

## 4.4 Summary and Conclusion

Five spectroscopic calibration models based on Vis-NIR underground reflectance spectra of three different fields have been examined. The fifth model (IM-integrated model) that incorporated soil from the three fields improved the accuracy of the three local model (M, Y and Ob) for MC, C-t and P-a. However, when IM was validated with the independent set, the prediction error of IM for P-a was higher than the local model. The integration of the model has good potential for minimizing the repetitiveness of developing calibration model every time for every different field. With this approach, the time and cost for obtaining the samples and laboratory analysis can be minimized and would simultaneously reduce the total production cost.

Nevertheless, more research is needed to determine the basis for this integrated calibration and whether it will be robust or limited to the conditions under which the calibration samples were obtained, example, same field; same soil type and texture; same crop; geographic area etc. The effects on the robustness of the integrated model due to difference in soil management need to be also investigated. For example, if the integrated model successfully predict the soil properties on one particular field, at one season, whether the similar integrated model is accurately predict the soil properties on the same field at other season which the soil management practice has been altered or changed, need to be examined. Moreover, the calibration sample selection methods need to be optimized which covering as much of the soil variation as possible within the calibration samples which comprise more variability in texture, colour, soil type, climate and origin of soil. Extending the integrated model application for all soil up to national or global level requires further research as an

integrated model probably has certain limitation such as it may be only applicable for the same soil type, colour, texture, moisture content and origin of the soil. Thus, incorporation of more soil samples from various types of cultivation fields at other regions of Japan is necessary in future studies as to improve the robustness of the calibration model that could be applied to all Japan soils with whatever the agricultural management background. The result from this study nevertheless could be used as a preliminary step towards establishment of a robust calibration model of Vis-NIR real-time soil sensing for various type of agriculture soil in future.

# Chapter 5

# Overall Summary and Conclusion

## 5.1 General Conclusion

Numerous researches have been done on quantifying agriculture soil properties and presented the information on soil maps by exploring the features of emerging technologies. Among of these technologies spectroscopy by means of Vis-NIR has huge interest among researchers. From lab-based to the field-based (real-time) spectra measurement for prediction of soil properties, the used of this technique has gone through some development since the last two decades and yet there are still many aspects need to be further improved towards sustainable agriculture practices. This study has presented improved technique and function of soil properties mapping using a Vis-NIR real-time soil sensor as to optimize the used of this state-of-the-art technology towards better agricultural management either for precision agriculture or precision carbon farming practice.

Three aspects of techniques improvement have been discussed in this study. The first aspect is about the measurement of the soil properties in depth direction. The result of

this study indicated that the incorporation of multi-depth soil properties measurement could increase the variability of the soil samples and hence improve the accuracy of the calibration model for prediction of soil properties. The generated maps exhibited variation in the distribution of soil properties not only horizontally but also at different depths. The information that can be derived from the multi-depth soil maps could provide comprehensive information on spatial at three-dimensional soil variability for making precision agronomic decisions.

The used of the Vis-NIR real-time soil sensor for mapping of 24 soil properties was another feature that has been introduced in this study for optimizing the used of this sensor for precision agriculture practice. This study indicates that 22 out of 24 soil properties can be predicted by just a single action of Vis-NIR scanning using a single soil sensor in real-time with different levels of model accuracy. Only two soil properties' models were categorized as unreliable which were N-a and N-n.

Another technique that has been introduced in this study for the improvement of the soil properties measurement using Vis-NIR real-time soil sensor is the integrated calibration modelling approach. The proposed integrated model that incorporated soil from the three fields improved the accuracy of the soil properties. The integration of the model is expected to minimize the repetitiveness of developing calibration model every time for every different field. The result from this study could be used as a preliminary step towards establishment of a robust calibration model of Vis-NIR real-time soil sensor for various type of agricultural soil in future.

## 5.2 Contributions

One of the contributions of this research is to provide improved method of agricultural soil mapping with the aid of real-time soil sensor for the efficiency of agricultural soil management. The technique developed in this research would capable reduce the cost and time in analysis of soil spatial variability for the precision agriculture and precision carbon farming practices which concomitantly increases the profit whilst reduces the environmental impact.

The proposed technique of soil property mapping could be a step towards variable-rate applications such as site specific irrigation, fertilizer and nutrient application in precision agriculture practice. The developed high-resolution soil map can be used as a tool for decision support system and integrated with other components as a production-based farming system. The improvement on the technique of soil quantification and mapping would lead to optimize production efficiency; optimize quality; minimize environmental impact; minimize risk at the site-specific level management practice for precision agriculture and carbon sequestration activity.

The integrated modelling approach has potential in reducing the cost, time and effort needed to transport and analyze the soil samples every time for calibration of the spectra to the soil constituents. Furthermore, the integrated modelling approach could be a step towards the establishment of spectral library for Japanese agriculture soil in future.

## 5.3 Uncertainties

Although the multi-depth soil mapping could provide comprehensive information on the distribution of soil properties in strata and depth direction, whether analysis of only soils'

surface or several soil layers will be sufficient or more likely, how to integrate surface scanning and more limited sub-surface data from perhaps cores, has not been answered. Running the RTSS on deeper soil depth may not be possible for all field conditions as some field possess high soil resistance and the use of RTSS is not practical for such condition. In this case large amounts of more easily acquired surface data will need to be integrated with lesser amounts of harder to get core/sub-surface data to provide an accurate estimate of the total soil properties within a given area/volume of soil especially for estimation of carbon sequestration rate in precision carbon farming practice.

Prediction error of calibration is commonly rooted in its calculation procedure, properties of reference data collected, and noise of spectral data record. Furthermore, natural soil heterogeneity, macro-aggregation, field moisture content are variables that can affect the performance of the soil prediction. The idea on using higher range of NIR for better prediction of some soil properties (such as nitrate) needs to be also considered in term of its noise occurrence. Although several researchers suggested to use further range of NIR for prediction of some soil properties, this method is would probably only suitable for lab-based spectra scanning. For real-time or online spectra acquisitions, where samples were fresh soil (field moist), Mouazen et al., 2006b, claimed that a full range NIR spectra was less advantageous.

Calibrations based on indirect measurements of soil properties that do not have direct spectra response e.g., measure X which correlates with properties Y of interest, are often referred to as surrogate calibrations and work only as long as the surrogate relationship applies to both sample sets (Reeves III, 2010). Results for other similar measures such as EC, CEC, P-a, K, Mg etc. have been found to vary greatly and are likely due to the surrogate nature of the calibrations. While surrogate based calibrations can be useful, one must keep in

mind that changes not related to the measure of interest could change the surrogate and thus make the calibration inaccurate without the user ever knowing (Reeves III, 2010). Another uncertainty is that the performances of the developed 24 calibration model were not tested on independent validation datasets. Thus, the robustness of the developed 24 models for prediction of the 24 soil properties in other seasons is still indistinct.

The basis for this integrated calibration whether it will be robust or limited to the conditions under which the calibration samples were obtained, example, same field; same soil type and texture; same climate; same crop; geographic area is also uncertain. The validation on the independent validation set was just performed on one of the field (Obihiro) that included in the calibration. The performance of the integrated calibration model on other fields that included in the calibration model (Matsuyama and Yamarsuri) and the fields that not included in the calibration model development is still ambiguous.

## 5.4 Suggestions for Future Research

The improvement in the soil properties mapping using the Vis-NIR real-time soil sensor has not come to the ending point. There are more researches need to be carried out in future study as to optimize the used of real-time soil sensor for mapping soil properties for either precision agriculture or precision carbon farming practices. The effects of the soil properties variation at different depths on the soil management such as fertilizer application need to be further investigated. The question on how much yield affected and how much excessive fertilizer applied if the grower observed the soil variability at a single depth is expected to be determine in future study. Furthermore, the idea of 3-dimensional mapping would probably give more comprehensive information about the soil variability. This approach could provide the distribution of the soil properties not only at a discrete

several layers but also in between layers. Moreover, Li (2013) pointed that the assessment of carbon sequestration needs to be considered up to the s 30 cm soil depth. Thus, the quantification of soil C, SOM and N at deeper soil depths need to be considered for carbon inventory in precision carbon farming.

The accuracy of the developed calibration models for 24 soil properties could also be further improved in future study. The low model accuracies some of the soil properties without direct response in the Vis-NIR range need for further investigation to understand and improve the calibration accuracy of these soil properties. Furthermore, the efficiency of the developed maps needs to be investigated on their applicability for soil management such as for variable-rate fertilizer application and soil treatment. Another aspect needs to be taken into account in future research is the economic feasibility on the use of the real-time soil sensor to the farmers. The high cost occurs when deploying this state-of-the art technology would always become one of the issues and become limitation for the adoption of this technology. Thus, the cost-benefit analysis need to be carried out in future study to arrive to a final conclusion on the potential of the Vis-NIR real-time soil sensor for multiple soil properties mapping and subsequently for variable-rate technology application in precision agriculture.

Validation on the integrated calibration model on the field that was not included in the calibration model development is needed to be carried out in future research. Moreover, further research is needed to upgrade the calibration models developed in this study using samples collected from a larger number of fields and regions with even distribution of concentrations along the entire concentration range encountered in agricultural soils. This is recommended to improve the prediction accuracy and robustness of models developed for the studied soil properties. The integrated model could be expand

applications to regional or national (Mouazen et al., 2006c), continental or even global (Brown, 2007) scales. Spectral libraries for global calibration models should include sufficient number of soil samples, which can illustrate the soil variability in the new target site where the prediction will be carried out (Viscarra Rossel et al., 2008; Guerrero et al., 2010). However, the large sample number may increase the prediction error. Therefore, before deciding on the scale of calibration, a decision on the degree of precision required has to be made. Cost evaluation for building calibration models need to be also considered.

# REFERENCES


Adamchuk, V. I., Lund, E., Dobermann, A. and Morgan, M. T. (2003). On-the-go mapping of soil properties using ion-selective electrodes. *In: Stafford, J., Werner, A. (Eds.), Precision Agriculture.* Wageningen Academic Publishers, Wageningen, The Netherlands, 27 – 33.

Adamchuk, V. I., Hummel, J. W., Morgan, M. T. and Upadhyaya, S. K., (2004). On-the-go soil sensors for precision agriculture. *Computers and Electronics in Agriculture*. 44, 71 – 91.

Adamchuk, V. I., Lund, E. D., Reed, T. M. and Ferguson, R. B. (2007). Evaluation of an on-the-go technology for soil pH mapping. *Computers and. Electronics in Agriculture*, 8, 139 – 149.

Barnes, R. J., Dhanoa, M. S. and Lister S. J. (1989). Standard normal variate transformation and detrending of near-infrared diffuse reflectance spectra. *Applied Spectroscopy* , 43, 772 – 777.

Barthes B. G., Brunet, D., Ferrer, H., Chotte, J. L. and Feller, C. (2006). Determination of total carbon and nitrogen content in a range of tropical soils using near infrared spectroscopy: influence of replication and sample grinding and drying. *Journal of Near Infrared Spectroscopy,* 14, 341 – 348.

Baumgardner M. F, Silva L. R. F, Biehl L. L. snd Stoner E. R. (1985). Reflectance properties of soils. *Advances in Agronomy* 38, 1 – 44. doi: 10.1016/S0065-2113(08)60672-0

Ben-Dor, E. and Banin, A. (1995). Near-infrared analysis as a rapid method to simultaneously evaluate several soil properties. *Soil Science Society of America Journal*, 59, 364 – 372.

Blackmer, A. M. and White, S. E., (1998). Using precision farming technology to improve management of soil and fertilizer nitrogen. *Australian Journal of Agricultural Research,* 49, 555 – 564.

Boulesteix A. N. and K. Strimmer. (2007). Partial Least Square: A Versatile Toll for the Analysis of High-dimensional Genomial Data, *Briefings in Bioinformatics,* 8, 32 – 44.

Brejda, J., Moorman, J., Smith, T. B., Karlen, J. L., Allan, D. L. and Dao, T. H. (2000). Distribution and variability of surface soil properties at a regional scale. *Soil Science Society of America Journal*, 64, 974 – 982.

Brenk, C., Pasda, G. and Zerulla, W. (1999). Nutrient mapping of soils – a suitable basis for site-specific fertilisation? In Precision Agriculture '99, (J. Stafford ed.), *Society of Chemical Industry*, 49 – 59.

Brereton, R. G. (2003). Chemometrics: Data Analysis for the laboratory and chemical Plant. John Wiley & Sons: Chichester, England

Bricklemyer, R. S. and Brown, D. J. (2010). On-the-go VisNIR: Potential and limitations for mapping soil clay and organic carbon. *Computers and Electronics in Agriculture,* 70, 209 – 216.

Bricklemyer, R. S., Brown, D. J., Barefield, J. E. and Clegg, S. M. (2011). Intact Soil Core Total, Inorganic, and Organic Carbon Measurement Using Laser-Induced Breakdown Spectroscopy. *Soil Science Society of America Journal*, 75, 1006 – 1018.

Brown, D. J., Shepherd, K. D., Walsh, M. G., Mays, M. D. and Reinsch, T. G. (2005). Global soil characterization with VNIR diffuse reflectance spectroscopy. *Geoderma,* 129 (3–4), 215 – 267.

Burrough P. A. and Mcdonnell, R. A. (1998). Principles of Geographic Information Systems (Oxford University Press) 356.

Cahn M. D, Hummel, J. W. and Brouer, B. H. (1994). Spatial analysis soil fertility for site-specific crop management. *Soil Science Society of America Journal*, 58, 1240 – 1248.

Castrignano, A., Giugliarini, L., Risaliti, R. and Martinelli, N. (2000). Study of spatial relationship among some soil physico-chemical properties of a field in central Italy using multivariate geostatistic, *Geoderma*, 97, 39 – 60.

Chang, C. W., Laird, D. A., Mausbach, M. J. and Hurburgh Jr., C. R. (2001). Near-infrared reflectancespectroscopy—principal components regression analysis of soil properties. *Soil Science Society of America Journal*, 65, 480 – 490.

Chang, C. W. and Laird, D. W. (2002). Near-infrared reflectance spectroscopic analysis of Soil C and N. *Soil Science,* 167, 110 – 116

Chang, C. W., Laird, D. A. and Hurburgh Jr., C. R. (2005). Influence of soil moisture on nearinfrared reflectance spectroscopic measurement of soil properties. *Soil Science*, 170, 244 – 255.

Chen, F., Kissel, D. E, West, L. T. and Adkins, W. (2000). Field-scale mapping of surface soil organic carbon using remotely sensed imagery. *Soil Science Society of America Journal*, 64, 746 – 753.

Cheng, B. and Wu, X. (2006). A Modified PLSR Method in Prediction. *Journal of Data Science,* 4, 257 – 274.

Christy C. D., Drummond, P. and Lund, E. (2010). Precision Agriculture Applications of an on-the-go Soil Infrared Reflectance Sensor, 1 – 12. Retrieved from http://www.veristech-com/pdf_files/Optical_8thinticonf.pdf on 26th November 2012.

Christy C. D., Drummond, P. and Laird, D. A. (2003). An on-the-go spectral reflectance sensor for soil. ASAE Paper No 031044. 2003 ASAE Annual Meeting, Las Vegas, NV

Christy, C. D. (2008). Real-time measurement of soil attributes using on-the-go near infrared reflectance spectroscopy. *Computers and Electronics in Agriculture*, 61 (1), 10 – 19.

Clark, R. N. (1999). Spectroscopy of rocks and minerals, and principles of spectroscopy. p. 3–52. *In* Rencz, N. (ed.), *Remote sensing for the earth sciences: manual of remote sensing*. John Wiley & Sons, New York.

Corwin, D. L., Kaffka, S. R., Hopmans, J. W., Mori, Y., van Groenigen, J. W., van Kessel, C., Lesch, S. M. and Oster, J. D. (2003). Assessment and field-scale mapping of soil quality properties of a saline-sodic soil. *Geoderma,* 114 (3–4), 231 – 259.

Cozzolino, D., Montossi, F. and San Julian, R. (2005). The use of Visible (Vis) and Near Infrared (NIR) reflectance spectroscopy to predict the fibre diameter in both clean and greasy wool samples. *Animal Science,* 80, 333 – 337.

Cozzolino, D. and Morron, F. (2006). Potential of Near-infrared Reflectance Spectroscopy and Chemometrics to Predict Soil Carbon Fractions. *Soil & Tillage Research,* 85, 78 – 85.

Dalal, R. C. and Henry, R. J. (1986). Simultaneous determination of moisture, organic carbon, and total nitrogen by near infrared reflectance. *Soil Science Society of America Journal,* 50, 120 – 123.

Daniel, K. W., Tripathi, N. K., Honda, K. (2003). Artificial neural network analysis of laboratory and in situ spectra for the estimation of macronutrients in soils of Lop Buri (Thailand). *Australian Journal of Soil Research,* 41, 47 – 59.

Debaene, G., Niedzwiecki, J. and Pecio, A. (2010). Visible and near-infrared spectrophotometer for soil analysis: preliminary results. *Polish Journal of Agronomy*, 3, 3 – 9.

Donovan, P. (2012). Measuring soil carbon change: a flexible, practical, local method, Retrieved from http://soilcarboncoalition.org/files/MeasuringSoilCarbonChange.pdf. on 3rd Oct 2013.

Ebinger, M. H., Norfleet, M. L., Breshears, D. D., Cremers, D. A., Ferris, M. J., Unkefer, P. J., Lamb, M. S., Goddard, K. L. and Meyer, C. W. (2003). Extending the applicability of laser-induced breakdown spectroscopy for total soil carbon measurement. *Soil Science Society of America Journal,* 67, 616 – 1619.

Ehsani, M. R., Upadhyaya, S. K., Slaughter, D., Shafii, S. and Pelletier, M. (1999). A NIR technique for rapid determination of soil mineral nitrogen. *Precision Agriculture*, 1, 217 – 234.

Fathi, H, Fathi, H. and Moradi, H. (2014). Spatial variability of soil characteristic for evaluation of agricultural potential in Iran Merit *Research Journal of Agricultural Science and Soil Sciences* (ISSN: 2350-2274), 2(2), 024 – 031.

Fidêncio, P. H., Poppi, R. J. and De Andrade, J. C. (2002). Determination of organic matter in soils using radial basis function networks and near infrared spectroscopy. *Analytica Chimica Acta,* 453, 125 – 134.

Franzen, D. W. and Peck. T. R. (1995). Statistical properties of the variable rate fertilization. *Journal of Production Agriculture*, 8, 568 – 574.

Franzluebbers, A. J. and Hons, F. M. (1996). Soil-profile distribution of primary and secondary plant-available nutrients under conventional and no tillage. *Soil & Tillage Research*. 39 (3–4), 229 – 239.

Futagawa, M., Iwasaki, T., Murata, H., Ishida, M. and Sawada, K. (2012). A miniature integrated multimodal sensor for measuring pH, EC and temperature for precision agriculture. *Sensors,* 12, 8338 – 8354.

Ge, Y., Morgan, C. L. S., Grunwald, S. Brown, D. J. and Sarkhot. D. V. S. (2011). Comparison of soil reflectance spectra and calibration models obtained using multiple spectrometers. *Geoderma*, 161 (3-4), 202 – 211.

Gehl, R. J. and Rice, C. W. (2007). Emerging technologies for in situ measurement of soil carbon. *Climatic Change*, 80, 43 – 54 DOI 10.1007/s10584-006-9150-2

Genot, V., Colinet, G., Bock, L., Vanvyve, D., Reusen, Y. and Darbenne, P. (2011). Near infrared reflectance spectroscopy for estimating soil characteristics valuable in the diagnosis of soil fertility. *Journal of Near Infrared Spectoscopy*, 19, 117 – 138.

Geladi, P. and Kowalski, B. R. (1986). Partial least-squares regression: A tutorial. *Analytica Chimica Acta*, 185, 1 – 17.

Godwin, R. J. and Miller, P. C. H. (2003). A review of the technologies for mapping within-field variability. *Biosystem Engineering*, 84 (4), 393 – 407.

Gotway, C. A., Ferguson, R. B. Hergert, G. W. and Peterson. T. A. (1996). Comparison of kriging and inverse-distance methods for mapping soil parameters. *Soil Science Society of America Journal,* 60, 1237 – 1247.

Haneklaus, S, Paulsen, H. M., Schrer, D., Leopold, U. and Schnug, E. (1998). Self-surveying: A strategy for efficient mapping of the spatial variability of time constant soil parameters. *Communication Soil Science Plant Analysis*, 29, 1593 – 1601.

Havlin, J., Beaton, J., Tisdale, S., Nelson, W. (1999). Soil Fertility and Fertilizers. 6th Edition. Prentice Hall, Inc. NJ 07458. USA.

Hoskinson, R. L., Hess, J. R. and Alessi, R. S. (1999). Temporal change in the spatial variability of soil nutrient. *In: Precision agriculture '99.J. V. Stafford (ed). 2nd European Conference on Precision Agriculture*, Odense, Denmark, 11 – 15 July 1999, SCI Sheffield Academic Press, 61 – 70.

Huang, X., Subramanian, S., Kravchenko A., Thelen, K. and Qi, J. (2007). Total carbon mapping in glacial till soils using near-infrared spectroscopy, Landsat imagery and topographical information. *Geoderma,* 141, 34 – 42, doi:10.1016/j.geoderma.2007.04.023

Hummel, J. W., Sudduth, K. A. and Hollinger, S. E. (2001). Soil moisture and organic matter prediction of surface and subsurface soils using an NIR soil sensor. *Computers and Electronics in Agriculture,* 32, 149 – 165.

Imade Anom, S. W., Shibusawa, S., Sasao, A. and Hirako, S. (2001). Soil parameters maps in paddy field using the real time soil spectrophotometer. *Journal of Japanese Society of Agricultural Machinery*, 63 (3), 51 – 58.

Islam, K., Singh, B. and McBratney, A. (2003). Simultaneous estimation of several soil properties by ultra-violet, visible, and near-infrared reflectance spectroscopy. *Australian Journal of Soil Research,* 41, 1101 – 1114. doi: 10.1071/SR02137

Islam, K., Singh, B., Schwenke, G., McBratney, A., (2004). Evaluation of vertosol soil fertility using ultra-violet, visible and near-infrared reflectance spectroscopy. SuperSoil 2004: *3rd Australian New Zealand Soils Conference,* 5 – 9 December 2004, University of Sydney, Australia.

Janik, L. J, Merry, R. H. and Skjemstad, J. O. (1998). Can mid infrared diffuse reflectance analysis replace soil extractions? *Australian Journal of Experimental Agriculture,* 38, 681 – 696.

Kanda, R. (2011). Redefinition of depth observation of real-time soil sensor *(in Japanese). Thesis of Bachelor of Agriculture,* Agriculture and Environmental Engineering, Tokyo University of Agriculture and Technology, Japan

Karydas, C. G., Gitas, I. Z., Koutsogiannaki, E., Lydakis-Simantiris, N. and Silleos, G. N. (2009). Evaluation of Spatial Interpolation Techniques for Mapping Agricultural Topsoil Properties in Crete. *European Association of Remote Sensing Laboratories eProceedings* 8, 1/2009 26 – 39.

Kodaira, M. and Shibusawa, S. (2013). Using a mobile real-time soil visible-near infrared sensor for high resolution soil property mapping. *Geoderma,* 199, 64 – 79.

Kodaira, M. and Shibusawa, S. (2014a). Calibration models for soil mapping of Twenty-five soil parameters using a Tractor-mounted Real-time soil sensor *(in Japanese). 73rd Annual Meeting of The Japanese Society of Agricultural Machinery and Food Engineers,* 16 – 19 May 2014, Okinawa, Japan.

Kodaira, M. and Shibusawa, S. (2014b). Twenty-five Soil Parameters Calibration Model Using a Real-Time Soil Sensor, *7th International Symposium on Machinery and Mechatronics for Agriculture and Biosystem Engineering*, 21 – 23 May 2013, Yilan, Taiwan.

Kodaira, M. and Shibusawa, S. (2014c). Soil Mapping And Modeling On Twenty-Five Ingredients Using A Real-Time Soil Sensor. *12th International Conference in Precision Agriculture*, 23 – 25 July 2014, California, USA.

Kravchenko, A. and Bullock, D. G. (1999). A Comparative Study of Interpolation Methods for Mapping Soil Properties. *Agronomy Journal*, 91, 393 – 400.

Krischenko, V. P., Samokhvalov, S. G., Fomina, L. G. and Novikova, G. A. (1991). Use of Infrared Spectroscopy for the Determination of Some Properties of Soil, *USSR. Interagrotech*, Moscow, USSR, 239 – 249.

Krull, E., Skjemstad, J., and Baldock, J. (2004). Functions of Soil Organic Matter and the Effect on Soil Properties: A Literature Review. *CSIRO Land and Water Client Report,* Adelaide: CSIRO Land and Water.

Kusumo, B. H., Hedley, C. B., Hedley, M. J., Hueni, A., Tuohy, M. P., and Arnold, G. C. (2008). The use of diffuse reflectance spectroscopy for in situ carbon and nitrogen analysis of pastoral soils. *Australian Journal of Soil Research,* 46, 623 – 635.

Kusumo, B. H. (2009). Development of Field Techniques to Predict Soil Carbon, Soil Nitrogen and Root Density from Soil Spectral Reflectance, *PhD. Thesis,* Massey University, Palmerston North, New Zealand.

Lal, R., (2004). Soil carbon sequestration impacts on global climate change and food security. *Science,* 304, 1623 – 1627.

Lal, R., Griffin, M., Apt, J., Lave, L. and Morgan, M. G. (2004). Managing soil carbon. *Science,* 304 – 393.

Lee, W. S., Alchanatis, V., Yang, C., Hirafuji, M., Moshou, D. and Li, C. (2010). Sensing technologies for precision specialty crop production. *Computers and Electronics in Agriculture,* 74, 2 – 33.

Li, Y., Shibusawa, S., Kodaira, M. Oomori, T. and Aliah, B. S. N. (2012). A scheme of precision carbon farming for paddy. *11th International Conference on Precision Agriculture,* International Society of Precision Agriculture, Indiana, USA, 15 – 18 July 2012 *(proceeding in CD.)*

Li, Y. (2013). Assessment of carbon sequestration potential and profitability of recommended carbon-capturing farming practices for Japanese paddy fields. *PhD. Thesis*, Agricultural and Environmental Engineering, Tokyo University of Agriculture and Technology, Japan.

Lyons, J. B., Garres, J. H. and Amador, J. A. (1998). Spatial and temporal variability of phosphorus retention in a riparian forest soil. *Journal of Environmental Quality*, 27, 895 – 903.

Maleki, M. R., Van Holm, L, Ramon, H., Merckx, R., De Baerdemaeker, J. and Mouazen A. M. (2006). Phosphorus Sensing for Fresh Soils using Visible and Near Infrared Spectroscopy. *Biosystems Engineering* 95(3), 425 – 436 doi:10.1016/j.biosystemseng.2006.07.015

Malengreau, N. Bedidi, A., Muller, J. P. and Herbillon, A. J. (1996). Spectroscopic Control of Iron Oxide Dissolution in Two Ferralitic Soil. *European Journal of Soil Science,* 47, 13 – 30.

Malhi, S. S., Grant, C. A., Johnston, A. M. and Gill, K. S. (2001). Nitrogen fertilization management for no-till cereal production in the Canadian Great Plains: a review. *Soil & Tillage Research*, 60 (3–4), 101 – 122.

Malley, D. F., Martin, P. D. and Ben-Dor, E. (2004). Application in analysis of soils. p. 729–784. In C.A. Roberts et al. (ed.) Near-infrared spectroscopy in agriculture. *Agronomy Monograph*, 44. ASA, CSSA, and SSSA, Madison, WI.

Martens, H. and Naes, T. (1989). Multivariate Calibration, 2nd edition. John Wiley & Sons, Ltd., Chichester, United Kingdom.

Martin, P. D., Malley, D. F., Manning, G. and Fuller, L. (2002). Determination of soil organic carbon and nitrogen at the field level using near-infrared spectroscopy. *Canadian Journal of Soil Science*, 82, 413–422.

McBratney, A. B. and Pringle, M. J. (1997). Spatial variability in soil-implications for precision agriculture. In: Stafford, J.V. (Ed.), Precision Agriculture '97 *Proceedings of the 1st European Conference on Precision Agriculture*, Oxford, UK, 639 – 643.

McBratney, A. B., Mendonca Santos, M. L. and Minasny, B. (2003). On digital soil mapping. *Geoderma,* 117, 3 – 52.

McCarty, G. W., Reeves III, J. B., Reeves, V. B., Follet, R. F. and Kimble, J. M. (2002). Mid-infrared and near-infrared diffuse reflectance spectroscopy for soil carbon measurement. *Soil Science Society of America Journal*, 66, 640 – 646.

McCauley, J. D., Engel, B. A., Scudder, C. E., Morgan, M. T. and Elliot, P. W. (1993). Assessing the spatial variability of organic matter. *ASAE Paper No. 93–1555*, American Society of Agricultural Engineers, St. Joseph, MI, USA.

Mengel K. and Kirby E. (2001). Principles of Plant Nutrition. Kluwer Academic Publishers. Dordretcht, The Netherlands.

Morgan, C. L. S., Waiser, T. H., Brown, D. J. and Hallmark, C. T (2009). Simulated in situ characterization of soil organic and inorganic carbon with visible near-infrared diffuse reflectance spectroscopy. *Geoderma,* 151, 249–256.

Morra, M. J., Hall, M. H. and Freeborn, L. L. (1991). Carbon and Nitrogen Analysis of Soil Fractions Using Near-Infrared Reflectance Spectroscopy. *Soil Science Society of American Journal,* 55 (1), 288 – 291.

Mouazen, A. M., Dumont, K., Maertens, K. and Ramon, H. (2003). Two-dimensional prediction of spatial variation in topsoil compaction of a sandy loam field based on measured horizontal force of compaction sensor, cutting depth and moisture content. *Soil & Tillage Research* 74 (1), 91 – 102.

Mouazen, A. M., De Baerdemaeker, J. and Ramon, H. (2005). Towards development of online soil moisture content sensor using a fibre-type NIR spectrophotometer. *Soil & Tillage Research,* 80 (1–2), 171 – 183.

Mouazen, A. M., Karoui, R., De Baerdemaeker, J. and Ramon, H. (2006a). Characterization of Soil Water Content using measured Visible and Near Infrared Spectra. *Soil Science Society of America Journal*, 70, 1295 – 1302.

Mouazen, A. M., De Baerdemaeker, J. and Ramon, H. (2006b). Effect of wavelength range on the measurement accuracy of some selected soil constituents using visual-near infrared spectroscopy. *Journal of Near Infrared Spectroscopy,* 14, 189 – 199.

Mouazen, A. M., Maleki, M. R. De Baerdemaeker, J. and Ramon, H (2007). On-line measurement of some selected soil properties using Vis-NIR sensor. *Soil & Tillage Research,* 93, 13 – 27.

Müller-Lindenlauf, M. (2009). Organic Agriculture and Carbon Sequestration Possibilities and constrains for the consideration of organic agriculture within carbon accounting systems. *Natural Resources Management and Environment Department Food and Agriculture Organization of the United Nations* Rome, December 2009. Retrieved from ftp://ftp.fao.org/docrep/fao/012/ak998e/ak998e00.pdf on 10th August 2012.

Niggli, U., Fliessbach, A., Hepperly, P. and Scialabba, N. (2009). Low Greenhouse Gas Agriculture: Mitigation and Adaptation Potential of Sustainable Farming Systems. FAO, April 2009, Rev. 2 – 2009. Retrieved from ftp://ftp.fao.org/docrep/fao/010/ai781e/ai781e00.pdf on 10th August 2012.

Ozaki Y., Morita S. and Du, Y. (2007). Spectral analysis. In 'Near-infrared spectroscopy in food science and technology'. (Eds Y Ozaki, W.F. McClure, A.A. Christy) (Wiley-Interscience, John Wiley & Sons, Inc.: Hoboken, New Jersy).

Quine, T. A. and Zhang, Y. (2002). An investigation of spatial variation in soil erosion, soil properties and crop production within an agricultural field in Devon, U.K. *Journal of Soil and Water Conservation*, 57, 50 – 60.

Raun, W. R., Solie, J. B. and Johnson, G. V. (1998). Microvariability in soil test, plant nutrient, and yield parameters in Bermudagrass. *Soil Science Society of America Journal*, 62, 683 – 690.

Reeves III, J. B, McCarty, G. W. and Reeves, V. B. (2001). Mid-infrared and diffuse reflectance spectroscopy for the quantitative analysis of agricultural soils. *Journal of Agricultural and Food Chemistry,* 49, 766 – 772.

Reeves III, J. B. and McCarty, G. W. (2001). Quantitative analysis of agricultural soils using near infrared reflectance spectroscopy and a fibre optic probe. *Journal of Near Infrared Spectroscopy,* 9, 25 – 34.

Reeves III, J. B., McCarty, G. W. and Mimmo, T. (2002). The potential of diffuse reflectance spectroscopy for the determination of carbon inventories in soils. *Environment Pollution,* 116, 277 – 284.

Reeves III, J. B. (2010). Near- versus mid-infrared diffuse reflectance spectroscopy for soil analysis emphasizing carbon and laboratory versus on-site analysis: Where are we and what needs to be done?. *Geoderma,* 158, 3 – 14

Redulla, C. A., Havlin, J. L., Kluitenberg, G. J., Zhang, N. and Schrock, M. D. (1996). Variable nitrogen management for improving groundwater quality. p. 1101-1110. In P.C. Robert et al. (ed.) *Proceeding of 3rd Internationa. Conference on Precision Agriculture*, Minneapolis, MN. 23-26 June 1996. ASA-CSSA-SSSA, Madison, WI.

Robertson, G. P., Paul, E. A. and Harwood, R. R. (2000). Greenhouse gases in intensive agriculture: contributions of individual gases to the radiative forcing of the atmosphere. *Science,* 289, 1922 – 1925.

Sarkhot, D. V., Grunwald, S., Ge, Y. and Morgan, C. L. S. (2011). Comparison and detection of total and available soil carbon fractions using visible/near infrared diffuse reflectance spectroscopy. *Geoderma*, 164, 22 – 32.

Savitzky, A. and Golay, M. J. E. (1964). Smoothing and differentiation of data by simplified least squares procedures. *Analytical Chemistry* 36, 1627–1639.

Scialabba, N. and Müller-Lindenlauf, M. (2010). Organic Agriculture and Climate Change. Renewable Agriculture and Food Systems. 25(2); 158–169 doi:10.1017/S1742170510000116

Shepherd, K. D. and Walsh, M. G. (2002). Development of reflectance spectral libraries for characterization of soil properties. *Soil Science Society of America Journal,* 66, 988 – 998.

Shibusawa, S., Hirako, S., Otomo, A., Li, M., (1999). Real-time underground soil spectrophotometer. *Journal of Japanese Society of Agricultural Machinery,* 61 (3), 131 – 133.

Shibusawa, S., Imade Anom, S. W., Sato, S., Sasao, A. and Hirako, S. (2001). Soil mapping using the real-time soil spectrophotometer In: Grenier, G., Blackmore, S. (Eds.), ECPA 2001, *3rd European Conference on Precision Agriculture*, vol. 1. Agro Montpellier, 497 – 508.

Shibusawa, S., Imade Anom, S. W., Hache, C., Sasao, A. and Hirako, S. (2003). Site-specific crop response to temporal tren of soil variability determined by the real-time soil spectrophotometer, In 'precision Agriculture. *Proceeding of the Joint European Conference of ECPA-ECPLF*. Berlin, Germany (Ed. JV Stafford), 639 – 643 (Wageningen Academic Publishers.

Shibusawa, S., Ehara K., Okayama, T., Umeda, H., and Hirako, S. (2005). A real-time multi-spectral soil sensor: predictability of soil moisture and organic matter content in a small field. *5th European Conference on Precision Agriculture*. Uppsala, Sweden. (Ed. JV Stafford), 495 – 502.

Shonk, J. L., Gaultney, L .D., Schulze, D. G. and Van Scoyoc, G. E. (1991). Spectroscopic sensing of soil organic matter content. *Transactions of ASAE* 34, 1978 – 1984.

Slaughter, D. C., Pelletier, M. G., Upadhyaya, S. K. (2001). Sensing soil moisture using NIR spectroscopy. *Applied engineering in agriculture*, 17 (12), 241 – 247.

Sonka, S. T., Bauer, M. E., Cherry, E. T., Colburn, J. W., Heimlich, R. E., Joseph, D. A., Leboeuf, J. B., Lichtenberg, E., Mortensen, D. A., Searcy, S. W., Ustin, S. L. and Ventura, S. J. (1997). Precision agriculture in the 21st century. Geospatial and information technologies in crop management. *Committee on Assessing Crop Yield:*

*Site-Specific Farming, Information Systems, and Research Opportunities,* Board of Agriculture, National Research Council. National Academy Press, Washington, DC.

Souma, S. and Kikuchi, K. (1992). Diagnostic Criteria for Soil and Crop Nutrition—Analysis Method (Revised). *Agriculture Research Department, Central Agricultural Experiment Station, Hokkaido* Research Organization; Agricultural Administration Division, Department of Agriculture, Hokkaido Government, Hokkaido, Japan.

Stenberg, B., Viscarra Rossel, R. A, Mouazen, A. M and Wetterlind, J. (2010). Visible and Near Infrared Spectroscopy in Soil Science. In Donald L. Sparks, editor: *Advances in Agronomy,* 107, 163 – 215. http://dx.doi.org/10.1016/S0065-2113(10)07005-7

Stevens, A., Wesemael, B. V.. Vandenschrick, G., Toure, S. and Tychon, B. (2006). Detection of carbon stock change in agricultural soilds using spectroscopic techniques *Soil Science Society of America Journal*, 70 (3), 844 – 850. doi: 10.2136/sssaj2005.0025,

Stevens, A., Van Wesemael, B., Bartholomeus, H., Rosillon, D., Tychon, B. and Ben-Dor, E. (2008). Laboratory, field and airborne spectroscopy for monitoring organic carbon content in agricultural soils. *Geoderma,* 144, 395–404.

Sudduth, K. A. and Hummel, J. W., (1993a). Portable, near-infrared spectrophotometer for rapid soil analysis. *Transaction of ASAE,* 36 (1), 185 – 193.

Sudduth, K. A. and Hummel, J. W. (1993b). Soil organic matter, CEC, and moisture sensing with a prototype NIR spectrometer. *Transactions of ASABE,* 36, 1571 – 1582.

Sudduth, K. A. and Hummel, J. W. (1996). Geographic operating range evaluation of a NIR soil sensor. *Transaction of ASAE* 39, 1599 – 1604.

Sudduth, K. A., Kitchen, N. R., Bollero, G. A., Bullock, D. G. and Wiebold, W. J. (2003). Comparison of electromagnetic induction and direct sensing of soil electrical conductivity. *Agronomy Journal,* 95, 472 – 482.

Sudduth, K. A., Kitchen, N. R., Sadler, E. J., Drummond, S. T. and Myers, D. B. (2010). VNIR spectroscopy estimates of within-field variability in soil properties. p. 153–163. *In R.A. Viscarra Rossel et al. (ed.) Proximal soil sensing.* Springer Science + Business Media, Dordrecht, the Netherlands.

Tekin, Y., Kuang, B. and Mouazen, A. M. (2013). Potential of On-line Visible and Near Infrared Spectroscopy for Measurement of pH for Deriving Variable Rate Lime Recommendations. *Sensors,* 3(8), 10177-10190; doi:10.3390/s130810177

Troeh, F. R. and Thompson, L. M. (2005). Soil and Soil Fertility. 6th edition. Blackwell. Iowa 50014, USA.

Udelhoven, T., Emmerling, C. and Jarmer, T. (2003). Quantitative analysis of soil chemical properties with diff use reflectance spectrometry and partial least-square regression: A feasibility study. *Plant Soil,* 251, 319 – 329. doi:10.1023/A:1023008322682

Vanden Auweele, W., Boon, W., Bries, J., Coppens, G., Deckers, S., Elsen, F., Mertens, J., Vandendriessche, H., Ver Elst, P. and Vogels, N. (2000). The Chemistry of Soil Fertility of Belgium Arable and Grass Lands. Belgium Soil Service Department, Heverlee, Belgium

Van Vuuren, J. A. J, Meyer J. H. and Classens, A. S. (2007). Potential Use of Near Infrared Reflectance monitoring in precision agriculture. *Communication in Soil Science and Plant Analysis,* 37, 2171 – 2184.

Vieira, S. R. and Paz Gonzalez, A. (2003). Analysis of the spatial variability of crop yield and soil properties in small agricultural plots. *Bragantia*, Campinas, 62, 127 – 138.

Viscarra Rossel, R. A. and McBratney, A. B. (1998). Laboratory evaluation of a proximal sensing technique for simultaneous measurement of soil clay and water content. *Geoderma,* 85, 19 – 39.

Viscarra Rossel, R. A. and Walter, C. (2004). Rapid, quantitative and spatial field measurements of soil pH using an ion sensitive field effect transistor. *Geoderma,* 119, 9 – 20.

Viscarra Rossel, R. A., McGlynn, R. N. and McBratney, A. B. (2006a). Determing the composition of mineral-organic mixes using UV-vis-NIR diffuse reflectance spectroscopy, *Geoderma,* 137, 70 – 82.

Viscarra Rossel, R. A., Walvoort, D. J. J., McBratney, A. B., Janik, L. J. and Skjemstad, J. O. (2006b). Visible, near infrared, mid infrared or combined diffuse reflectance spectroscopy for simultaneous assessment of various soil properties. *Geoderma,* 131, 59 – 75.

Viscarra Rossel, R.A. (2007). Robust modelling of soil diffuse reflectance spectra by bagging-partial least squares regression. *Journal of Near Infrared Spectroscopy,* 15, 39 – 47.

Viscarra Rossel, R. A., Cattle, S. R., Ortega, A. and Fouad, Y. (2009). In situ measurements of soil colour, mineral composition and clay content by Vis–NIR spectroscopy. *Geoderma*, 150, 253 – 266.

Viscarra Rossel, Rizzo, R. A. R., Dematte, J. A. M. and Behrens, T. (2010). Spatial modeling of a soil fertility index using visible-near-infrared spectra and terrain attributes. *Soil Science Society of American Journal*, 4, 1293 – 1300.

Vrindts, E., Mouazen, A. M., Reyniers, M., Martens, K., Maleki, M. R., Ramon, H. and De Baerdemaeker, J. (2005). Management zones based on correlation between coil compaction, yield and crop data. *Biosystem Engineering*, 92 (4), 419 – 428.

Waiser, T. H., Morgan, C. L. S., Brown, D. J. and Hallmark, C. T. (2007). In situ characterization of soil clay content with visible near-infrared diffuse reflectance spectroscopy. *Soil Science Society of America Journal,* 71, 389 – 396.

Warrick, A. W, and Nielsen, D. R. (1980). Spatial variability of soil physical properties in the field. In: Hillel, D., Editor,. *Applications of Soil Physics*. Academic Press. New York.

Weber, D. and Englund, E. (1992). Evaluation and comparison of spatial interpolators. *Journal of Mathematical Geology,* 24, 381 – 391.

Weisz, R., Fleischer, S. and Smilowitz, Z. (1995). Map generation in high-value horticultural integrated pest management: Appropriate interpolation methods for site-specific pest management of Colorado potato beetle (Coleoptera: Chrysomelidae). *Journal of Economic Entomology,* 88, 1650 – 1657.

Wetterlind, J., Stenberg, B., and Jonsson, A. (2008). Near infrared reflectance spectroscopy compared with soil clay and organic matter content for estimating within-field variation in N uptake in cereals. *Plant and Soil,* 302, 317 – 327.

Wetterlind, J., Stenberg, B. and Söderström, M. (2010) .Increased sample point density in farm soil mapping by local calibration of visible and near infrared prediction models. *Geoderma,* 156, 152 – 160.

Whipker, B. E. and Cavins, T. J. (2000). Electrical Conductivity (EC): Unit and Conversions. North Carolina State University.

Wielopolski, L., Mitra, S., Hendrey, G., Rogers, H., Torbert, A. and Prior, S. (2003). Non-destructive *in situ* soil carbon analysis: principles and results. *Proc 2nd Nat Conf carbon sequestration: developing and validating the technology base to reduce carbon intensity*. 5 – 8 May, 2003, Alexandria, VA.

Williams, P. C., and Norris. K. (2001). Variables affecting near-infrared spectroscopic analysis, 171 – 185. In P. Williams and K. Norris (ed.) Near-infrared technology in the

agricultural and food industries. 2nd ed. *American Association of Cereal Chemists*., St. Paul, MN.

Williams P C (2003). Near-infrared technology—getting the best out of light. PDK Grain, PDK Project, Inc., 10.

Wold, S., Martens, H., Wold, H. (1983). The multivariate calibration method in chemistry solved by the PLS method. In: Ruhe, A., Kagstrom, B. (Eds.), *Proc. Conf. Matrix Pencils,* Lecture Notes in Mathematics. Springer-Verlag, Heidelberg, 286 – 293.

Wollenhaupt, N. C., Wolkowski, R. P. and Clayton. M. K. (1994). Mapping soil test phosphorus and potassium for variable-rate fertilizer application. *Journal of Production Agriculture,* 7, 441 – 448.

Wu, C.Y., Jacobson., A. R ., Laba, M., Kim, B. and Baveye, P. C. (2010). Surrogate Correlations and Near-Infrared Diffuse Reflectance Sensing of Trace Metal Content in Soils. *Water Air Soil Pollution,* 209, 377 – 390. DOI 10.1007/s11270-009-0206-6

Xie, H. T., Yang, X. M., Drury, C. F., Yang, J. Y. and Zhang, X. D. (2011). Predicting soil organic carbon and total nitrogen using mid- and near-infrared spectra for Brookston clay loam soil in Southwestern Ontario, Canada. *Canadian Journal of Soil Science*, 91, 53 – 63.

Yang, H., Kuang, B. and Mouazen, A. M. (2011). Prediction of soil TN and TC at a farm-scale using VIS-NIR spectroscopy. *Advanced Materials Research*, 225 – 226 (1-2), 1258 – 1261.

Yemefack, M., Rossiter, D. G. and Njomgang, R. (2005). Multi-scale characterization of soil variability within an agricultural landscape mosaic system in southern Cameroon. *Geoderma*, 125, 117 – 143.

Young, L. M. (2003). Carbon sequestration in agriculture: the US policy context. *American Journal of Agricultural Economics,* 85, 1164 – 1170.

# List of Publications

## Journal

**Aliah**, **B. S. N.,** Shibusawa, S., Kodaira, M. and Kanda, R. (2014), Multiple Depths Mapping of Soil Properties using Visible-near Infrared Real-time Soil Sensor for a Paddy Field. *Engineering in Agriculture, Environment and Food Journal*. **(accepted on 23rd Aug 2014)**

## Proceedings and Conference Presentations

**Aliah, B. S. N**, Shibusawa, S., Kodaira, M. and Inoue, K. (2014), Comparison of Calibration Models Developed For A Visible-Near Infrared Real-Time Soil Sensor, *proceeding of the 12th International Conference on Precision Agriculture*, 20 – 23 July 2014, California, USA

**Aliah, B. S. N.,** Shibusawa, S., Kodaira, M. and Inoue, K. (2014), Mapping Of Soil Properties For Paddy Field In Fukushima Using Visible-Near Infrared Real-Time Soil Sensor. *proceeding of the 7th International Symposium on Machinery and Mechatronics for Agriculture and Biosystems Engineering (ISMAB)*, 21 – 23 May 2014, Yilan, Taiwan

**Aliah**, **B. S. N.,** Shibusawa, S., Kodaira, M. and Kanda, R. (2013), Utilization of Visible-Near Infrared Real-time Soil Sensor as a Practical Tool For Precision Carbon Farming Practice, *proceeding of International Conference on Green Agro-Industry*, Yogyakarta, Indonesia , 11 – 13 November 2013

**Aliah, B. S. N.**, Shibusawa, S., Kodaira, M. and Inoue, K. (2013) Paddy Soil Mapping with Real-time Soil Sensor toward Traceable Management, *The 72nd Japanese Society of Agricultural Machinery Meeting*, Obihiro, Hokkaido, Japan, 10 – 13 September 2013

**Aliah**, **B. S. N.,** Shibusawa, S., Kodaira, M. and Kanda, R. (2013), Effects of Sensing Depth Variation on Total Carbon and Total Nitrogen Mapping using Real-time Soil Sensor, *proceeding of the 5th Asian Conference on Precision Agriculture*, Jeju, Korea, 25 – 28 June 2013

**Aliah, B. S. N.,** Kodaira, M. and Shibusawa, S., (2013), The Potential of Visible – Near Infrared Spectroscopy for Mapping of Multiple Soil Properties using Real-time Soil Sensor, *proceeding of The 1st International Conference on Sensing Technologies for Biomaterial, Food and Agriculture*. Yokohama, Japan, 23 – 26 April 2013

**Aliah, B. S. N.,** Shibusawa, S. and Kodaira, M. (2012), Calibration Model for Carbon and Nitrogen Measurement of Field Soil using Real-time Soil Sensor, *Joint Conference on Environmental Engineering in Agriculture*, Utsunomiya, Tochigi, Japan, 11 – 14 September 2012

## Co-author

Inoue, K., Shibusawa, S. and Kodaira, M., **Aliah, B. S. N.** and Ookuma, S. (2014), Soil Parameters Of Paddy Field In Yamatsuri Town, Fukushima, Japan, *proceeding of the 7th International Symposium on Machinery and Mechatronics for Agriculture and Biosystems Engineering* (ISMAB), 21-23 May 2014, Yilan, Taiwan

Inoue, K., Shibusawa, S. and Kodaira, M., **Aliah, B. S. N.** and Ookuma, S. (2014), Properties of paddy soil in Fukushima Prefecture Yamatsuri Town, *The 73rd Annual Meeting of the Japanese Society of Agricultural Machinery and Food Engineers 2014*, Okinawa, Japan (in Japanese)

Kanda, R., Shibusawa, S., Kodaira, M., **Aliah, B. S. N.** and Usui, K. (2013), Three-dimensional variability of Soil Components in a Small Paddy Field*, proceeding of the 5th Asian Conference on Precision Agriculture*, Jeju, Korea, 25 – 28 June 2013

Shibusawa, S., Kodaira, M., Li, Y., Oomori, T. and **Aliah, B. S. N.** (2012), A Scheme for Precision Carbon Farming for Paddy, *proceeding of the 11th International Conference on Precision Agriculture*, Indianapolis, Indiana, USA, 15 – 18 July 2012.

## Invited Presentation

Aliah, B. S. N., Precision Agriculture Technology in Malaysia, *presented to the undergraduate students of Agriculture Technology, Universitas Udayana, Bali, Indonesia*, 15 Nov 2013